UNIVERSITÀ DEGLI STUDI DI MILANO
Dipartimento di Scienze Farmacologiche e Biomolecolari

Scuola di Dottorato di Ricerca in
Scienze Biochimiche, Nutrizionali e Metaboliche
Dottorato di ricerca in Biochimica ciclo XXVI
Settore scientifico disciplinare: BIO/10

The use of Atomic Force Microscopy together with classical biochemical techniques to study alterations of membrane microdomains induced by DHA in MDA-MB-231 breast cancer cells

Dottorando:
Dott. Andrea Cremona
Matricola: R09276

Tutor: Dott.ssa Angela Maria Rizzo
Coordinatore: Prof. Francesco Bonomi

A.A. 2012-2013

Index

Abbreviations

AA = arachidonic acid
ALA = α-linolenic acid
AFM = atomic force microscopy
LA = linoleic acid
Cer = ceramides
Chol = cholesterol
CLA = conjugated linoleic acid
COX = ciclooxygenase
DAG = diacylglycerol
DHA = docosahesaenoic acid
DGLA = dihomo-gamma-linolenic acid
DPA = docosapentaenoic acid
DRM = detergent-resistant membrane
DSC = differential scanning calorimetry
EFA = essential fatty acids
EGFR = epidermal growth factor receptor
Elov = elongase
EM = electron microscopy
EPA = eicosapentaenoic acid
ESR = electron spin resonance
FA = fatty acid
FASN = fatty acid synthase
FBS = fetal bovine serum
FCS = fluorescence correlation spectroscopy
FM = fluorescence microscopy
FRET = fluorescence resonance energy transfer
GC = gas chromatography
GLA = gamma linolenic acid
GPI = glycosylphosphatidylinositol-linked proteins
GPLs = glycerophospholipids
GPMVs = giant plasma membrane vesicles
GSLs = glycosphingolipids
^{2}H-NMR = deuterium-based nuclear magnetic resonance
HPLC/ELSD = high performance liquid chromatography/evaporative light scattering detector
HP-TLC = high performance thin layer chromatography
IL = interleuchin

LCPUFA = long chain polyunsaturated fatty acids
Ld = liquid disordered phase
Lo = liquid ordered phase
LOX = lipoxygenase
LT = leucotriens
LX = lipoxine
MAPK = mitogen-activated protein kinase
MaR = maresins
MUFA = monounsaturated fatty acids
NF-κB = nuclear transcription factor κB
NMR = nuclear magnetic resonance
n-6 PUFAs = omega 6 polyunsaturated fatty acids
n-3 PUFAs = omega 3 polyunsaturated fatty acids
PALM = photoactivated localization microscopy
PC = phosphatidylcholine
PE = phosphatidylethanolamine
PGs = prostaglandins
PI = phosphatidylinositol
PI3K = phosphatidylinositol 3-kinase
PIP2 = phosphatidylinositol 4,5-bisphosphate
PIP3 = phosphatidylinositol 3,4,5-trisphosphate
PL = phospholipid
PLA = phospholipase A
PLAP = placental alkaline phosphatase
PPAR = peroxisome proliferator activated receptor
PD = protectins
PLCγ = phospholipase Cγ
PS = phosphatidylserine
PUFAs = polyunsaturated fatty acids
Rv = resolvins
SDC-1 = syndecan-1
SEM = scanning electron microscopy
SFA = saturated fatty acid
SLBs = supported lipid bilayers
SLs = sphingolipids
SM = sphingomyelin
So = solid-ordered phase
SPM = scanning probe microscopy
STED = stimulated emission depletion microscopy
STM = scanning tunneling microscopy

TEM = transmission electron microscope
Tm = melting temperature
TNF = tumor necrosis factor
TX = tromboxane

Summary

Today, the Western diet is substantially enriched in n-6 PUFAs (shifting the balance from the optimal n-6:n-3 ratio of 1–5:1 to approximately 20:1) due to the increased consumption of food items rich in n-6 and simultaneous reduction of fish intake. Diet enriched in n-6 PUFAs determines an unbalance between bioactive lipid mediators that are involved in regulating inflammation. These bioactive products can contribute to the development of numerous chronic diseases, including cancer. Many studies have demonstrated that genetic factors contribute only for 5% to the onset of cancer, while 95% is due to environmental conditions factors, including lifestyle-related factors (tobacco, alcohol and physical activity), external stimuli (radiation and infections) and diet that represents about 30–35% of the risk factors.

There are *in vitro* and *in vivo* evidences that the DHA and EPA administration is able to reduce cancer proliferation increase apoptosis as well as inhibit angiogenesis and metastasis, and to influence cancer differentiation. Several molecular mechanisms have been proposed for the anticancer activity of n-3 PUFAs, including inhibition of cell proliferation, anti-angiogenic action and enhancement of apoptosis. The multiple actions of n-3 PUFAs appear to involve multiple mechanisms that connect the cell membrane, the cytosol, and the nucleus. N-3 PUFAs may act also modulating cell membrane FA composition.

The plasma membrane is involved in many aspects of cell biology, including proliferation, differentiation and apoptosis. Phospholipids (PLs) fatty acid composition within cell membrane play a key role in maintaining its fluidity, structure and function. Thus, changes in membrane PLs fatty acid composition can influence the function of cells. In particular, n-3 PUFAs incorporated into membrane PLs can potentially affect a variety of plasma membrane physical properties including membrane thickness, fluidity and elasticity, structure and function in particular of membrane microdomains (lipid rafts); moreovere they can cause alteration of cell signaling pathways that lead to altered transcription factor activity and changes in gene expression. We have observed that DHA is incorporated in breast cancer cell membrane with different specificity for the PLs moiety. Moreover, we have demonstrated that the treatment with DHA determines a reduction of cell proliferation, inhibition of EGFR activity and induction of apoptotic process, suggesting that these effects might be the consequences of cell membrane alterations induced by FAs.

The main purpose of my research project was to analyze the effects of PUFA administration on membrane microdomain structure and function in breast cancer cells by a combination of biophysical and biochemical techniques. In my study I have used Atomic Force Microscopy (AFM) to perform a morpho-dimensional characterization of lipid rafts as Detergent-Resistant Membrane (DRM) isolated from MDA-MB-231 breast cells (estrogen receptor negative and over-expressing Epidermal growth factor receptor (EGFR)).

AFM providing nanometer spatial resolution and operating in physiological-like conditions without fixation, staining, or labeling, appears to be a useful tool to visualize and quantitatively characterize the topology of biological membranes as well as of their protein content.

AFM imaging of DRM fractions showed membrane patches whose height corresponds to the one awaited for a single lipid bilayer as well as the presence of microdomains with lateral dimensions in the order of a few hundreds of nanometers. Moreover, AFM-immunolabeling using specific antibodies suggested the presence, in these microdomains, of a characteristic marker of lipid rafts, the protein flotillin-1. In addition, my results suggested that AFM could be an useful tool to study the phase coexistence of a Liquid-disordered (Ld) and Liquid-ordered (Lo) domain in purified membrane microdomains.

Finally, I have investigated the role of lipid changes induced by DHA in membrane microdomain structure and function by biochemical tecniques. The data showed that the incubation with DHA determines its incorporation in all PLs, with different specificity for PI, PS and PC, and a reduction of sphingomyelin (SM) and cholesterol (Chol) content in membrane microdomains. Moreover, I have demonstrated that DHA can exclude key proteins, such as EGFR and Ras, from membrane microdomains, modifying their downstream signaling, such as Erk1/2 and Akt.

Chapter 1

N-3 Polyunsaturated Fatty Acids

1.1 N-6 and n-3 fatty acids: structure and metabolism

From a chemical point of view, fatty acids (FAs) are carboxylic acids characterized by a long hydrocarbon chain with a carboxyl group at one end and a methyl group at the other. Fatty acids (FAs) differ in the length of the carbon chain: short-chain FAs have less than 8 carbons, whereas long-chain FAs have 16 or more carbons. The number and the type of bonds (single or double) between the carbons define the different kind of fatty acids. In particular, FAs without double bonds are known as saturated, while FAs with double bonds are known as unsaturated. Unsaturated fatty acids include Monounsaturated Fatty Acids (MUFAs) and Polyunsaturated Fatty Acids (PUFAs).

PUFAs are grouped into two main families. ω-6 (or n-6) and ω-3 (or n-3), distinguished by a position of the first double bond closest to the methyl end. Linoleic acid (LA, C18:2n-6) and α-linolenic acid (ALA, C18:3n-3) with 18 carbon atoms in acyl chain and two (LA) or three (ALA) double bonds, are the precursors of n-6 and n-3 PUFAs, respectively. From a nutritional point of view, LA and ALA are identified as ‘‘Essential’’ fatty acids (EFA), because in mammalians, including humans, they cannot be synthesized *de novo* due to the absence of Δ12- and Δ15-desaturases, and therefore they must be obtained from the diet.

For example, vegetable oils such as soybean, corn, sunflower, safflower and cotton seed oils are enriched to n-6 FAs, while linseed and canola oils are rich in n-3 FAs **[1]**.

Normally, in healthy subjects, most of part of LA and ALA assimilated by dietary are used to produce energy **[2]**, and approximately only 3.0% and 1.5% of them are metabolized into longer PUFAs to satisfy the metabolic need. Starting from LA and ALA, using enzyme system, it is possible to produce longer and more unsaturated PUFAs by the same microsomal **[3].** In particular, LA is converted into Arachidonic acid (AA, C20:4n-6), and ALA is converted first into Eicosapentanoic acid (EPA, C20:5n-3) and, subsequently, into Docosahexanoic acid (DHA, C22:6n-3) the longest and the most unsaturated fatty acid (**Figure 1.1**).

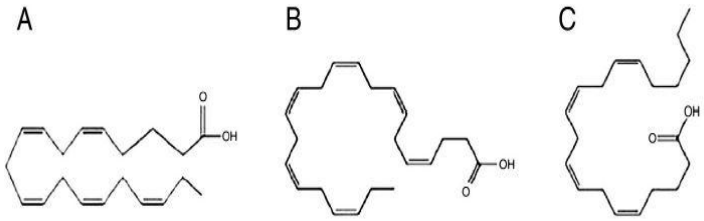

Figure 1.1. Polyunsaturated fatty acids (PUFAs) structures (from Raposo *et al.*,2013 [4]).

A) Eicosapentaenoic acid (EPA), B) Docosahexaenoic acid (DHA), and C) Arachidonic acid (AA).

The human body converts LA and ALA into these higher unsaturated derivatives by a series of desaturation and elongation steps. As shown in **Figure 1.2**, the Δ6-desaturase recognizes and converts LA and ALA into γ-linolenic acid (GLA, C18:3n-6), and octadecatetraenoic (stearidonic, C18:4n-3) acids, respectively.

This step is followed by a cycle of elongation via elongase (Elov-l) and desaturation by Δ5-desaturase to generate AA and EPA. AA is either metabolized to tetracosapentaenoic acid (C24:5n-6) by two cycles of elongations and one of desaturation by Δ6-desaturase, and eventually β-oxidized to docosapentaenoic acid (DPA, C22:5n6). EPA is either metabolized to DHA, this conversion involves the addition of two carbons by two consecutive elongase Elovl-5 and 2 to produce tetracosapentaenoic acid (C24:5n-3) and a desaturation using Δ6-desaturase to produce tetracosa-hexaenoic acid (C24:6n-3). Finally, tetracosapentaenoic acid (C24:5n-6) and tetracosahexaenoic acid (C24:6n-3) are translocated from the endoplasmic reticulum (ER) to the peroxisomes, where the β-oxidation pathway involves acyl chain shortening of C2 to produce DPA and DHA, and then back to endoplasmic reticulum (ER) **[5].**

Since biosynthesis of FAs and phospholipids (PLs) occurs in ER, the intermediates of the PUFA metabolism can either be incorporated into PLs, or become the substrate for further elongation/desaturation reactions.

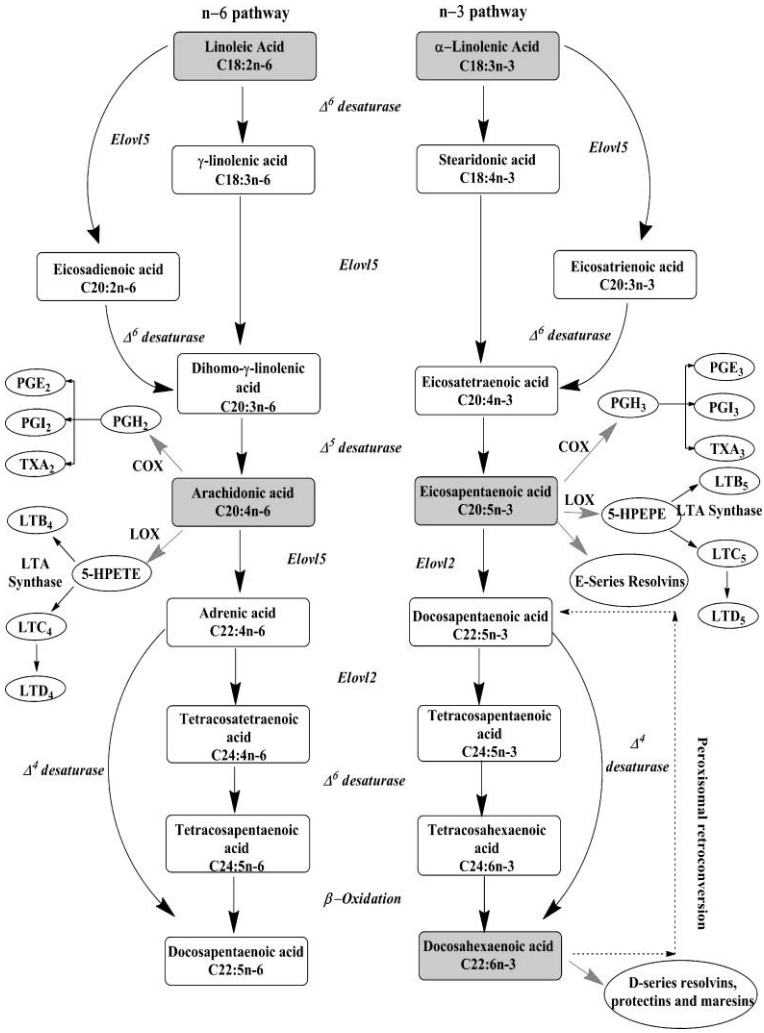

Figure 1.2. PUFA metabolic pathways (from Poudyal *et al.*, 2011[6]).

PGs prostaglandins; PGI prostacyclins; LT leukotriene; TX thromboxane.

1.2 Health benefits of n-3 PUFAs

Today, the Western diet is substantially enriched in n-6 PUFAs (shifting the balance from the optimal n-6:n-3 ratio of 1–5:1 to approximately 20:1) **[7,8]** due to the increased consumption of food items rich in n-6 and simultaneous reduction of fish intake. Diet enriched of n-6 PUFAs determines an unbalance between bioactive lipid mediators that are involved in regulating inflammation. These bioactive products can contribute to the development of numerous chronic diseases, including cardiovascular and inflammatory disorders. On the other hand, n-3 PUFAs are very important fatty acids in human nutrition, indeed, they have a wide range of physiological functions in the human body. As components of structural PLs in the cell membrane, they modulate cellular signalling, cellular interaction, and membrane fluidity **[9]**. The potential health benefits of n-3 PUFAs, DHA and EPA in particular, have been the focus of many researches since 1980, when epidemiologic data showed that populations consuming large quantities of fish (e.g. salmon, tuna, mackerel, and sardines) had lower rates of inflammation **[10,11]**. In the past decade, a lot of studies have shown the benefits of dietary consumption of n-3 PUFAs in cardiovascular disease **[12-15]**, atherosclerosis **[16]**, diabetes **[17]**, metabolic syndrome **[6]**, neurological/neuropsychiatric disorders **[18,19]**, osteoporosis **[20,21],** pregnancy **[23,23]** and autoimmune diseases **[24,25]**.

The protective effects of n-3 PUFAs are particularly convincing for cardiovascular diseases (CVD). The first observation dates back almost 50 years, when Dyerberg and coworkers observed the low incidence of mortality rate from coronary heart disease in Greenland Eskimos (a population consuming a diet enriched in n-3 PUFAs) **[26,27]**. In the past years, the most compelling evidence for the cardiovascular benefit obtained by n−3 PUFAs, derives from an analysis of pooled data from 3 controlled trials of 32,000 participants. These trials showed reductions in cardiovascular events of 19% to 45% **[28]**. Among the possible mechanisms that may contribute to the cardiovascular benefits of n-3 PUFAs, there are their ability to lowering of plasma triglycerides **[29]**, decreasing blood pressure **[30]** and improving vasodilatation **[31].** Other mechanisms include the generation of less-potent inflammatory mediators (*e.g.* 3-series prostanoids and 5-series leukotrienes) that compete for AA metabolism and pro-inflammatory effects of AA derived eicosanoids **[32]**. N-6 and n-3 PUFAs are substrates for the production of various eicosanoids and docosanoids. The mono-hydroxylated PUFA metabolites of AA, 15- hydroxyeicosatetraenoic acid (15-HETE) and 5- hydroxyeicosatetraenoic acid (5-HETE) are direct precursors for Lipoxins (LXA4 and LXB4), which, in contrast to Prostaglandins (PGs) and Leukotrienes (LTs), attenuate the inflammatory effect. Moreover, current evidence indicates that n-3 PUFAs are precursors of a distinct set of lipid mediators. The novel n-3 PUFA-pro-resolution lipid mediators like Resolvins (Rv), Protectins (PD) and Maresins (MaR) are responsible for the active resolution of inflammation **[33-35]**.

EPA and DHA are substrates for various classes of Rv of the E (originating from EPA) and D (originating from DHA) series, respectively (**Figure 1.3**).

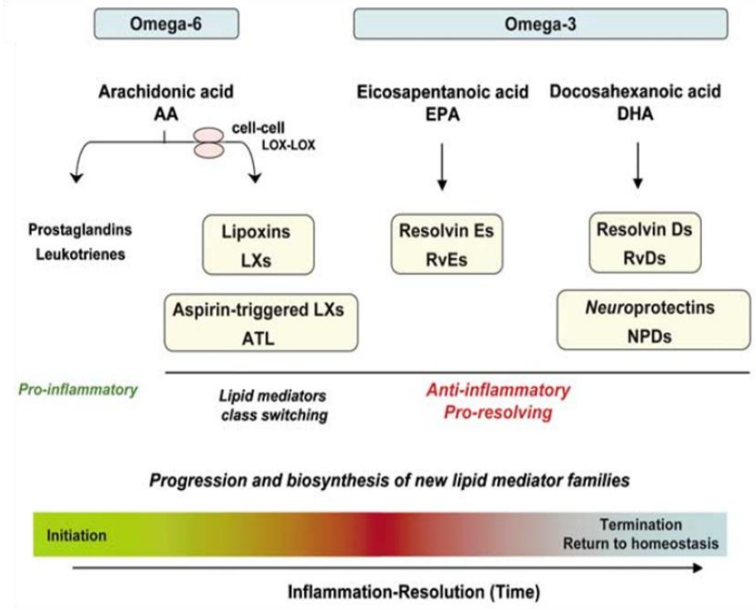

Figure 1.3. New families of PUFA-derived lipid mediators (from Serhan & Chiang 2008 [35]).

These mediators include n-6 (AA)-derived Lipoxins (LXs) and aspirin-triggered LXs (ATL); n-3 (EPA)-derived Resolvin E-series (RvEs); (DHA)-derived Resolvin D-series (RvDs) and Protectins (PDs).

1.3 N-3 PUFA, diet and cancer

Many studies have demonstrated that genetic factors contribute only for 5% to the onset of cancer, while 95% is due to environmental conditions factors, including lifestyle-related factors (tobacco, alcohol and physical activity), external stimuli (radiation and infections) and diet that represents about 30–35% of the risk factors **[36]**. Indeed, for the past few decades, epidemiologic studies have suggested a relationship between dietary lipids and development/progression of cancer **[37]**. Specific dietary fatty acids, such as n-3 PUFAs, have been suggested to play a key role. In fact, PUFAs are important for the normal development and function of the organism, and are essential in maintaining human health. There are *in vitro* and *in vivo* evidences that the DHA and EPA administration is able to reduce cancer proliferation and to increase apoptosis **[38,39]** as well as inhibit angiogenesis and metastasis, and to influence cancer differentiation **[40,41]**.

This is a result of various pathways including, for example, inhibition of AA metabolism and independent effects on various cytokines involved in tumourigenesis. These data suggest that PUFAs can show a potential antitumor activity representing an effective adjuvant in cancer chemotherapy, and improve a few of the secondary complications associated with cancer, like cachexia **[42]**. Moreover, the efficacy of various cancer chemotherapy drugs, such as doxorubin, **[43,44]**, tamoxifen **[45]**, and mitomycin C **[46]**, and of radiation therapy **[47]** has been increased, when the n-3 PUFAs were included in the diet of rodents or in cell culture medium. Several molecular mechanisms have been proposed for the anticancer activity of n-3 PUFAs, including

inhibition of cell proliferation, enhancement of apoptosis and anti-angiogenic action **[38,48]**.

Moreover, new mechanisms are frequently reported as we gain additional knowledge of the regulation of gene expression by FAs. For these reasons, it is likely that suppression of tumor cell growth is related to the combination of different mechanisms instead than a single, unique activity that is the main mechanism of action.

1.4 Mechanisms of Action of n-3 PUFAs in cancer

The multiple actions of n-3 PUFAs appear to involve multiple mechanisms that connect the cell membrane, the cytosol, and the nucleus. For some actions, n-3 PUFAs appear to act via receptors or sensors, so regulating signaling processes that influence patterns of gene expression. Moreover, n-3 PUFAs seem to involve changes in cell membrane FA composition. Changing membrane composition can in turn affect membrane order, lipid rafts formation, intracellular signaling processes, gene expression, and the production of both lipid and peptide mediators **[49]**.

Some of the mechanisms proposed for the action of n-3 PUFAs include:

- suppression of AA-derived eicosanoid biosynthesis;
- influences on transcription factor activity and gene expression;
- alteration of estrogen metabolism;
- increased or decreased production of free radicals and reactive oxygen species;
- mechanisms involving alterations of cell membrane fluidity and structure.

Inhibition of AA– derived eicosanoid biosynthesis

The eicosanoids are short-lived, hormone-like bioactive lipid mediators with chain lengths of 20 carbons associated with inflammation. They include different classes of substances: Prostaglandins (PGs), Prostacyclins, Thromboxanes (TXs) and Leukotrienes (LTs). AA, EPA and DHA are the endogenous precursors for the biosynthesis of eicosanoids. The synthesis of eicosanoids begins with the release of PUFAs from the sn-2 position of membrane phospholipids by the action of the enzyme phospholipase A2. Thereafter, these PUFAs are metabolized by two major enzyme pathways: Cyclooxygenases (COX), Lipoxygenases (LOX) or cytochrome P450 monooxygenases. The COX give rise to prostaglandins and thromboxanes, whereas the LOX produce LTs and lipoxins. The relative proportions of PUFAs in cell membranes are the primary factors in regulating of eicosanoid that will be generated. Because the major PUFA in cell membranes is AA, most eicosanoids produced will be of the 2-series prostanoids (PGs and TXs) and of the 4-series leukotrienes. AA-derived eicosanoids, such as prostaglandin E2 (PGE2), leukotriene B4 and thromboxane A2, have promoting effects in cancer cell growth, angiogenesis, and invasion **[50]**. For example, PGE2 promotes tumor cell survival by inhibition of apoptosis and stimulation of cell proliferation. If n-3 PUFAs are included in the diet and are incorporated into cell membranes, they can inhibit the biosynthesis of AA-derived eicosanoids. This effect is achieved at several levels. N-3 PUFAs can partially replace AA into membrane phospholipids, thereby decreasing the availability of AA precursors and favoring the biosynthesis of EPA-

derived eicosanoids. Moreover, they can suppress COX-2 and compete with n-6 PUFAs for COX to form eicosanoids. N-3 PUFAs compete with n-6 PUFAs for desaturases and elongases, and n-3 PUFAs have greater affinities for the enzymes than n-6 PUFAs. Thus, a higher intake of n-3 PUFAs reduces the desaturation and elongation of LA to AA and thus the production of AA-derived eicosanoids **[51]**. Finally, as discussed above EPA and DHA can also be metabolized to resolvins and protectins.

These compounds possess immune-regulatory actions and it is well documented that inflammation plays an important role in the development of numerous human malignancies, including cancer. Thus one other possible mechanism for inhibition of tumor growth by n-3 PUFAs is the resolution of inflammation process through production of these immune-regulatory compounds.

Influence on transcription factor activity and gene expression

PUFAs and their metabolites can modulate gene expression acting as ligand to nuclear receptors such as Peroxisome Proliferator-Activated Receptors (PPARs) and Nuclear transcription Factor κB (NF-κB).

Peroxisome Proliferator-Activated Receptor

PPARs are nuclear hormone receptors, and are composed of three isotypes: PPARα, PPARγ, and PPARδ. During recent years, the intensive study of PPARs has revealed their importance in both normal physiology and in the pathology of various tissues.

PPARs play an important role in the gene regulation involved in lipid metabolism including fatty acid transport and mitochondrial oxidation, inflammation and the development of atherosclerosis or diabetes **[52]**. Moreover, they are involved in proliferation and differentiation of cancer, for example, an increase of PPARα mRNA has been found in rat mammary gland carcinomas **[53]**.

The involvement of PPARs in cancer has been examined using synthetic pharmacological PPAR agonists. K.Y. Kim *et al.* **[54]** have showed that PPARγ activation may induce the inhibition of cell proliferation. In particular, they have investigated the effects of two different PPARγ agonists, rosiglitazone and KR-62980, on MCF-7 breast cancer cells. Their results showed an up-regulation of tumor suppresor PTEN with a decrease of Akt phosphorylation. Moreover, in PTEN knockdown cells, the actions of both agonists are abolished, indicating a key role of PTEN in the anti-proliferative effects of PPARγ activation. These results suggest that PPARγ activation may cause the inhibition of cell proliferation by apoptosis, indicating a potential role of PPARγ agonists in breast cancer therapy. PPARs are activated by non-covalent binding of both exogenous and endogenous ligands (**Table 1**), including n-3 PUFAs and various eicosanoid mediators.

N-3 PUFAs alter PPARs cell signaling by acting as direct ligands for the receptors. DHA has been shown to modulate PPAR receptor expression, induce cellular apoptosis and inhibit cell growth **[55]**. Zand *et al.*, have demonstrated that DHA induces apoptosis in Reh and Ramos cells and the apoptotic effect of DHA is regulated through PPARγ. Furthermore, they have found that DHA increase the expression of p53 protein in Reh cells in a PPAR-γ-dependent manner.

The up-regulation of p53 protein induces apoptosis in Reh cells, through the activation of caspases 9 and 3, suggesting a role for p53 in DHA-mediated apoptosis process. These data may suggest a new signaling pathway, DHA-PPAR-c-p53, in regulating the apoptotic effect of DHA in Reh cells **[56]**.

Exogenous PPAR ligands		**Endogenous PPAR ligands**	
PPAR α	**PPAR γ**	**PPAR α**	**PPAR γ**
WY-14.643	Indomethacin	Palmitic acid	Arachidonic acid
Clofibrate	Ibuprofen	Stearic acid	Eicosapentaenoic acid
Gemvibrozil	Piroxicam	Palmitoleic acid	PGJ2
Nafenopin	Pioglitazon	Oleic acid	15 deoxy PGJ12
Bezafibrate	Ciglitazon	Linoleic acid	
	Englitazon	Arachidonic acid	
	BRL-49653	Eicosapentaenoic acid	

Table 1. Exogenous and endogenous PPARs ligands (from Vavrušová *et al.*, 2002 [52]).

Rovito *et al.*, have showed that two ethanolamide derivatives from DHA and EPA, namely Docosahexaenoyl Ethanolamine (DHEA) and Eicosapentaenoyl Ethanolamine (EPEA), are able to reduce cell viability in MCF-7 breast cancer cells.

Their results showed that DHEA and EPEA treatment can enhance PPARγ expression, confirmed by the increased expression of its target gene PTEN, the inhibition of AKT-mTOR pathways and the induction of phosphorylation of Bcl-2 in MCF-7 breast cancer cells, whereas they did not elicit any effects in MCF-10A non-tumorigenic breast epithelial cells. In summary, their data showed that the two n-3 ethanolamides exert anti-proliferative effects by inducing autophagy in breast cancer cells highlighting their potential use as breast cancer preventive and/or therapeutic agents **[57]**.

Moreover, recent studies on human breast cancer showed that n-3 PUFAs can up-regulate Syndecan 1 (SDC-1) synthesis by PPARγ transcriptional pathway [57]. SDC-1 is the major proteoglycan expressed on the surface of mammary epithelial cells and known to regulate many biological processes, including cell-cell adhesion and growth factor signaling **[59]**. Sun and coworkers have studied effects of n-3 PUFAs on SDC-1 expression in human mammary cell lines. In particular, they have observed that the treatment with n-3–PUFAs significantly increased the expression of SDC-1 mRNA. The activation of PPARγ determines up-regulation of SDC-1 target gene, inducing apoptosis (**Figure 1.4**) **[60]**.

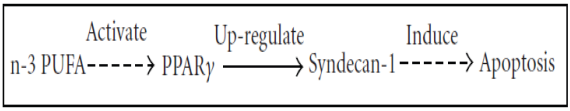

Figure 1.4. The syndecan-1 pathway for n-3 PUFA induction of apoptosis (from Edwards & O'Flaherty 2008 [58]).

Dashed lines indicate that effects may be indirect with involvement of other metabolites and signaling molecules.

Nuclear transcription Factor κB (NF-κB)

NF-κB is one of the most complex transcription factors. At quiescence state, NF-κB forms homo- or heterodimer usually located in the cytoplasm associated with an inhibitor protein (IκB). Upon stimulation by extracellular signals (i.e. inflammatory cytokines and oxidative stress) IκB is phosphorylated via kinases allowing dissociation from NF-κB. Phosphorylated IκB is degraded through the ubiquitination–proteasome pathway, while the active NF-κB dimer is translocated to the nucleus **[61]**. Abundant data support a key role for NF-κB signaling pathway in cell cycle activation, apoptosis, and carcinogenesis. In particular, the constitutive activation of NF-κB appears to play a role in controlling the initiation and progression of human cancer **[62]**. A large variety of extracellular signals are known to activate NF-κB and then the expression of 200 responsive genes **[63]**, including cytokines and other proteins implicated in inflammation, such as COX-2, and inducible NO synthase **[63]**, that are likely to promote the oncogenic phenotype (**Figure 1.5**).

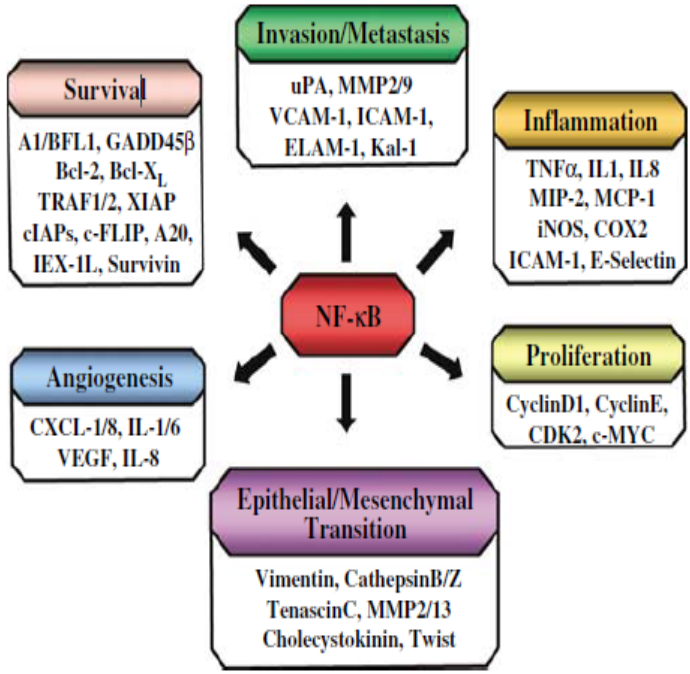

Figure 1.5. NF-κB dependent targets involved in different aspects of oncogenesis (from Basse`res and Baldwin 2006 [65]).

The regulation of the activity of pro-inflammatory transcription nuclear factor NF-κB is an important therapeutic effect of the major n-3 PUFAs, EPA and DHA. Activation of NF-κB and the PPAR-Bcl-2 feedback loop may control the life-death continuum in colon cells and can be further associated with the expression of COX-2.

Suppression of the activation of NF-κB by DHA reduces the production of pro-proliferative eicosanoids formed by COX-2 and also decreases the production of other NF-κB–induced cytokines that promote cancer cell growth. DHA, decreasing NF-κB activity, also sensitizes tumour cells to gamma irradiation and induction of apoptosis **[66]**. Moreover, Novak *et al.*, in their experimental study, have showed that n-3 PUFAs can inhibit the activation of NF-κB in LPS-stimulated macrophage. In particular, they have demonstrate that a mechanism for pro-inflammatory cytokine inhibition in murine macrophages by n-3 PUFAs is mediated, in part, through inactivation of the NF-κB signal transduction pathway and secondary to inhibition of IκB phosphorylation **[67]**.

Alterations of cell membrane fluidity and structure

The plasma membrane is involved in many aspects of cell biology, including proliferation, differentiation and apoptosis. Fatty acids in the cell membrane phospholipids (PLs) of cell membranes play a key role in maintaining the fluidity, structure and function of the membrane. Thus, changes in membrane PLs fatty acid composition can influence the function of cells. In particular, n-3 PUFAs incorporated into membrane PLs can potentially affect a variety of plasma membrane physical properties including membrane thickness, fluidity, elasticity, permeability, structure and function of membrane microdomains (lipid rafts) and alteration of cell signaling pathways that lead to altered transcription factor activity and changes in gene expression **[68]**.

Here I will concentrate on the effect of DHA on membrane structure and function, with a major focus on membrane microdomains. In mammals DHA levels are not homogeneously distributed. DHA is found in high concentration only in select tissues, such as the retinal rod outer segment, sperm and neurons. DHA can approach 50 mol% of the total PL acyl chains in these membranes. In contrast to the few tissues containing high levels of DHA, there are other tissues where DHA is often found below 5 mol% of the total phospholipid acyl chains. In low-DHA tissues, the PUFA-content can be influenced by dietary supplementation with foods rich in this n-3 FA. Probably the health benefits of DHA result from its incorporation into membranes that normally exhibit low levels of this PUFA **[69]**. *In vitro* studies have demonstrated that DHA can be taken up into cells and incorporated into plasma membrane PLs. Corsetto *et al.*, **[39]** have observed that DHA is incorporated in breast cancer cell membrane with different specificity for the PLs moiety. In particular, the results showed that the concentration of DHA increases especially in PE (about 6,3 fold), in PI (about 7,5 fold) and in PC (about 26,6 fold) in MDA-MB-231 cells, while the DHA exposure of MCF7 cells determines the increase of DHA especially in PC (about 11,9 fold), in PE (about 8 fold) and in PS (about 7,3 fold). Moreover, they have demonstrated that the treatment with DHA determines a reduction of cell proliferation, inhibition of EGFR activity and induction of apoptotic process, suggesting that these effects might be the consequences of cell membrane alterations induced by FAs.

"Lipid rafts are small (10–200nm), heterogeneous, highly dynamic, sterol- and sphingolipid-enriched domains that compartmentalize cellular processes.

Small rafts can sometimes be stabilized to form larger platforms through protein-protein and protein-lipid interactions." **[70]**. The composition of lipid rafts is important for their function. There are literature evidences that the administration of DHA is able to modify the lipid rafts composition, in particular SM, Chol and raft-associated signaling proteins content, altering the lipid rafts function. The Chapkin laboratory assessed the effect of n-3 PUFAs on rafts lipid composition in multiple cell types, such as immortalized young adult mouse colonocytes (YAMC) and mouse splenic T-cells. In particular, they have evaluated the effects of n-3 PUFAs administration on Chol and SM content. Their results have showed a reduction of Chol (46%) and SM (30%) in YAMC and mouse splenic T-cells fed n-3 PUFAs, respectively **[71]**. Several reports have shown that the incorporation of n−3 PUFAs into lipid rafts may alter the localization and function of raft-associated signaling proteins by inducing changes in physical properties **[72]**. The Chapkin laboratory showed that dietary n-3 PUFAs are capable of displacing acylated proteins from lipid raft both *in vivo* and *in vitro* models. Feeding mice a diet enriched in n-3 PUFAs and treating immortalized young adult mouse colonocytes (YAMC) with DHA decreased the localization of H-Ras in lipid raft domains. Upon further examination of the effect of n-3 PUFAs on localization of lipid raft proteins in colonocytes, their lab found that DHA inhibited the plasma membrane targeting of lipidated proteins, including H-Ras, suggesting that changes in membrane lipid composition directly influence the intracellular trafficking and subcellular localization of lipidated proteins **[72]**.

In MDA-MB-231 breast cancer cell line, Altenburg & Siddiqui, observed that n-3 PUFAs exposure resulted in a partial displacement of the chemokine receptor CXCR4 from lipid rafts. In particular, the treatment with n-3 PUFAs resulted in reduced surface expression of CXCR4, but had no effect on overall CXCR4 expression. CXCR4-mediated signaling and migration requires thus the cholesterol-rich membrane microdomains. Treatment with n-3 PUFAs disrupted the membrane microdomains in a manner similar to methyl-β-cyclodextrin, suggesting that DHA, due to its incompatibility with Chol, could be the cause of the distruption of lipid rafts, with a partial displacement of CXCR4 **[73]**.

The localization of Epidermal Growth Factor Receptor (EGFR) in lipid rafts is believed to be crucial for downstream receptor signaling controlling proliferation and apoptosis, which in turn could be altered by n-3 PUFA incorporation. Many experimental data have showed in several cell types that administration of n-3 PUFAs, in particular DHA, can exclude EGFR proteins from lipid raft, suppressing the activation of several downstream pathways, including ERK1/2, Akt and Fatty Acid Synthase (FASN) protein **[74-76]**.

Chapkin *et al.,* investigated the mechanistic link between EGFR function and DHA, both *in vivo* and *in vitro*. In particular, using YAMC cells, they observed that DHA induces shift of EGFR localization within the plasma membrane modifying the ability of the receptor to dimerize and trans-phosphorylate. In addition, DHA antagonizes the EGF-induced activation signaling by increasing receptor internalization and its degradation, and suppressing several downstream pathways, including Erk1/2 and STAT3.

Moreover, they showed that feeding a DHA-enriched diet resulted in an increase in EGFR phosphorylation and a suppression of Erk1/2 and STAT3 activation in mouse colonic epithelium.

These data suggest that EGF/Ras/Erk signaling might be disrupted in DHA-treated cells by the exclusion of EGFR protein from lipid rafts **[77]**.

Chapter 2

Microdomain organization in cell membranes

2.1 The plasma membrane

The plasma membrane defines the outer perimeter of the cell and maintains separate the inner part of the cell and the outer environment. This simple fact allows at the plasma membrane to act as a selective permeable barrier between the cell and the extracellular environment regulating as well the transport of water, ions and other molecules.

In 1925, Gorter & Grendel **[78]** observed that, in aqueous solutions, the lipids of red blood cells (RBC) were capable of forming bilayers, this basic organizing principle of lipid self-aggregation remains the oldest still valid molecular model of cellular structures. Only in 1972, the nature of this molecular organization as a bilayer of amphipathic phospholipids was elucidated. Thanks to electron microscopy images, Singer & Nicolson proposed the "fluid mosaic" model of biological membranes **[79]**. As a key property, Singer & Nicolson assigned to the lipid bilayer a certain degree of fluidity. In fact, at physiological temperature, the phospholipids (PLs) fatty acyl chains are in a fluid phase. Thus, the cellular membrane appears to be a two-dimensional solutions of integral membrane proteins in a lipid bilayer solvent **[80,81]**, allowing the lateral movement of membrane components. Because such movements are lateral or rotational, the fatty acyl tails remain in the hydrophobic core of the membrane.

Occasionally, PLs can also migrate from one leaflet of the membrane to the other, in a so called flip-flop movement which involves a head-tail inversion. However, flip-flop movements are energetically unfavorable because the polar head of a PL must be transported through the central hydrophobic interior of the membrane.

The membrane components can be organized in a non-homogeneous lateral distribution, leading to obtain the "ordered structures that differ in lipid and/or protein composition from the surrounding membrane", defined "membrane domains". The existence of membrane domains with different molecular composition and supermolecular organization is linked to the multiple important roles played by biological membranes. Indeed, the biological membrane has to serve as a matrix for the organization of multimolecular interactions that are dynamic in time and space such as the signaling transduction pathways **[82]**.

The basic matrix of eukaryotic plasma membrane is the lipid bilayer containing mainly amphipathic lipids such as glycerophospholipids (GPLs) and sphingolipids (SLs) and cholesterol (Chol). GPLs are the major structural lipids in cellular membranes, and include phosphatidylserine (PS), phosphatidylethanolamine (PE), phosphatidylinositol (PI), and phosphatidylcholine (PC). Their hydrophobic portion is a diacylglycerol (DAG), which contains saturated or cis-unsaturated fatty acyl chains of varying lengths. PC accounts for >50% of all cell membrane phospholipids, is the main bilayer-forming lipid. It self-organizes spontaneously as a planar bilayer in which each PC has a nearly cylindrical molecular geometry, with the lipidic tails facing each other and the polar headgroups interfacing with the aqueous phase. Most PC molecules have one cis-unsaturated fatty acyl chain, which renders them fluid at room temperature **[83]**. The SLs constituite another class of structural lipids.

They are defined as a category by the presence of amine-containing lipid backbones, the so-called sphingoid bases, which are represented by sphingosine, the major sphingoid base found in mammals. Free sphingoid bases are typically present in very small amounts because most are amide-linked with a long- or very-long-chain fatty acid to form ceramides (Cer) that can be further derivatized by addition of a headgroup (at C1) to form more complex sphingolipids such as sphingomyelin (SM), glucosylceramide (GlcCer), galactosylceramides (GalCer) and more complex glycosphingolipids (GSLs), such as gangliosides (sialic acid-containing GSLs) **[84]**. Although SLs are minor components of plasma membrane of mammalian cells, their local concentration can be high. Indeed, they are particularly abundant in certain cells and tissues such as the myelin sheath and neurons. Generally SLs adopt a solid "gel" phase, but are fluidized by sterols, which preferentially interact with them in the membrane. Because of their preferential interaction with Chol, SLs are enriched in the external side of the plasma membrane **[85]**. SLs have saturated (or trans-unsaturated) tails so they are able to form taller and narrower cylinders with respect to PC lipids of the same chain length and they pack more tightly. Moreover, SLs have extensive hydrogen-bonding capabilities which together with their saturated nature facilitate the formation of SLs-enriched lateral domains in membranes. The major SLs in mammalian cells are SM and the GSLs, which contain mono-, di-oligosaccharides based on GlcCer **[86]**.

Gangliosides are typical components of neuronal plasma membranes. The first ganglioside structure, that of ganglioside GM1, was elucidated by Kuhn & Wiegand **[87]**. Complex GLs serve as adhesion sites for proteins and carbohydrates from the extracellular matrix and neighboring cells.

Additionally, GLs modulate the function of the proteins on the same cell an often cited example is the inhibition of the Epidermal Growth Factor (EGF) receptor tyrosine kinase by ganglioside GM3, which has been suggested to be due to a glycan–glycan interaction involving multivalent GlcNAc termini on the EGF receptor **[88]**.

Sterols are the major non-polar lipids of cell membranes, and Chol predominates in mammalian cell (typically accounts for 20–25% of the lipid molecules). The unique puckered four-ring structure of Chol confers special biophysical properties that increase the ordering (cohesion and packing) of neighbouring lipids. Because of the rigid sterol backbone, Chol is preferentially positioned in close proximity to saturated hydrocarbon chains of neighbouring lipids, as these are more inflexible and elongated compared with those of unsaturated lipids **[89]**. This increased lateral ordering of lipids consequently affects the biophysical properties of the membrane, by decreasing fluidity and reducing the permeability of polar molecules.

There is a remarkable lipid asymmetry in the lipid composition of the two mono layers of the plasma membrane bilayer. In particular, the outer leaflet is enriched in SM, PC and Chol, while the inner leaflet is enriched in PS, PI, and PE.

2.2 Lipid rafts

Today, the view on biological membranes has gradually evolved from the "fluid mosaic" model of the early 1970s to the “membrane microdomains” concept. The “membrane microdomains” hypothesis proposes that the lipid bilayer is not a structurally passive solvent, but that the preferential association between SLs, sterols, and specific proteins confers cell membranes with lateral segregation potential.

This concept whereby the membrane lipids can be organized in macro- and microdomains was introduced in 1982 **[90]**. Subsequently, in 1988, Simons and van Meer proposed a new concept that describes the formation of glycosphingolipid-cholesterol microdomains or “rafts” that function as transport carriers for protein and lipid from the trans-Golgi network (TGN) to the apical membrane of polarized epithelial cells. Briefly, in epithelial cells the plasma membranes are polarized into apical, enriched in SLs (GLs and SM), and basolateral, enriched in PC, **[91,92]** domains.

The components of these apical and basolateral domains are immiscible because of the diffusion barrier formed by the tight junction that separates the domains. Simons & Van Meer observed in epithelial MDCK cells that the delivery and sorting of newly synthesized SLs takes place in the TGN and that these lipids are preferentially sorted to the apical membrane **[93]**. The hypothesis postulated that favorable molecular interactions induce the formation of cholesterol-sphingolipid-enriched domains, referred to as “lipid rafts”, within the plasma membrane **[94]**.

Moreover, the difference in each membrane protein's affinity for raft and non-raft lipid species regulates their localization within the plasma membrane, and, consequently, its proximity to potential binding partners.

One subset of lipid rafts is found in cell surface invaginations called caveolae. These flask-shaped plasma membrane invaginations were firsty identified on the basis of their morphology by Palade and Yamada in the 1950s. Caveolae are formed from lipid rafts by polymerization of caveolins-hairpin-like palmitoylated integral membrane proteins that tightly bind cholesterol. They have been implicated in endocytosis of albumin and other proteins across the endothelial monolayer. Moreover, they also function during signal transduction, but they are not absolutely required as several cell types that lack caveolin, such as lymphocytes and neurons, can nevertheless signal through rafts **[95]**.

"Lipid rafts" were initially proposed to function in sorting and transport of lipids and proteins as well as in signal transduction **[94]**. During the past two decades, the concept of "lipid rafts" has become extremely popular among cell biologists, and these structures have been suggested to be involved in a great variety of cellular functions and biological events, and the definition of a "lipid raft" has been revised. Today, "lipid rafts" are defined as small, dynamic, ordered domains of cholesterol, sphingolipids, and specific proteins that may combine into larger structures due to lipid–lipid, lipid–protein, and protein–protein interactions that are hypothesized to exist in the plasma membranes of eukaryotic cells **[96,97]**.

2.2.1 *Lipid phase behavior and raft formation*

Under physiological conditions, lipid bilayers exist in a liquid disordered (Ld) phase, upon cooling below the melting point, the lipid acyl chains are frozen in an solid-ordered phase (So) where their mobility is restricted. However, because of the high concentration of Chol in the plasma membrane, a third physical phase, the liquid ordered (Lo) phase **[98]**, can be observed. In the Lo state, acyl chains of lipids are extended and tightly packed. In this sense, the Lo state is similar to the gel state, and lipids that favor gel state formation, and thus have a high melting temperature (Tm) in the absence of Chol, tend to form the Lo state in the presence of Chol.

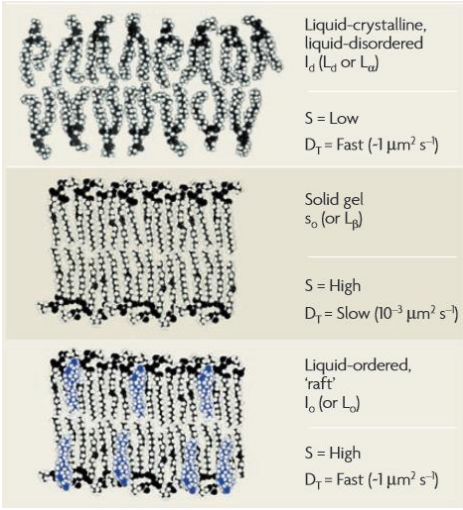

Figure 2.1. Lipid phases in membranes (from van Meer *et al.*, 2008 [83]).

On the other hand, lateral diffusion in the Lo state appears to be almost as rapid as in the fluid Ld state (**Figure 2.1**). Thus, in a sense the Lo state has properties intermediate between gel and Ld states **[99]**. The "lipid rafts" structure appears to arise from the phase separation of a Ld phase and a cholesterol-rich Lo phase. The first, non-rafts phase consists mainly of the unsaturated lipid and is depleted of Chol; the second, raft-like phase is enriched in both Chol and high Tm lipids such as SM **[100]**.

The membrane lipids are highly heterogeneous in their hydrophobic portions: GPLs contain unsaturated acyl chains that ensures the fluidity of biological bilayers, while, SLs (e.g. SM) have long and saturated acyl chains and this allows them to be tightly packed with a high degree of order in the hydrophobic core of a bilayer, obtaining much higher Tm than membrane PLs.

It is now clear that tight acyl chain packing is a key feature of membrane microdomain organization **[101]**. In fact, the differential packing ability of SLs and phospholipids is most likely one of the major forces leading to phase separation in lipid mixtures, including bilayers.

The coexistence of domains in Lo and Ld phases has been extensively characterized. Studies of membrane model systems strongly suggest that lipids could laterally segregate in membranes under certain conditions, and could form distinct lipid domains with particular structural characteristics (i.e. a particular lipid phase). Early evidence of fluid phase separation was reported in the early 1970s by Phillips *et al.*, who evaluated lateral mixing of different PC species using differential scanning calorimetry (DSC) **[102]**.

Two phase coexistence in binary mixtures of a lipid with cholesterol was observed by Shimshick & McConnell who mapped out phase diagrams for lateral phase separation by using electron spin resonance (ESR) **[103]**. Moreover, using nuclear magnetic resonance (NMR), Schmidt *et al.*, have observed that sphingomyelin might form microdomains in biological membranes **[104]**. Gebhardt *et al.*, considered the known lipid compositional heterogeneity in biological membranes and predicted that lipid lateral segregation might occur under particular environmental conditions such as those that mimic a physiological state **[105]**.

More recently, using a variety of techniques, such as Fluorescence Resonance Energy Transfer (FRET), Deuterium-based Nuclear Magnetic Resonance (^{2}H-NMR) and Atomic Force Microcopy (AFM), it is possible to observe macroscopic (>200nm) or microscopic (<100nm) separation of Lo and Ld phases **[106]**. For example, donor-quenching FRET analysis shows nanoscale domain formation (a few tens of nm) in lipid bilayers with a similar composition to that of the outer plasma membrane, at physiological temperature **[107]**.

AFM has been extensively used for topographic characterization of membrane models, and in particular, for identification and visualization of lipid domains and phase transitions in monolayers and in supported lipid bilayers (SLBs) **[108]**. Tokumasu *et al.*, have observed that nanoscopic and microscopic domains can coexist under a range of composition mixtures at room temperature with or without cholesterol in membrane bilayers from a DLPC/DPPC/Chol **[109]**.

Yuan *et al.,* have studied the distribution of ganglioside GM1 in model membranes composed of ternary lipid mixtures (SM/Chol/DOPC) that mimic the composition of lipid rafts. Their results demonstrate that addition of GM1 to lipid monolayers leads to the formation of small ganglioside-rich microdomains, with lateral dimension in the order of a few tens of nm, that are localized preferentially in the ordered SM/Chol-rich phase **[110]**.

A number of lipid mixtures have been used to mimic the biophysical characteristics of rafts in membrane model systems. Recent studies have confirmed the importance of using natural raft mixtures rich in SM (synthetic 16:0 or natural), Chol and in some cases small amounts of the ganglioside GM1 compared to mixtures containing raft lipid "model" such as DPPC. Ternary mixtures designed to mimic the coexisting of raft and non-raft domains are usually composed of Chol, SM and unsaturated phospholipids (DOPC or POPC) **[111]**.

It is generally believed that the interaction of DOPC with the high melting lipid is so unfavorable that over an extensive region of composition space, phase separation of Ld and Lo occurs. Phase domains are macroscopic, and a single domain can extend also for some microns due to the effective local cholesterol concentration **[112-114]**. Indeed varying the Chol content from ~10% to 35% progressively increases the size of Lo domains from small (<20nm), through intermediate sizes (20–75 nm) detected by FRET imaging, to larger domains (>100 nm) that are visible by standard microscopy **[115]**.

Chol has important effects on phase behavior. In particular, in the Lo phase, cholesterol is preferentially positioned in close proximity to saturated hydrocarbon chains of the bilayer-forming lipid, as these are more inflexible and elongated compared with those of unsaturated lipids, so increasing the ordering (cohesion and packing) of neighbouring lipids **[82,101]**. Precisely how Chol drives the formation of the Lo phase remains unclear. Several schemes, derived from *in vitro* studies, have been generated to explain the mechanisms of Chol–lipid interactions (**Figure 2.2**).

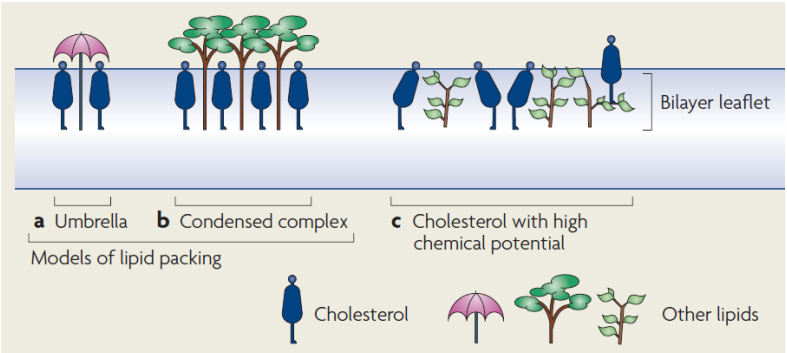

Figure 2.2. Models of cholesterol interactions with other lipids (from Ikonen 2008 [116].

In the "*condensed complex model*" McConnell *et al.*, have suggested that cholesterol can form reversible oligomeric chemical complexes with phospholipids. The formation of these complexes has been proposed to lead to the "condensing" effect of Chol, in the other words the surface area occupied by the PLs is decreased by interaction

with Chol **[117]**. While Huang & Feigenson have presented another model of Chol-phospholipid mixing: the "*umbrella model*" **[118,119]**. They propose a model in which non-polar Chol relies on the coverage of polar headgroups of the neighboring PL to prevent the unfavorable free energy of exposure of the non polar body part to water. Chol is generally regarded as a key lipid component of "lipid rafts" **[97]**. However, understanding the role of Chol in stabilizing membrane domains is hampered by the lack of precise information regarding its trans-bilayer distribution, which is largely asymmetric **[120]**. Importantly, in membranes that comprise appropriate mixtures of SM, unsaturated phospholipids and Chol, Lo and Ld phases can coexist **[115]**.

Model systems have greatly improved our understanding of the structure and function of cell membranes, but the membrane model does not reflect the complexity of the lipid environment or the interactions between lipids and proteins in a cell membrane. The main reason for this difference is that model systems are too simplistic to simulate all the chemical complexity of the cell membrane. Indeed, the plasma membrane contains a plethora of lipid-anchored and transmembrane proteins, is not a static platform and cannot be considered an equilibrated membrane. Moreover, there is a remarkable lipid asymmetry in the lipid composition of the two mono layers of the plasma membrane, and the cholesterol is excluded from the immediate vicinity of transmembrane proteins; therefore the local concentration of cholesterol will vary on a nanometer-length scale **[121]**. For these reasons, became particularly important the introduction of giant plasma membrane vesicles (GPMVs), microscopic spheres of plasma membranes harvested from live cells following chemical treatment **[122]**.

They are probably the closest models of cell plasma membranes in terms of chemical composition, as in addition to lipids they contain also membrane proteins. Fluid phase separation has been reported in giant GPMVs obtained from mast cells and fibroblasts **[123-125]**, from CHO-K1 **[126]**, RBL-2H3 **[127]** and A431 cells **[128]**.

For example, in a study of GPMVs composed of native pulmonary surfactant membranes, Bernardino de la Serna **[129]** observed by Fluorescence Microscopy (FM) and AFM under physiological conditions, that the native material showed the coexistence of two distinct micrometer sized fluid phases, ordered and disordered-like phases. Their results provide a clear example of the notion that specialized regions with particular lateral packing properties coexist in natural membranes and control specific molecular interactions in agreement with the raft hypothesis. Moreover, they have obtained evidence that at physiological temperature the observed lateral structure in native pulmonary surfactant membranes is dependent on the concentration of a few key lipid species. In particular, the phase separation is dramatically affected by the extraction of cholesterol, an effect not observed upon extraction of the surfactant proteins. These GPMVs offer an good opportunity to study the phase preference of lipids and proteins in complex biological membranes. However, even GPMVs are not perfect models of plasma membranes of live cells.

Recent studies suggest that the amount of Lo phase in plasma membranes of eukaryotic live cells can be significantly above 50% **[130],** while this is clearly not the case in GPMVs **[131]**.

Membrane models and giant plasma membrane vesicles show clearly separated microscopic domains of Lo/Ld phases, while in cell plasma membranes these domains have not been really observed except in some rare exceptions **[132,133]**. In particular, Gaus *et al.*, have directly visualized membrane lipid structure of living cells by using two-photon microscopy at physiological temperature. In particular, in macrophages, Lo domains were particularly enriched on membrane protrusions and cover 10-15% of the cell surface. Finally, by deconvoluting the images, they have demonstrated the existence of phase separation in vivo, thereby providing strong support for the lipid raft hypothesis **[132]**.

However, in live cells, the domains are probably too small and dynamic, so that only recently introduced super-resolution techniques may access these tiny enigmatic structures **[134,135]**.

2.2.2 *Lipid rafts isolated as Detergent-Resistant Membranes (DRMs)*

To biochemically demonstrate an association between the locally concentrated membrane proteins and lipids, Brown & Rose (Brown & Rose, 1992) described a simple detergent extraction method where they demonstrated that GPI-anchored proteins can be inserted in detergent-resistant membranes or DRMs. This was the first evidence supporting the "lipid raft" hypothesis of Simons & van Meer **[92]**.

These insoluble membranes appear to derive from cholesterol-sphingolipid-rich membrane microdomains (rafts) in the tightly packed Lo state. Furthermore, experiments on membrane models under the conditions used to extract cells show that monolayers and bilayers SM and Chol content are more resistant to solubilization by Triton X-100 than the pure membrane SM. Hydrogen bonding between cholesterol and SM may be important for this, and can provide a rational explanation for the detergent insolubility of DRMs **[136]**.

Thus, there is a close relation between rafts and DRMs, and isolation of DRMs is became one of the most widely used methods for studying lipid rafts.

The standard method of isolation of membrane rafts involves solubilization of the membrane at 4°C using the non-ionic detergent, typically Triton X-100. Due to their low relative density, due to of their high lipid-to-protein ratio, membrane rafts are separated by centrifugation on discontinuous or continuous sucrose gradients (usually DRMs are isolated in the low-density fractions corresponding to the 5% and 30% sucrose interface) **[137,138]**. Low-density detergent-insoluble fractions were isolated from a wide variety of cultured cells, including almost all the mammalian cell types **[139-141]**, yeast **[142]**, and plant cells **[143]**.

Analyses of this type of raft preparation have revealed a membrane domain of unique lipid composition. Thus Triton-X-100-resistant lipid rafts are distinguished from bulk plasma membrane because they are enriched in Chol and SLs, but are relatively depleted in GPLs **[144,145]**.

As report above (**section 2.2.1**), under physiological conditions, lipid bilayers exist in a Ld phase, upon cooling below the melting point, the lipid acyl chains are frozen in an solid-ordered phase (So) where their mobility is restricted. However, because of the high concentration of Chol in the plasma membrane, a third physical phase, the Lo phase can be observed. The L*o* phase is characterized by a high order degree of lipid acyl chains (as in the So phase), but with higher lateral mobility (characteristic of Ld phase). GPLs present in the membrane in a Ld phase are dissolved by treatment with non-ionic detergent at low temperature, and they are thus removed from the membrane through the formation of mixed detergent/lipid micelles **[146]**. While Lo phase components are insoluble in Triton X-100, and they remain thus laterally organized in microsome-like or planar structures, as shown schematically in **Figure 2.3 [147]**.

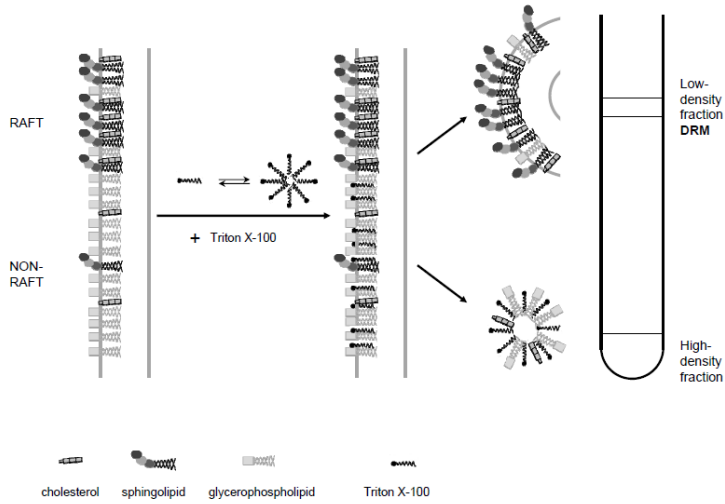

Figure 2.3. Insolubility of lipid raft components in the presence of Triton X-100 and preparation of DRMs (from Sonnino & Prinetti 2013 [82]).

Although Triton X-100 is the best characterized and most widely used detergent for DRM purification, other isolation procedures which involve the use of different detergents including Lubrol WX, Brij 96, Brij 98, Nonidet P40 and CHAPS have been used to prepare detergent resistant membrane domains **[148-151]**. The use of these different detergents in the preparation of rafts yields membrane domains with lipid compositions different from those of standard Triton-X-100-resistant membranes. For example, Schuck *et al.,* **[152]** observed that rafts prepared in Triton X-100 were strongly enriched in SLs and Chol as compared with total cell membranes, while, extraction with Tween 20, Brij 58 or Lubrol WX yielded low density membranes that showed relatively little enrichment in either of these traditional raft lipids.

Moreover, DRMs prepared with Brij 96 or Brij 98 were moderately enriched in Chol and SM. In conclusion, Schuck *et al.,* described these differences as being due to the "DRM selectivities" of the different detergents, where, Triton X-100 was the most selective, whereas Tween 20 and Brij 58 were the least selective. Moreover, use of mild detergents such as Brij 98 is preferable, compared with Triton X-100, because it has a reduced tendency to solubilise PLs localized in the inner leaflet or cause fusion of membrane fragments from different sources to form an amalgamated detergent-resistant membrane **[153]**. The observation that different detergents can lead to the isolation of DRMs with different composition suggests that there is some underlying heterogeneity among rafts that gives rise to these differences.

A variety of studies have suggested that detergent extraction (in particular Triton X-100) causes fusion of rafts, as well as lipid exchange between membranes **[154-156]**.

Heerklotz *et al.,* suggested that Triton X-100 could induce domain formation in POPC/SM/Chol raft model membrane system (otherwise miscible lipid mixtures). NMR and calorimetric measurements were used to follow micellization of lipids, an indication of membrane solubilization, as a function of temperature and Triton X-100 concentration and thermal transitions. Their results suggest that the large SM/Chol-rich domains isolated from detergent do not reliably report on the organization of these lipids in the cell membrane **[157]**. Nevertheless recent data demonstrated that Triton X-100 does not induce domain formation or increase the fraction of the bilayer in the ordered state, although it does increase domain size by coalescing pre-existing domains **[158]**.

These results have important implications for the reliability of Triton X-100 insolubility as a method to detect ordered domains. Another problem associated with the use of Triton X-100 is the possibility that of treatment with detergents might generate clusters of raft lipids and proteins that did not exist in the intact cells **[159]**. Cross-linking experiments showed that GPI-anchored proteins aggregate into large clusters in the presence of detergent, but not in its absence **[160]**.

To avoid the complications associated with preparing lipid rafts using detergent extraction procedures, several "detergent-free" methods have been established. Mcdonald & Pike **[161]**, developed a simplified and rapid method for the purification of detergent-free lipid rafts, starting from the protocols of Song *et al.,* and Smart *et al.,* **[162,163]**. Briefly, Chinese hamster ovary (CHO) and HeLa cells were lysed by passage through a needle. Lysates were centrifuged and the resulting postnuclear supernatant was mixed with an equal volume of buffer containing OptiPrep™. A 0% to 20% continuous OptiPrep™ gradient was poured on top of the lysate. The gradient was centrifuged for 90 min at 52,000 g and different fractions were collected. This method yields a membrane fraction that is highly enriched in cholesterol and protein markers of lipid rafts, with no contamination from non-raft plasma membrane or intracellular membranes. Other detergent-free methods have used sodium carbonate and OptiPrep™; magnetic bead; or silica-based isolations using raft/caveolar proteins as markers or the use of cationic buffers, which may stabilize raft-associated proteins **[164, 165]**.

These preparations seem to retain a greater fraction of inner leaflet membrane lipids **[144]** than DRM rafts and may therefore yield domains in which the coupling between raft leaflets is maintained. **[166-168]**. For these reasons, rafts prepared by non-detergent methods seem more likely to reproduce the *in vivo* composition of these microdomains accurately. Comparative analyses have shown that the compositions of DRM versus non-detergent membrane fractions obtained after cell lysis under different experimental conditions appear to be similar but not identical **[144]**.

The finding that non-detergent rafts are similar to some forms of detergent resistant rafts suggests that there is some overlap in the type of domain that is being isolated by these different methods. In particular, these results suggest that the highly ordered supramolecular structures corresponding to the native cores of lipid rafts can be isolated using these procedures, despite the procedures can alter the lateral order of biological membranes to some extent **[82]**.

Several reviews on the different methods of isolation of membrane lipid rafts are available for the interested reader **[169,170]**.

2.2.3 *The organization of proteins within the lipid rafts*

According to the lipid raft hypothesis, cholesterol- and sphingolipid-enriched domains can modulate protein–protein interactions, in particular, lipid rafts can include or exclude proteins, for this reason, they may be involved in the regulation of different cellular processes. While most of the cell membrane proteins are found in non-raft domains, some proteins are preferentially concentrated into the raft domains.

As examples include glycosylphosphatidylinositol-linked proteins (GPI), which are anchored to the outer leaflet of the membrane by the GPI anchor, palmitoylated/myristoylated proteins such as flotillins **[171]**, which are localized to the inner leaflet of the membrane and probably function as raft organizers. In addition, many proteins associated with rafts are receptors or proteins involved in signal transduction, such as the Epidermal Growth Factor Receptor (EGFR) **[95]**.

Post-translational modifications allow for rapid modulation of protein structure, localization, and function. An important class is lipid modifications, which includes the addition of saturated lipids or specific targeting sequence (e.g., a cholesterol-binding). The cellular purpose of protein lipidation is often to anchor the modified polypeptide to membranes. Several evidence suggest that a protein lipidation can increase the concentration of both, peripheral and transmembrane proteins within rafts, while short, unsaturated, and/or branched hydrocarbon chains prevent raft association **[172]**. The well-characterized examples of lipid modifications determining protein association with membrane rafts are GPI-anchored proteins.

Several experimental data confirm that GPI-anchored proteins are concentrated into lipid rafts by virtue of the interaction of their hydrophobic anchors with raft domains. Varma & Mayor using FRET showed that GPI-anchored folate receptors attached to a fluorescent folic acid analogue were clustered in domains of a size less than 70nm. Moreover, depleting the cell membrane of Chol resulted in a decreased FRET efficiency, consistent with an increased distance between folate receptors. Addition of Chol to the cell resulted in restoration of the proteins to ordered domains. These results confirmed that lipid-linked proteins are organized in Chol-dependent submicron sized domains **[173]**. An direct measure of component partitioning between coexisting fluid domains has been provided by observations of reconstituted proteins in model membranes containing a phase separating mixture of raft lipids (SM, an unsaturated phosphatidylcholine, and Chol). For example, GPI-AP Thy-1 reconstituted in model membranes showed a significant distribution into the model raft domain **[174]**. Similar results have been obtained observing GPI-AP placental alkaline phosphatase (PLAP) into a model bilayer; here PLAP partitioned into the ordered phase and this partitioning can be greatly enhanced by antibody-mediated oligomerization **[175]**.

Cysteine S-palmitoylation, another raft-targeting motif, can increase an affinity of protein for rafts **[176]**. Indeed, membrane proteins can be reversibly palmitoylated and can lose its raft association after depalmitoylation. Palmitoylation and rafts association were shown for Src-family of kinases (SFKs) Lck and its substrate Fyn **[177]**, for the T-cell transmembrane co-receptor CD4 **[178]** and for the cytotoxic T-cell co-receptor component CD8β **[179]**.

An important class of intracellular proteins whose raft association appears to be mediated by palmitoylation are GTP-binding switches, including small GTPases of the Ras family **[180]**. Prior *et al.,* combining detergent resistance, non detergent fractionation, antibody patching, and Electron Microscopy (EM) have showed that the doubly palmitoylated H-Ras was raft associated, whereas K-Ras, the non-palmitoylated isoform, was excluded from these microdomains **[168, 180]**.

2.2.3 *Lipid rafts and signal transduction: the EGFR pathway*

The lipid raft has become extremely popular and has been implicated in a wide variety of cellular functions and biological events **[181,182]** such as membrane trafficking, signal transduction, and regulation of the activity of membrane proteins **[95,183]**. As shows in **Table 2.1**, several classes of proteins, identified by biophysical, biochemical, and immuno-localization methods, and involved in signal transduction mechanisms, have been reported to be associated with lipid rafts.

Protein	Selected references
FcεRI receptor	40
T-cell receptor	47, 48
B-cell receptor	90
EGF receptor	35, 91
Insulin receptor	92
EphrinB1 receptor	93
Neurotrophin	94
GDNF	63, 65
Hedgehog	68
H-Ras	66
Integrins	95, 96
eNOS	97, 98

Table 2.1. Examples of protein components of lipid rafts (from Simons &Toomre 2000 [95]).

The EGFR is a 170 kDa transmembrane tyrosine kinase receptor. It is synthesized from a 1210 amino acid polypeptide precursor; after cleavage of the N-terminal sequence, an 1186-residue protein is inserted into the cell membrane. EGF receptors have a highly conserved extracellular binding domain, a single transmembrane lipophilic region, and a cytoplasmic tyrosine kinase domain **[184]**.

Several ligands, including EGF, transforming growth factor-alpha (TGF-α), epiregulin (EPR) and betacellulin bind and activate the EGFR receptors **[185]**.

Upon ligand binding, EGF receptors form homo or heterodimers that, following trans-phosphorylation of their intracellular tyrosine kinase domains, recruit signaling proteins, such as Shc, Grb7, Grb2, the phospholipase Cγ (PLCγ), the intracellular kinases Src and PI3K, responsible for the initiation of several signaling pathways. These intracellular signaling cascades result in alterations of gene expression, which determine the biological response to receptor activation.

The EGFR signaling has multiple routers, as shown in **Figure 2.4**. The two major downstream signalling pathways includes the Ras/Raf/mitogen-activated protein kinase (MAPK) for proliferation and the phosphatidylinositol 3-kinase (PI3K)/Akt for survival **[186-188]**.

The Ras/Raf/mitogen-activated protein kinase (MAPK) pathway is well-characterised. This begins with the recruitment of Grb2, that can bind either directly to the phosphorylated EGFR. Grb2 is constitutively bound to the Ras exchange factor Sos and is normally localized to the cytosol. Relocation of the Grb2/Sos complex to the receptor at the plasma membrane facilitates the interaction of membrane-associated Ras with Sos, resulting in activation of Ras via the exchange of its associated GDP with GTP. Ras in turn activates the serine/threonine kinase Raf-1, which leads to the activation of the MAPK pathway.

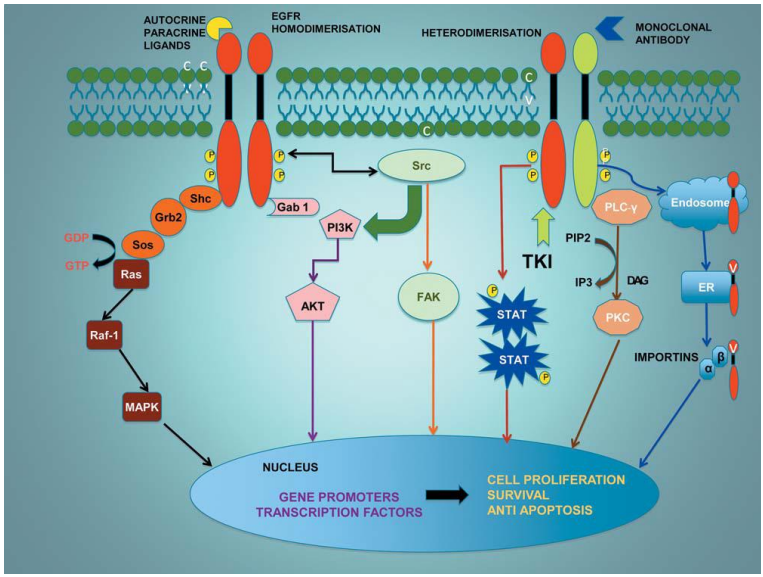

Figure 2.1. EGFR signaling (from Ayyappan *et al.*, 2013 [189]).
Intracellular signaling pathways include RAS/ Raf-1/ MAPK, PI3K/AKT, PLCγ/PKC pathways which require the adaptor molecules for signaling. Src and STAT pathways are directly activated by phosphorylated receptors.

This involves the phosphorylation of MEK (MAPKinase) and the activation and translocation of Erk1 and Erk2 to the nucleus, where they phosphorylate transcription factors, such as Elk, stimulating cell proliferation and motility **[190]**. Another EGFR signaling pathway, is the PI3K/Akt pathway. PI3K can be activated by K-Ras or by EGFR itself. PI3K phosphorylates phosphatidylinositol 4,5-bisphosphate (PIP2) to phosphatidylinositol 3,4,5-trisphosphate (PIP3) that stimulates the activity of serine/threonine kinase Akt (also known as protein kinase B) by binding to its Pleckstrin Homology (PH) domain.

Akt can phosphorylate proteins such as CREB (cAMP response element binding protein), pro-caspase-9, BAD and is involved in the regulation of apoptosis, gene expression, cell proliferation migration and angiogenesis **[191,192]**. As mentioned above, lipid rafts are enriched in Chol, SLs, and saturated FAs, characterized by higher order, that function as signaling platforms **[95,96]**. The ability of EGFR to activate downstream pathways is its localization in lipid raft domains of the plasma membrane **[193-195]** probably due to co-localization with downstream mediators within lipid rafts. In addition, disruption of lipid rafts results in the re-localization of EGFR to bulk membrane regions, which alters EGFR activation and signaling **[77]**. EGFR is an important mediator of cancer cell proliferation, differentiation and survival; indeed, overexpression or activation of EGFR has been strongly linked to the etiology of several human cancers, including esophago-gastric **[189]** and breast cancer **[196]**.

Chapter 3

Atomi Force Microscopy: a biophysical tool to visualize lipid rafts

3.1 Developments in microscopy

A growing need for techniques to study the basis of essential processes for life in even greater detail were developed in the last decades. A wide variety of biochemical techniques is now available to allow a functional study of the molecular origin of these processes. However, there are only a limited number of tools available to study the structure of biomolecules, which are generally only few µm large. Conventional optical microscopes use light beams to image objects. Their spatial resolution is limited by the used wavelengths. For this reason it is not possible to visualize the structure of individual biomolecules and their complexes. X-ray scattering techniques have contributed a lot to the structural determination of biomolecules. Using these techniques, Crick and Watson discovered the DNA double helix structure in 1954, thanks to the analysis of the crystal diffraction pattern **[197].** Nowadays a great number of biomolecules have been structurally resolved with atomic resolution using X-ray crystallography. Unfortunately these techniques usually resolve only an average crystal structure, neglecting the dynamics of molecular processes. Moreover, not all proteins can be crystallized. The hydrophilic environment of crystallization can also modify the physiological conformation of the protein, which happens in the case of transmembrane proteins.

In 1960, the invention of the Electron Microscope (EM), allowed the observation of nanometer-sized objects such as DNA, proteins and other biological macromolecules.

However, because the biological matter is transparent compared with an electron beam, the sample must be frozen, fixed, dried, and/or processed to gain contrast prior to imaging. The use of these invasive treatments limits the possibility of applying this technique to study samples in physiological conditions as well as to study the dynamic processes. Many other techniques were also developed to obtain more information regarding the dynamics of biological processes such as the molecular motion, conformational changes and interaction receptor-ligand. Some examples are the use of optical dichroism studies to measure molecular motion, and fluorescence quenching experiments to get information about the interaction of proteins. Obviously, all these techniques offer information about few, very specific aspects of the system under study. Moreover, the biological system must be prepared (and often denatured) in order to make it accessible to a particular method of analysis. In microscopy, many invasive sample preparations can be found, such as drying of the samples for EM investigations and metal coating in the case of Scanning Electron Microscopy (SEM) imaging.

The imaging and the manipulation of molecules at the atomic scale have been a dream become true at the early 80's with a new revolutionary kind of microscopy known as Scanning Probe Microscopy (SPM). SPM, a branch of non-optical microscopy, has rapidly evolved into a family of powerful techniques able to visualize the sample surface with high resolution, down to the level of molecules and groups of atoms, in three dimensions.

A wide variety of materials, including biological systems, can be measured and many surface properties that other microscopes cannot see, can be studied by SPM.

SPM uses no light or focused electrons, but rather an extremely sharp tip (10-50nm radius of curvature) mounted on a flexible cantilever, allowing the tip to follow the surface profile. The interactions between the tip and the atoms composing the sample surface can be recorded and processed to form 3D image of sample surface. The invention of the Scanning Tunneling Microscopy (STM) in 1982 by Binnig *et al.*, at the IBM Zurich Research Laboratory allowed to study surfaces of solid materials at atomic scale **[198]**, imaging individual atoms and molecules. For this reason, the developments in SPM have led to the birth of a new techniques such as Atomic Force Microscopy (AFM) and Near-field Scanning Optical Microscope (NSOM).

Today, new high-resolution imaging methods (*e.g.* Fluorescence Resonance Energy Transfer (FRET), Fluorescence Correlation Spectroscopy (FCS) and Stimulated Emission Depletion (STED) Microscopy have allowed advances in the membrane research, such as evaluation of lipid–lipid and lipid–protein interactions in the cell bilayer. The use of these new high-resolution imaging methods to study membrane microdomains are extensively described in a recent review **[82,97]**.

3.2 Atomic Force Microscope (AFM)

AFM was developed in a collaboration between IBM Zurich Research Laboratory and Stanford University in 1986 by Binnig, Quate & Gerber **[199]**. The success of AFM has been its capability to overcome the main drawback of the STM technique, namely the requirement to have a conductive surface. AFM is now the most versatile branch of Scanning Probe Microscopy (SPM) to study samples regardless of their conductive properties. AFM is able to collect 3D topography images with high lateral and vertical resolutions, in the order of nanometre, without any sample preparation such as fixation, staining, or labeling. In addition, AFM can visualize samples in air and liquid without the need to operate under vacuum. AFM can analyze almost any type of surface: ceramics, polymers, synthetic and biological membranes, biological macromolecules like nucleic acids and proteins, cells and tissues, metals, glass and semiconductors.

Since its invention, the number of publications related to AFM has increasing constantly, and the instrument is now a fundamental tool in several fields of research, from biochemistry to biology, from materials science to engineering, in studies of the most varied phenomena, such as characterization of nanostructures and molecules **[200]**, surface elasticity **[201**], and friction **[202]**. In biological field, in the last 20 years, AFM has been used to visualize cells, membranes and smallest biomolecules, such as proteins, phospholipids, RNA and DNA under near-physiological conditions **[203-206]**.

Besides imaging, AFM allowed to measure mechanical properties of biological samples like elasticity and stiffness and it has been used for manipulation of individual biomolecules **[207-210]**.

3.2.1 *Functional principles*

Traditional microscopes use electromagnetic radiation, such as photon or electron beams, to create an image. On the contrary AFM is a mechanical imaging instrument that collects three-dimensional topography images as well as physical properties of a surface with a thin probe. **Figure 4.1** shows a typical AFM set up composed of a cantilever-tip assembly and an optical detector to evaluate the cantilever bending induced by the forces interacting between the tip and the sample surface. The sample is scanned in three-dimensions (X,Y,Z) by the AFM probe with angstrom precision.

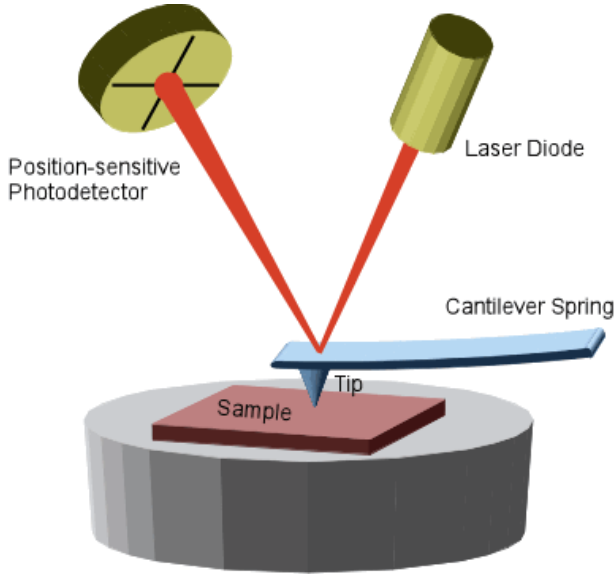

Figure 4.1. Scheme of an Atomic Force Microscope (AFM).
It shows the scanning probe, the piezo electric scanner and the laser deflection system.

The AFM heart is the scanning probe, composed of a tip, mounted at the end of a flexible cantilever (**Figure 4.2**). The tip is the part that interacts directly with the sample, and is used to scan its surface, senses the topographical variations of the sample surface, and generates three dimensional images.

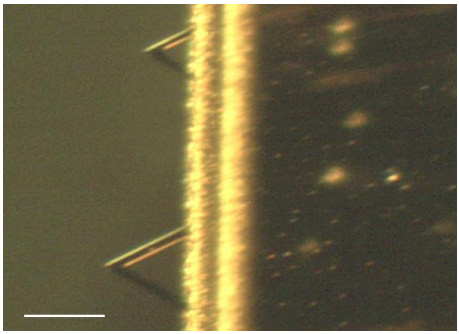

Figure 3.2. AFM probe.
In particular the picture shows a V-shaped cantilever. Scale bar: 200nm.

In 1986, Binnig *et al.*, built the first AFM tip-cantilever system based on a tiny shard of diamond glued at the end of a rectangular strip of gold foil **[199]**. This construction allowed to resolve lateral features as small as 30nm. The structural resolution of AFM depends strongly on the sharpness of the tip **[211]** and therefore the technical developments have been focused on improving the performances of this component. The ideal AFM tip should have a high aspect ratio (ratio between height and width of the tip) with a radius of curvature as small as possible, a pyramidal or conical geometry which makes the terminal point of the tip very sharp in order to be able to penetrate in small pits of the surface. Moreover, it should be mechanically and chemically robust so that its structure is not altered while imaging in air or fluid environments.

Today, the typical tip-cantilever assembly is micro-fabricated from silicon (Si) or silicon nitride (Si_3N_4). The tips are pyramidal in shape with cone angles of 20–30° and radius of curvature of 5–10nm (Si) or 20–60nm (Si_3N_4).

The cantilevers are mainly of two shapes: rectangular and V-shaped **[212]**. Moreover, their were coated with a thin layer of gold on the backside (the one not in closest proximity with the sample) to enhance its reflectivity.
The cantilever should have:

- a relatively low spring constant, typically between 0.1 and 10N/m, enabling to measure a deflection caused to a small force;
- high resonance frequency to minimize the sensitivity of the cantilever to mechanic vibrations of low frequency (around 10-100kHz);
- high lateral stiffness to reduce the effect of lateral forces.

To describe the topography of the sample, the tip is raster scanned over the object surface, and the cantilever deflection is simultaneously recorded. Interaction forces between the tip and the sample surface cause a vertical deflection of the cantilever according to Hooke's law:

$$F = k\,x$$

where k is the spring constant of the cantilever (N/m), and x the cantilever vertical deflection (nm).

The interaction forces are evaluated using the force curves, which reflect the relationship between the cantilever deflection and the vertical movements of the cantilever.

The cantilever deflection is measured by an optical detection system like optical lever method, with sub-angstrom sensitivity **[213,214]**. The scanning over an uneven surface causes the cantilever deflection, which is measured by focusing a laser beam on the back of cantilever and its upward and downward deviations are collected on a rotating mirror and into a position sensitive detector (PSD, **Figure 4.3**). The direction of the reflected laser beam is sensed by the PSD, which is typically divided in four quadrants, as illustrated in **Figure 4.3**. The optical lever is a mechanical amplifier which is able to increase the movements of the tip generating an extremely high sensitivity. The sensitivity of this detection system is in the order of 10^{-3} Å/$(Hz)^{1/2}$, both for deflection and torsion of the cantilever **[215]**. Using this method, the vertical deflection of the cantilever can be monitored. In particular, when the cantilever is in rest position, the reflected laser beam should be centred on the PSD (red spot in **Figure 4.3**). During the scanning, the vertical deflection of the cantilever, due to attractive or repulsive interactions of the tip with the sample surface, causes a vertical shift of the beam spot on the PSD (occupying the position indicated in blue in **Figure 4.3**).

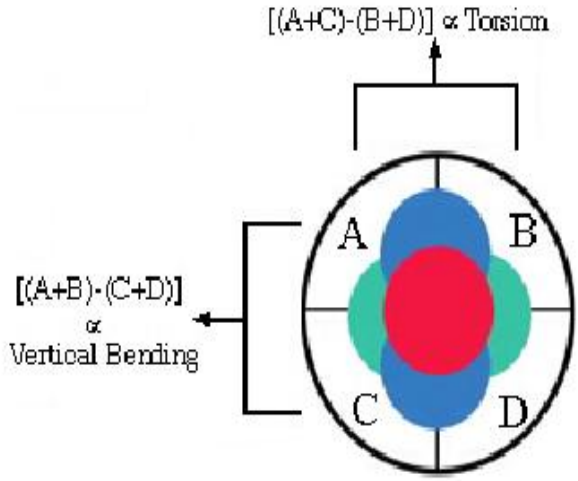

Figure 4.3. Position sensitive detector (PSD) divided in four quadrants A, B, C and D, employed in the optical detection method.

Moreover, the optical detection system allows measuring frictional forces acting on the tip **[216]**: these are manifested in a lateral shift of the laser beam spot (green spots in **Figure 4.3**). The vertical or lateral movements of the laser spot are detected by calculating the differences of the signal due to the different quadrants of the PSD. The differences in signal in the vertical and horizontal direction are proportional to the vertical and torsional deflection of the cantilever respectively.

3.2.2 *AFM imaging mode*

AFM can operate in different imaging modes that depend on the region of the force field between tip and sample as schematically shown in **Figure 4.4**.

"Contact mode" has been the first imaging mode developed in AFM where the cantilever is placed few Ångstrom far from the sample surface **[199]**. During the scanning, the tip is constantly in contact with the sample, and the repulsive interaction forces (i.e. Coulomb forces) determine the cantilever deflection. The cantilever deflection is proportional to the topographical variations of the sample surface **[217]**. In contact mode AFM can be operated in either *height* or *deflection mode*. When operated in *height mode*, the system monitors the changes in piezo-vertical position, producing an accurate three-dimensional image also called "topography" image of the sample surface.

When operated in *deflection mode*, the z-piezo remains stationary, while the deflection data, determined by the movement of the laser on the photodetector in response to topographical changes, are recorded to form sample surface. The resulting images are called "deflection" or "error signal" images. Images produced in *error signal* do not give quantitative information in the z-direction, but often are very useful for direct imaging of the small corrugations on the sample surface. *Contact mode* can operate in air, but the ambient humidity is sufficient to create a thin water layer on sample surface causing capillary forces between tip and sample.

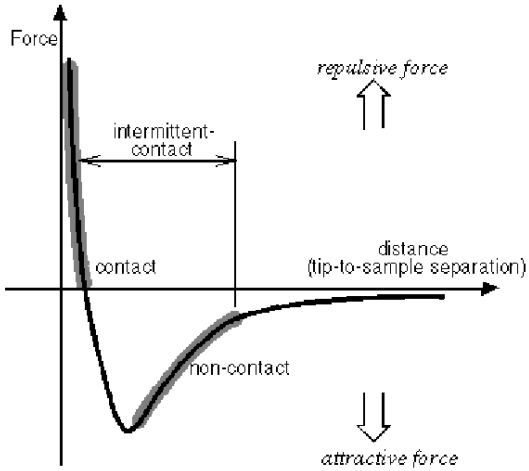

Figure 4.4. Diagram illustrating the force regimes under which the most common AFM imaging operate.

The capillary forces are attractive forces (10^{-8}N), which keep the tip in contact with the sample surface. Because of this effect, the control on applied pressures in AFM imaging performed in *contact mode* in air is limited, which is a problem especially with soft biological samples. The total force exerted by the tip on the sample can be reduced, operating under aqueous environment, even of one order of magnitude compared with air **[218]**. The imaging in solutions has become very popular because it is potentially less destructive to soft samples. *Contact mode* is typically used to obtain nanometre resolution images to flat, hard and stable samples, such as 2D protein crystals.

A drawback of the *contact mode* is the presence of strong lateral forces derived from the lateral movement of the tip in contact with the sample. This problem is particularly evident for the biological samples, which are easily damageable. To overcome this problem another mode of imaging, *non-contact* and *intermittent modes*, have been developed. The magnitude of the forces applied to the sample by the AFM tip can be further reduced by applying *non-contact* mode **[219,220]**. This mode operates by bringing a probe, which is vibrating at its resonant frequency, into the attractive force region (within 10nm to the sample). It does not come into physical contact with the surface, but is able to detect force gradients as it is raster scanned across the surface by either shifts in the resonant frequency or amplitude of the cantilever.

Non-contact mode is desirable as it allows to investigate the sample topography with a complete lack of sample damage. However, the long range attractive forces that operate between the sample and probe are relatively low and less sensitive to probe-sample separation as such, images obtained from this imaging mode inevitably display a lower spatial resolution. A reduction of lateral forces can be achieved imaging the sample using *intermittent* or *tapping mode* **[221]**.

Tapping mode allow to study soft materials as biological samples. It uses an oscillating cantilever at its resonance frequency, placed near the sample surface, and only at the end of each oscillation cycle the tip interacts with the surface. Because the tip is not continuously in contact with the surface, both tip and sample degradations are minimized.

While the tip is moved towards the surface, a feedback system constantly adjusts the z-piezo to maintain the amplitude of the freely oscillating probe as a constant pre-set value **[222]**. The measured vertical displacements allow high resolution topography images of the sample surface to be reconstructed. The main advantage of this mode, as compared to the contact mode, is that lateral forces and friction are reduced. Hence, the oscillation mode is particularly convenient for AFM imaging of soft and weakly sample, such as living cells, biological membranes, proteins and DNA, both in air and in solution **[223-226]**.

3.3 Tools to detect lipid rafts

In 2007, K. Jacobson, O. Mouritsen and R. Anderson published a review entitled ‘‘Lipid rafts: at a crossroad between cell biology and physics”. They stated that ‘‘. . the physical tools to study biological membranes as a liquid in space and time are still being developed…and the development of new tools are needed to understand the dynamic heterogeneity of biological membranes. . .” **[227]**. Studying lipid rafts is challenging since they are too small and elusive to be resolved by techniques such as optical and fluorescence microscopy.

Electron microscopy (EM) allows the ultra-high spatial resolution necessary for the investigation of membrane lateral heterogeneity at the nanoscale. Using immunogold-EM and colloidal gold particles linked to anti-GSL antibodies has been possible observed that GSLs form clusters at the cell surface **[228,229]**.

This method allows, observing the distribution of colloidal gold particles, to estimate average lipid raft size and the total membrane area occupied by lipid rafts.

On the other hand, this method requires sample manipulation, such as the use of organic solvents and/or chemical fixatives that do not allow to preserve the in situ localization of membrane lipids **[230]**. A freeze-fracture replica labeling method can overcome some of the disadvantages of conventional immuno-EM, allowing quantitative analysis of the distribution of membrane lipids at a nanometer scale. In this method, living cells without pretreatment are flash-frozen, later the fractured membrane is coated by a thin layer of carbon and platinum via vacuum evaporation, fixing the membrane components **[231]**. This method has allowed to observe the distribution of GM3 and GM1 into indipendent clusters (<100 nm diameter) at the cell surface **[232]**. EM, allowed the observation of nanometer-sized biological macromolecules, however, because the biological matter is transparent compared with an electron beam, the sample must be frozen and/or fixed to gain contrast prior to imaging.

The use of these invasive treatments limit the possibility of applying this technique to study samples in physiological conditions as well as to study the dynamic processes.

Today, high-resolution techniques that utilize fluorescent probes are available for studies of membrane heterogeneity in intact cells, allowing the study of small and elusive microdomains *in vivo* (**Table 2**) **[82,233,234]**.

Some of these techniques are particularly appealing because of their capability to reveal the dynamics of membrane domains.

Technique	Primary observable(s)
Fluorescence correlation spectroscopy (FCS)	Translational mobility of fluorophore
Fluorescence renonance energy transfer (FRET)	Donor-acceptor proximity
Stimulated emission depletion (STED) microscopy	Time traces of single molecule diffusion of a fluorescence-labeled probe at the nano-scale

Table 2. High-resolution techniques for detecting and characterizing membrane microdomains.

The basic idea behind Stimulated Emission Depletion (STED) microscopy is the spatially selective deactivation of fluorophores, preventing their participation in image formation. Briefly, a laser beam that excites fluorescence, that is, which switches fluorescence ON, is focused onto a small (diffraction-limited) spot.

Scanning this spot over the sample and detecting the fluorescence for each scanning position permits the reconstruction of an image by providing the spatial distribution of the fluorescent-labeled molecules. The addition of a second laser beam that switches off the fluorescence emission permits the observation of spots of nanoscopic size **[235, 236]**.

This technique can be applied to investigate the ultrastructural organization of living cells, for example, for to test the lipid raft hypothesis.

The Eggeling laboratory, using STED microscopy, showed for the first time a non-invasive imaging of lipid molecules and proteins with high spatial resolution within the membrane in live cells. In particular, they have demonstrated that lipid raft markers, such as GPI-anchored proteins, SM, and GM1, were confined into membrane areas with diameters about 20nm. These complexes were transient and had an average lifespan about 10^{-2}sec. The complexes appeared to be Chol-dependent, as the trapping was reduced upon Chol depletion **[134,237]**.

Photoactivated Localization Microscopy (PALM) is another powerful approach for investigating protein/lipid organization. Combining pair-correlation analysis with PALM provided a method to analyze complex patterns of protein organization across the plasma membrane demonstrating a distinct nanoscale organization of plasma membrane proteins with different membrane anchoring and lipid partitioning characteristics in COS-7 cells as well as dramatic changes in GPI-anchored protein arrangement under varying perturbations **[238,239]**.

Moreover, PALM imaging proved that Chol- and SL-enriched microdomains occupy different regions on the plasma membrane with lateral dimensions in the order of a hundred of nanometers **[240]**. In the super-resolution fluorescence microscopy, the major limitation is the necessity of using fluorescent probes or fluorescence-tagged antibodies against the target molecule, with the problems related to the use of probes, such as the generation of artifacts *e.g.*, the multivalency of the

probe (as in the case of anti-glycolipid antibodies, which are usually IgM), chemical modifications introduced in the marker molecule, or the use of an extrinsic label **[127]**.

3.3.1 *AFM to study lipid rafts*

In the past decade, the AFM has emerged as a powerful tool to obtain nano-structural details and biomechanical properties (such as stiffness and viscoelasticity) of soft and fragile materials such as proteins and lipids, which is more challenging because of the easy deformability of the samples. AFM is unique in that it allows to study biological structures, using buffer solutions, in order to study functional complexes, to monitor their dynamic changes and to understand the range of conformations underlying different functions. Compared with Scanning Electron Microscopy (SEM), AFM provides extraordinary topographic contrast, direct height measurements and, not requiring a metal coating of the sample, in situ views of surface features. AFM has some advantages also on Transmission Electron Microscopy (TEM), principally the capability to obtain three dimensional images without cumbersome sample preparation and to yield far more complete information than the two dimensional profiles available from cross-sectioned samples. AFM operating in physiological-like conditions and providing nanometer spatial resolution without fixation, staining, or labeling, appears to be a powerful tool to quantitatively perform a morpho-dimensional characterization of lipid rafts **[241]**. AFM has been employed to study structure and dynamics of lipid rafts based on model membranes **[109,242,243]**.

Rinia *et al.,* used AFM to study supported lipid bilayers, consisting of PE, SM and Chol. They observed domains which the morphology and size depended on the cholesterol concentration.

Moreover, they showed the resistance of domains against non-ionic detergent. This study shows that it is possible to directly visualize SM/cholesterol domains and their resistance to detergent using AFM, illustrating the usefulness of this technique in raft studies **[244]**. Moreover, the change, at the nanometer level, of the lipid rafts in model membranes treated with Triton X-100 has been observed by Real-time AFM. This work indicates that AFM is a unique tool to investigate the structure of biological membranes in situ **[245]**.

The Le Grimellec laboratory have studied the interactions between GPI-anchored alkaline phosphatases (AP-GPI) and rafts models using AFM. Their data showed that AP-GPI molecules inserted in membrane models can be easily imaged by AFM, in physiological buffer. In particular, they have observed that AP-GPI were generally observed in the most ordered domains of model membranes under phase separation, (i.e. presenting both fluid and ordered domains). This direct access to the membrane structure at a mesoscopic scale provides direct evidence for the temperature-dependent distribution of a GPI protein between fluid and ordered membrane domains. Moreover, these data strongly suggest that, within a membrane, subclasses of different GPI proteins can colocalize in subsets of microdomains enriched in sphingolipids and cholesterol **[246]**.

The use of AFM to study membrane microdomains in supported planar lipid bilayers (SLB) is extensively described in a recent review by **[247]**.

Recently, Cai *et al.*, **[248]** have directly confirmed the existence of lipid rafts in native erythrocyte membranes using in situ atomic force microscopy. Their results indicate that most of the lipid rafts have lateral dimension in the order of hundred nm with irregular shape.

Moreover, the Chol content contributes significantly to the formation and stability of the protein domains. Finally Band III is an important protein of lipid rafts in the inner leaflet of erythrocyte membranes, indicating that lipid rafts are exactly the functional domains in plasma membrane. This work provides evidence of the presence of lipid rafts at a resolution of a few nanometers, which will might open the way for studying their structure and functions in detail.

However, AFM studies on whole cell are much more difficult to execute. In particular, intact membranes often contain numerous structures, many of which may be indistinguishable by AFM. It is difficult to obtain well-flattened and fixed plasma membrane samples as required to achieve the highest possible resolution in AFM. Furthermore, cell surfaces are covered by a cellular matrix consisting of proteins, proteoglycans, making direct access to the lipid surface difficult. Nonetheless, the application of AFM to live cells is holds promise.

References

1. Russo GL: **Dietary n-6 and n-3 polyunsaturated fatty acids: from biochemistry to clinical implications in cardiovascular prevention**. *Biochemical pharmacology* 2009, **77**(6):937-946.
2. Cunnane SC, Anderson MJ: **The majority of dietary linoleate in growing rats is beta-oxidized or stored in visceral fat**. *The Journal of nutrition* 1997, **127**(1):146-152.
3. Sprecher H: **Biochemistry of essential fatty acids**. *Progress in lipid research* 1981, **20**:13-22.
4. de Jesus Raposo MF, de Morais RM, de Morais AM: **Health applications of bioactive compounds from marine microalgae**. *Life sciences* 2013, **93**(15):479-486.
5. Sprecher H, Chen Q: **Polyunsaturated fatty acid biosynthesis: a microsomal-peroxisomal process**. *Prostaglandins, leukotrienes, and essential fatty acids* 1999, **60**(5-6):317-321.
6. Poudyal H, Panchal SK, Diwan V, Brown L: **Omega-3 fatty acids and metabolic syndrome: effects and emerging mechanisms of action**. *Progress in lipid research* 2011, **50**(4):372-387.
7. DeFilippis AP, Sperling LS: **Understanding omega-3's**. *American heart journal* 2006, **151**(3):564-570.
8. Simopoulos AP: **The omega-6/omega-3 fatty acid ratio, genetic variation, and cardiovascular disease**. *Asia Pacific journal of clinical nutrition* 2008, **17**:131-134.
9. Roynette CE, Calder PC, Dupertuis YM, Pichard C: **n-3 polyunsaturated fatty acids and colon cancer prevention**. *Clinical nutrition (Edinburgh, Scotland)* 2004, **23**(2):139-151.

10. Beare-Rogers JL, Gray L, Nera EA, Levin OL: **Nutritional properties of poppyseed oil relative to some other oils**. *Nutrition and metabolism* 1979, **23**(4):335-346.
11. Kromann N, Green A: **Epidemiological studies in the Upernavik district, Greenland. Incidence of some chronic diseases 1950-1974**. *Acta medica Scandinavica* 1980, **208**(5):401-406.
12. Dallongeville J, Yarnell J, Ducimetiere P, Arveiler D, Ferrieres J, Montaye M, Luc G, Evans A, Bingham A, Hass B *et al*: **Fish consumption is associated with lower heart rates**. *Circulation* 2003, **108**(7):820-825.
13. Whelton SP, He J, Whelton PK, Muntner P: **Meta-analysis of observational studies on fish intake and coronary heart disease**. *The American journal of cardiology* 2004, **93**(9):1119-1123.
14. Barrett SJ: **The role of omega-3 polyunsaturated fatty acids in cardiovascular health**. *Alternative therapies in health and medicine* 2013, **19**:26-30.
15. Casula M, Soranna D, Catapano AL, Corrao G: **Long-term effect of high dose omega-3 fatty acid supplementation for secondary prevention of cardiovascular outcomes: A meta-analysis of randomized, double blind, placebo controlled trials**. *Atherosclerosis* 2013, **14(**2):243-251.
16. Erkkila AT, Lichtenstein AH, Mozaffarian D, Herrington DM: **Fish intake is associated with a reduced progression of coronary artery atherosclerosis in postmenopausal women**

with coronary artery disease. *The American journal of clinical nutrition* 2004, **80**(3):626-632.

17. Wu JH, Micha R, Imamura F, Pan A, Biggs ML, Ajaz O, Djousse L, Hu FB, Mozaffarian D: **Omega-3 fatty acids and incident type 2 diabetes: a systematic review and meta-analysis**. *The British journal of nutrition* 2012, **107**:S214-227.
18. Lin PY, Chiu CC, Huang SY, Su KP: **A meta-analytic review of polyunsaturated fatty acid compositions in dementia**. *The Journal of clinical psychiatry* 2012, **73**(9):1245-1254.
19. Dacks PA, Shineman DW, Fillit HM: **Current evidence for the clinical use of long-chain polyunsaturated n-3 fatty acids to prevent age-related cognitive decline and Alzheimer's disease**. *The journal of nutrition, health & aging* 2013, **17**(3):240-251.
20. Salari P, Rezaie A, Larijani B, Abdollahi M: **A systematic review of the impact of n-3 fatty acids in bone health and osteoporosis**. *Med Sci Monit* 2008, **14**(3):RA37-44.
21. Kelly OJ, Gilman JC, Kim Y, Ilich JZ: **Long-chain polyunsaturated fatty acids may mutually benefit both obesity and osteoporosis**. *Nutrition research* 2013, **33**(7):521-533.
22. Koletzko B, Lien E, Agostoni C, Bohles H, Campoy C, Cetin I, Decsi T, Dudenhausen JW, Dupont C, Forsyth S *et al*: **The roles of long-chain polyunsaturated fatty acids in pregnancy, lactation and infancy: review of current knowledge and consensus recommendations**. *Journal of perinatal medicine* 2008, **36**(1):5-14.

23. Rogers LK, Valentine CJ, Keim SA: **DHA supplementation: current implications in pregnancy and childhood**. *Pharmacol Res* 2013, **70**(1):13-19.
24. Calder PC: **Immunomodulation by omega-3 fatty acids**. *Prostaglandins, leukotrienes, and essential fatty acids* 2007, **77**(5-6):327-335.
25. Mehta LR, Dworkin RH, Schwid SR: **Polyunsaturated fatty acids and their potential therapeutic role in multiple sclerosis**. *Nature clinical practice* 2009, **5**(2):82-92.
26. Dyerberg J, Bang HO, Hjorne N: **Fatty acid composition of the plasma lipids in Greenland Eskimos**. *The American journal of clinical nutrition* 1975, **28**(9):958-966.
27. Bang HO, Dyerberg J, Hjoorne N: **The composition of food consumed by Greenland Eskimos**. *Acta medica Scandinavica* 1976, **200**(1-2):69-73.
28. Lee JH, O'Keefe JH, Lavie CJ, Marchioli R, Harris WS: **Omega-3 fatty acids for cardioprotection**. *Mayo Clinic proceedings* 2008, **83**(3):324-332.
29. Harris WS, Bulchandani D: **Why do omega-3 fatty acids lower serum triglycerides?** *Current opinion in lipidology* 2006, **17**(4):387-393.
30. Ueshima H, Stamler J, Elliott P, Chan Q, Brown IJ, Carnethon MR, Daviglus ML, He K, Moag-Stahlberg A, Rodriguez BL *et al*: **Food omega-3 fatty acid intake of individuals (total, linolenic acid, long-chain) and their blood pressure: INTERMAP study**. *Hypertension* 2007, **50**(2):313-319.

31. Morgan DR, Dixon LJ, Hanratty CG, El-Sherbeeny N, Hamilton PB, McGrath LT, Leahey WJ, Johnston GD, McVeigh GE: **Effects of dietary omega-3 fatty acid supplementation on endothelium-dependent vasodilation in patients with chronic heart failure**. *The American journal of cardiology* 2006, **97**(4):547-551.
32. Yashodhara BM, Umakanth S, Pappachan JM, Bhat SK, Kamath R, Choo BH: **Omega-3 fatty acids: a comprehensive review of their role in health and disease**. *Postgraduate medical journal* 2009, **85**(1000):84-90.
33. Elabdeen HR, Mustafa M, Szklenar M, Ruhl R, Ali R, Bolstad AI: **Ratio of pro-resolving and pro-inflammatory lipid mediator precursors as potential markers for aggressive periodontitis**. *PloS one* 2013, **8**(8):e70838.
34. Anderson P, Delgado M: **Endogenous anti-inflammatory neuropeptides and pro-resolving lipid mediators: a new therapeutic approach for immune disorders**. *Journal of cellular and molecular medicine* 2008, **12**(5B):1830-1847.
35. Serhan CN, Chiang N: **Endogenous pro-resolving and anti-inflammatory lipid mediators: a new pharmacologic genus**. *British journal of pharmacology* 2008, **153**:S200-215.
36. Baena Ruiz R, Salinas Hernandez P: **Diet and cancer: Risk factors and epidemiological evidence**. *Maturitas* 2013, **pii: S0378-5122**(13)00360-5.
37. Hardman WE: **Omega-3 fatty acids to augment cancer therapy**. *The Journal of nutrition* 2002, **132**:3508S-3512S.

38. Serini S, Piccioni E, Merendino N, Calviello G: **Dietary polyunsaturated fatty acids as inducers of apoptosis: implications for cancer**. *Apoptosis* 2009, **14**(2):135-152.
39. Corsetto PA, Montorfano G, Zava S, Jovenitti IE, Cremona A, Berra B, Rizzo AM: **Effects of n-3 PUFAs on breast cancer cells through their incorporation in plasma membrane**. *Lipids in health and disease* 2011, **12;10**:73.
40. Merendino N, Costantini L, Manzi L, Molinari R, D'Eliseo D, Velotti F: **Dietary omega -3 polyunsaturated fatty acid DHA: a potential adjuvant in the treatment of cancer**. *BioMed research international*, 2013, **2013**:310186.
41. Vaughan VC, Hassing MR, Lewandowski PA: **Marine polyunsaturated fatty acids and cancer therapy**. *British journal of cancer* 2013, **108**(3):486-492.
42. Colomer R, Moreno-Nogueira JM, Garcia-Luna PP, Garcia-Peris P, Garcia-de-Lorenzo A, Zarazaga A, Quecedo L, del Llano J, Usan L, Casimiro C: **N-3 fatty acids, cancer and cachexia: a systematic review of the literature**. *The British journal of nutrition* 2007, **97**(5):823-831.
43. Hardman WE, Moyer MP, Cameron IL: **Dietary fish oil sensitizes A549 lung xenografts to doxorubicin chemotherapy**. *Cancer letters* 2000, **151**(2):145-151.
44. Hardman WE, Avula CP, Fernandes G, Cameron IL: **Three percent dietary fish oil concentrate increased efficacy of doxorubicin against MDA-MB 231 breast cancer xenografts**. *Clin Cancer Res* 2001, **7**(7):2041-2049.

45. DeGraffenried LA, Friedrichs WE, Fulcher L, Fernandes G, Silva JM, Peralba JM, Hidalgo M: **Eicosapentaenoic acid restores tamoxifen sensitivity in breast cancer cells with high Akt activity**. *Ann Oncol* 2003, **14**(7):1051-1056.
46. Shao Y, Pardini L, Pardini RS: **Dietary menhaden oil enhances mitomycin C antitumor activity toward human mammary carcinoma MX-1**. *Lipids* 1995, **30**(11):1035-1045.
47. Colas S, Paon L, Denis F, Prat M, Louisot P, Hoinard C, Le Floch O, Ogilvie G, Bougnoux P: **Enhanced radiosensitivity of rat autochthonous mammary tumors by dietary docosahexaenoic acid**. *International journal of cancer* 2004, **109**(3):449-454.
48. Field CJ, Schley PD: **Evidence for potential mechanisms for the effect of conjugated linoleic acid on tumor metabolism and immune function: lessons from n-3 fatty acids**. *The American journal of clinical nutrition* 2004, **79**:1190S-1198S.
49. Calder PC: **Mechanisms of action of (n-3) fatty acids**. *The Journal of nutrition* 2012, **142**(3):592S-599S.
50. Lone AM, Tasken K: **Proinflammatory and immunoregulatory roles of eicosanoids in T cells**. *Frontiers in immunology* 2013, **4**:130.
51. Rose DP, Connolly JM: **Omega-3 fatty acids as cancer chemopreventive agents**. *Pharmacol Ther* 1999 **83**(3):217-44.
52. Ehrmann J, Jr., Vavrusova N, Collan Y, Kolar Z: **Peroxisome proliferator-activated receptors (PPARs) in health and disease**. *Biomedical papers of the Medical Faculty of the*

University Palacky, Olomouc, Czechoslovakia 2002, **146**(2):11-14.

53. Roberts-Thomson SJ, Snyderwine EG: **Characterization of peroxisome proliferator-activated receptor alpha in normal rat mammary gland and 2-amino-l-methyl-6-phenylimidazo[4, 5-b]pyridine-induced mammary gland tumors from rats fed high and low fat diets**. *Toxicology letters* 2000, **118**(1-2):79-86.
54. Kim KY, Kim SS, Cheon HG: **Differential anti-proliferative actions of peroxisome proliferator-activated receptor-gamma agonists in MCF-7 breast cancer cells**. *Biochemical pharmacology* 2006, **72**(5):530-540.
55. Wannous R, Bon E, Maheo K, Goupille C, Chamouton J, Bougnoux P, Roger S, Besson P, Chevalier S: **PPARbeta mRNA expression, reduced by n-3 PUFA diet in mammary tumor, controls breast cancer cell growth**. *Biochimica et biophysica acta* 2013, **1831**(11):1618-1625.
56. Zand H, Rhimipour A, Bakhshayesh M, Shafiee M, Nour Mohammadi I, Salimi S: **Involvement of PPAR-gamma and p53 in DHA-induced apoptosis in Reh cells**. *Molecular and cellular biochemistry* 2007, **304**(1-2):71-77.
57. Rovito D, Giordano C, Vizza D, Plastina P, Barone I, Casaburi I, Lanzino M, De Amicis F, Sisci D, Mauro L *et al*: **Omega-3 PUFA ethanolamides DHEA and EPEA induce autophagy through PPARgamma activation in MCF-7 breast cancer cells**. *Journal of cellular physiology* 2013, **228**(6):1314-1322.

58. Edwards IJ, O'Flaherty JT: **Omega-3 Fatty Acids and PPARgamma in Cancer**. *PPAR Res* 2008, **2008**:358052.
59. Edwards IJ, Sun H, Hu Y, Berquin IM, O'Flaherty JT, Cline JM, Rudel LL, Chen YQ: **In vivo and in vitro regulation of syndecan 1 in prostate cells by n-3 polyunsaturated fatty acids**. *The Journal of biological chemistry* 2008, **283**(26):18441-18449.
60. Sun H, Berquin IM, Edwards IJ: **Omega-3 polyunsaturated fatty acids regulate syndecan-1 expression in human breast cancer cells**. *Cancer research* 2005, **65**(10):4442-4447.
61. Perkins ND: **Integrating cell-signalling pathways with NF-kappaB and IKK function**. *Nature reviews* 2007, **8**(1):49-62.
62. Schwartz SA, Hernandez A, Mark Evers B: **The role of NF-kappaB/IkappaB proteins in cancer: implications for novel treatment strategies**. *Surgical oncology* 1999, **8**(3):143-153.
63. Gilmore TD: **Introduction to NF-kappaB: players, pathways, perspectives**. *Oncogene* 2006, **25**(51):6680-6684.
64. Sigal LH: **Basic science for the clinician 39: NF-kappaB-function, activation, control, and consequences**. *J Clin Rheumatol* 2006, **12**(4):207-211.
65. Basseres DS, Baldwin AS: **Nuclear factor-kappaB and inhibitor of kappaB kinase pathways in oncogenic initiation and progression**. *Oncogene* 2006, **25**(51):6817-6830.
66. Skender B, Vaculova AH, Hofmanova J: **Docosahexaenoic fatty acid (DHA) in the regulation of colon cell growth and cell death: a review**. *Biomedical papers of the Medical Faculty*

of the University Palacky, Olomouc, Czechoslovakia 2012, **156**(3):186-199.

67. Novak TE, Babcock TA, Jho DH, Helton WS, Espat NJ: **NF-kappa B inhibition by omega -3 fatty acids modulates LPS-stimulated macrophage TNF-alpha transcription**. *American journal of physiology* 2003, **284**(1):L84-89.
68. Wassall SR, Brzustowicz MR, Shaikh SR, Cherezov V, Caffrey M, Stillwell W: **Order from disorder, corralling cholesterol with chaotic lipids. The role of polyunsaturated lipids in membrane raft formation**. *Chemistry and physics of lipids* 2004, **132**(1):79-88.
69. Wassall SR, Stillwell W: **Docosahexaenoic acid domains: the ultimate non-raft membrane domain**. *Chemistry and physics of lipids* 2008, **153**(1):57-63.
70. Pike LJ: **The challenge of lipid rafts**. *Journal of lipid research* 2009, **50**:S323-328.
71. Turk HF, Chapkin RS: **Membrane lipid raft organization is uniquely modified by n-3 polyunsaturated fatty acids**. *Prostaglandins Leukot Essent Fatty Acids* 2013, **88**(1):43-7.
72. Biondo PD, Brindley DN, Sawyer MB, Field CJ: **The potential for treatment with dietary long-chain polyunsaturated n-3 fatty acids during chemotherapy**. *The Journal of nutritional biochemistry* 2008, **19**(12):787-796.
73. Altenburg JD, Siddiqui RA: **Omega-3 polyunsaturated fatty acids down-modulate CXCR4 expression and function in MDA-MB-231 breast cancer cells**. *Mol Cancer Res* 2009, **7**(7):1013-1020.

74. Rogers KR, Kikawa KD, Mouradian M, Hernandez K, McKinnon KM, Ahwah SM, Pardini RS: **Docosahexaenoic acid alters epidermal growth factor receptor-related signaling by disrupting its lipid raft association**. *Carcinogenesis* 2010, **31**(9):1523-1530.
75. Ravacci GR, Brentani MM, Tortelli T, Jr., Torrinhas RS, Saldanha T, Torres EA, Waitzberg DL: **Lipid raft disruption by docosahexaenoic acid induces apoptosis in transformed human mammary luminal epithelial cells harboring HER-2 overexpression**. *The Journal of nutritional biochemistry* 2013, **24**(3):505-515.
76. Lee EJ, Yun UJ, Koo KH, Sung JY, Shim J, Ye SK, Hong KM, Kim YN: **Down-regulation of lipid raft-associated onco-proteins via cholesterol-dependent lipid raft internalization in docosahexaenoic acid-induced apoptosis**. *Biochimica et biophysica acta* 2014, **1841**(1):190-203.
77. Turk HF, Barhoumi R, Chapkin RS: **Alteration of EGFR spatiotemporal dynamics suppresses signal transduction**. *PloS one* 2012, **7**(6):e39682.
78. Gorter E, Grendel F: **On Bimolecular Layers of Lipoids on the Chromocytes of the Blood**. *The Journal of experimental medicine* 1925, **41**(4):439-443.
79. Singer SJ, Nicolson GL: **The fluid mosaic model of the structure of cell membranes**. *Science (New York, NY* 1972, **175**(4023):720-731.

80. Jacobson K, Mouritsen OG, Anderson RG: **Lipid rafts: at a crossroad between cell biology and physics**. *Nature cell biology* 2007, **9**(1):7-14.
81. Coskun U, Simons K: **Membrane rafting: from apical sorting to phase segregation**. *FEBS letters* 2010, **584**(9):1685-1693.
82. Sonnino S, Prinetti A: **Membrane domains and the "lipid raft" concept**. *Current medicinal chemistry* 2013, **20**(1):4-21.
83. van Meer G, Voelker DR, Feigenson GW: **Membrane lipids: where they are and how they behave**. *Nature reviews* 2008, **9**(2):112-124.
84. Merrill AH, Jr.: **Sphingolipid and glycosphingolipid metabolic pathways in the era of sphingolipidomics**. *Chemical reviews* 2011, **111**(10):6387-6422.
85. van Meer G, de Kroon AI: **Lipid map of the mammalian cell**. *Journal of cell science* 2011, **124**:5-8.
86. van Meer G, Lisman Q: **Sphingolipid transport: rafts and translocators**. *The Journal of biological chemistry* 2002, **277**(29):25855-25858.
87. Sandhoff K, Harzer K: **Gangliosides and gangliosidoses: principles of molecular and metabolic pathogenesis**. *J Neurosci* 2013, **33**(25):10195-10208.
88. Merrill AH, Jr., Wang MD, Park M, Sullards MC: **(Glyco)sphingolipidology: an amazing challenge and opportunity for systems biology**. *Trends in biochemical sciences* 2007, **32**(10):457-468.

89. Simons K, Vaz WL: **Model systems, lipid rafts, and cell membranes**. *Annual review of biophysics and biomolecular structure* 2004, **33**:269-295.
90. Karnovsky MJ, Kleinfeld AM, Hoover RL, Dawidowicz EA, McIntyre DE, Salzman EA, Klausner RD: **Lipid domains in membranes**. *Annals of the New York Academy of Sciences* 1982, **401**:61-75.
91. van Meer G: **Lipid traffic in animal cells**. *Annual review of cell biology* 1989, **5**:247-275.
92. Rodriguez-Boulan E, Nelson WJ: **Morphogenesis of the polarized epithelial cell phenotype**. *Science (New York, NY* 1989, **245**(4919):718-725.
93. van Meer G, Simons K: **Lipid polarity and sorting in epithelial cells**. *Journal of cellular biochemistry* 1988, **36**(1):51-58.
94. Simons K, Ikonen E: **Functional rafts in cell membranes**. *Nature* 1997, **387**(6633):569-572.
95. Simons K, Toomre D: **Lipid rafts and signal transduction**. *Nature reviews* 2000, **1**(1):31-39.
96. Kraft ML: **Plasma membrane organization and function: moving past lipid rafts**. *Molecular biology of the cell* 2013, **24**(18):2765-2768.
97. Simons K, Sampaio JL: **Membrane organization and lipid rafts**. *Cold Spring Harbor perspectives in biology* 2011, **3**(10):a004697.
98. Ipsen JH, Karlstrom G, Mouritsen OG, Wennerstrom H, Zuckermann MJ: **Phase equilibria in the**

phosphatidylcholine-cholesterol system. *Biochimica et biophysica acta* 1987, **905**(1):162-172.

99. Heberle FA, Feigenson GW: **Phase separation in lipid membranes**. *Cold Spring Harbor perspectives in biology* 2011, **3**(4): a004630.
100. Risselada HJ, Marrink SJ: **The molecular face of lipid rafts in model membranes**. *Proceedings of the National Academy of Sciences of the United States of America* 2008, **105**(45):17367-17372.
101. Brown DA, London E: **Structure and function of sphingolipid- and cholesterol-rich membrane rafts**. *The Journal of biological chemistry* 2000, **275**(23):17221-17224.
102. Phillips MC, Ladbrooke BD, Chapman D: **Molecular interactions in mixed lecithin systems**. *Biochimica et biophysica acta* 1970, **196**(1):35-44.
103. Shimshick EJ, McConnell HM: **Lateral phase separations in binary mixtures of cholesterol and phospholipids**. *Biochemical and biophysical research communications* 1973, **53**(2):446-451.
104. Schmidt CF, Barenholz Y, Thompson TE: **A nuclear magnetic resonance study of sphingomyelin in bilayer systems**. *Biochemistry* 1977, **16**(12):2649-2656.
105. Gebhardt C, Gruler H, Sackmann E: **On domain structure and local curvature in lipid bilayers and biological membranes**. *Zeitschrift fur Naturforschung* 1977, **32**(7-8):581-596.
106. Hancock JF: **Lipid rafts: contentious only from simplistic standpoints**. *Nature reviews* 2006, **7**(6):456-462.

107. Silvius JR: **Fluorescence energy transfer reveals microdomain formation at physiological temperatures in lipid mixtures modeling the outer leaflet of the plasma membrane**. *Biophysical journal* 2003, **85**(2):1034-1045.
108. Picas L, Milhiet PE, Hernandez-Borrell J: **Atomic force microscopy: a versatile tool to probe the physical and chemical properties of supported membranes at the nanoscale**. *Chemistry and physics of lipids* 2012, **165**(8):845-860.
109. Tokumasu F, Jin AJ, Feigenson GW, Dvorak JA: **Atomic force microscopy of nanometric liposome adsorption and nanoscopic membrane domain formation**. *Ultramicroscopy* 2003, **97**(1-4):217-227.
110. Yuan C, Furlong J, Burgos P, Johnston LJ: **The size of lipid rafts: an atomic force microscopy study of ganglioside GM1 domains in sphingomyelin/DOPC/cholesterol membranes**. *Biophysical journal* 2002, **82**(5):2526-2535.
111. Goni FM, Alonso A, Bagatolli LA, Brown RE, Marsh D, Prieto M, Thewalt JL: **Phase diagrams of lipid mixtures relevant to the study of membrane rafts**. *Biochimica et biophysica acta* 2008, **1781**(11-12):665-684.
112. Veatch SL, Keller SL: **Miscibility phase diagrams of giant vesicles containing sphingomyelin**. *Physical review letters* 2005, **94**(14):148101.
113. Bartels T, Lankalapalli RS, Bittman R, Beyer K, Brown MF: **Raftlike mixtures of sphingomyelin and cholesterol**

investigated by solid-state 2H NMR spectroscopy. *Journal of the American Chemical Society* 2008, **130**(44):14521-14532.

114. Sodt AJ, Sandar ML, Gawrisch K, Pastor RW, Lyman E: **The molecular structure of the liquid-ordered phase of lipid bilayers**. *Journal of the American Chemical Society* 2014, **136**(2):725-732.
115. de Almeida RF, Loura LM, Fedorov A, Prieto M: **Lipid rafts have different sizes depending on membrane composition: a time-resolved fluorescence resonance energy transfer study**. *Journal of molecular biology* 2005, **346**(4):1109-1120.
116. Ikonen E: **Cellular cholesterol trafficking and compartmentalization**. *Nature reviews* 2008, **9**(2):125-138.
117. McConnell HM, Radhakrishnan A: **Condensed complexes of cholesterol and phospholipids**. *Biochimica et biophysica acta* 2003, **1610**(2):159-173.
118. Huang J, Feigenson GW: **A microscopic interaction model of maximum solubility of cholesterol in lipid bilayers**. *Biophysical journal* 1999, **76**(4):2142-2157.
119. Ali MR, Cheng KH, Huang J: **Ceramide drives cholesterol out of the ordered lipid bilayer phase into the crystal phase in 1-palmitoyl-2-oleoyl-sn-glycero-3 phosphocholine/cholesterol/ceramide ternary mixtures**. *Biochemistry* 2006, **45**(41):12629-12638.
120. Wood WG, Igbavboa U, Muller WE, Eckert GP: **Cholesterol asymmetry in synaptic plasma membranes**. *Journal of neurochemistry* 2011, **116**(5):684-689.

121. Zhang W, McIntosh AL, Xu H, Wu D, Gruninger T, Atshaves B, Liu JC, Schroeder F: **Structural analysis of sterol distributions in the plasma membrane of living cells**. *Biochemistry* 2005, **44**(8):2864-2884.
122. Scott RE: **Plasma membrane vesiculation: a new technique for isolation of plasma membranes**. *Science (New York, NY* 1976, **194**(4266):743-745.
123. Baumgart T, Hammond AT, Sengupta P, Hess ST, Holowka DA, Baird BA, Webb WW: **Large-scale fluid/fluid phase separation of proteins and lipids in giant plasma membrane vesicles**. *Proceedings of the National Academy of Sciences of the United States of America* 2007, **104**(9):3165-3170.
124. Veatch SL, Cicuta P, Sengupta P, Honerkamp-Smith A, Holowka D, Baird B: **Critical fluctuations in plasma membrane vesicles**. *ACS chemical biology* 2008, **3**(5):287-293.
125. Levental I, Byfield FJ, Chowdhury P, Gai F, Baumgart T, Janmey PA: **Cholesterol-dependent phase separation in cell-derived giant plasma-membrane vesicles**. *The Biochemical journal* 2009, **424**(2):163-167.
126. Nikolaus J, Scolari S, Bayraktarov E, Jungnick N, Engel S, Pia Plazzo A, Stockl M, Volkmer R, Veit M, Herrmann A: **Hemagglutinin of influenza virus partitions into the nonraft domain of model membranes**. *Biophysical journal* 2010, **99**(2):489-498.
127. Sezgin E, Levental I, Grzybek M, Schwarzmann G, Mueller V, Honigmann A, Belov VN, Eggeling C, Coskun U, Simons K *et al*: **Partitioning, diffusion, and ligand binding of raft lipid**

analogs in model and cellular plasma membranes. *Biochimica et biophysica acta 2012,* **1818**(7):1777-1784.

128. Lingwood D, Simons K: **Lipid rafts as a membrane-organizing principle**. *Science 2008,* **327**(5961):46-50.
129. Bernardino de la Serna J, Perez-Gil J, Simonsen AC, Bagatolli LA: **Cholesterol rules: direct observation of the coexistence of two fluid phases in native pulmonary surfactant membranes at physiological temperatures**. *The Journal of biological chemistry* 2004, **279**(39):40715-40722.
130. Owen DM, Williamson DJ, Magenau A, Gaus K: **Sub-resolution lipid domains exist in the plasma membrane and regulate protein diffusion and distribution**. *Nature communications* 2012, **3**:1256.
131. Sengupta P, Hammond A, Holowka D, Baird B: **Structural determinants for partitioning of lipids and proteins between coexisting fluid phases in giant plasma membrane vesicles**. *Biochimica et biophysica acta* 2008, **1778**(1):20-32.
132. Gaus K, Gratton E, Kable EP, Jones AS, Gelissen I, Kritharides L, Jessup W: **Visualizing lipid structure and raft domains in living cells with two-photon microscopy**. *Proceedings of the National Academy of Sciences of the United States of America* 2003, **100**(26):15554-15559.
133. Gousset K, Wolkers WF, Tsvetkova NM, Oliver AE, Field CL, Walker NJ, Crowe JH, Tablin F: **Evidence for a physiological role for membrane rafts in human platelets**. *Journal of cellular physiology* 2002, **190**(1):117-128.

134. Eggeling C, Ringemann C, Medda R, Schwarzmann G, Sandhoff K, Polyakova S, Belov VN, Hein B, von Middendorff C, Schonle A *et al*: **Direct observation of the nanoscale dynamics of membrane lipids in a living cell**. *Nature* 2009, **457**(7233):1159-1162.
135. Owen DM, Magenau A, Williamson D, Gaus K: **The lipid raft hypothesis revisited--new insights on raft composition and function from super-resolution fluorescence microscopy**. *Bioessays* 2012, **34**(9):739-747.
136. Edidin M: **The state of lipid rafts: from model membranes to cells**. *Annual review of biophysics and biomolecular structure* 2003, **32**:257-283.
137. Brown DA, Rose JK: **Sorting of GPI-anchored proteins to glycolipid-enriched membrane subdomains during transport to the apical cell surface**. *Cell* 1992, **68**(3):533-544.
138. London E, Brown DA: **Insolubility of lipids in triton X-100: physical origin and relationship to sphingolipid/cholesterol membrane domains (rafts)**. *Biochimica et biophysica acta* 2000, **1508**(1-2):182-195.
139. Prinetti A, Chigorno V, Prioni S, Loberto N, Marano N, Tettamanti G, Sonnino S: **Changes in the lipid turnover, composition, and organization, as sphingolipid-enriched membrane domains, in rat cerebellar granule cells developing in vitro**. *The Journal of biological chemistry* 2001, **276**(24):21136-21145.
140. Corsetto PA, Cremona A, Montorfano G, Jovenitti IE, Orsini F, Arosio P, Rizzo AM: **Chemical-physical changes in cell**

membrane microdomains of breast cancer cells after omega-3 PUFA incorporation. *Cell biochemistry and biophysics* 2012, **64**(1):45-59.

141. Podyma-Inoue KA, Hara-Yokoyama M, Shinomura T, Kimura T, Yanagishita M: **Syndecans reside in sphingomyelin-enriched low-density fractions of the plasma membrane isolated from a parathyroid cell line**. *PloS one* 2012, **7**(3):e32351.
142. Tanigawa M, Kihara A, Terashima M, Takahara T, Maeda T: **Sphingolipids regulate the yeast high-osmolarity glycerol response pathway**. *Molecular and cellular biology* 2012, **32**(14):2861-2870.
143. Fujiwara M, Hamada S, Hiratsuka M, Fukao Y, Kawasaki T, Shimamoto K: **Proteome analysis of detergent-resistant membranes (DRMs) associated with OsRac1-mediated innate immunity in rice**. *Plant & cell physiology* 2009, **50**(7):1191-1200.
144. Pike LJ, Han X, Chung KN, Gross RW: **Lipid rafts are enriched in arachidonic acid and plasmenylethanolamine and their composition is independent of caveolin-1 expression: a quantitative electrospray ionization/mass spectrometric analysis**. *Biochemistry* 2002, **41**(6):2075-2088.
145. Prinetti A, Chigorno V, Tettamanti G, Sonnino S: **Sphingolipid-enriched membrane domains from rat cerebellar granule cells differentiated in culture. A compositional study**. *The Journal of biological chemistry* 2000, **275**(16):11658-11665.

146. Dennis EA: **Formation and characterization of mixed micelles of the nonionic surfactant Triton X-100 with egg, dipalmitoyl, and dimyristoyl phosphatidylcholines**. *Archives of biochemistry and biophysics* 1974, **165**(2):764-773.

147. Schroeder RJ, Ahmed SN, Zhu Y, London E, Brown DA: **Cholesterol and sphingolipid enhance the Triton X-100 insolubility of glycosylphosphatidylinositol-anchored proteins by promoting the formation of detergent-insoluble ordered membrane domains**. *The Journal of biological chemistry* 1998, **273**(2):1150-1157.

148. Roper K, Corbeil D, Huttner WB: **Retention of prominin in microvilli reveals distinct cholesterol-based lipid micro-domains in the apical plasma membrane**. *Nature cell biology* 2000, **2**(9):582-592.

149. Drevot P, Langlet C, Guo XJ, Bernard AM, Colard O, Chauvin JP, Lasserre R, He HT: **TCR signal initiation machinery is pre-assembled and activated in a subset of membrane rafts**. *The EMBO journal* 2002, **21**(8):1899-1908.

150. Slimane TA, Trugnan G, Van ISC, Hoekstra D: **Raft-mediated trafficking of apical resident proteins occurs in both direct and transcytotic pathways in polarized hepatic cells: role of distinct lipid microdomains**. *Molecular biology of the cell* 2003, **14**(2):611-624.

151. Loberto N, Prioni S, Bettiga A, Chigorno V, Prinetti A, Sonnino S: **The membrane environment of endogenous cellular prion protein in primary rat cerebellar neurons**. *Journal of neurochemistry* 2005, **95**(3):771-783.

152. Schuck S, Honsho M, Ekroos K, Shevchenko A, Simons K: **Resistance of cell membranes to different detergents**. *Proceedings of the National Academy of Sciences of the United States of America* 2003, **100**(10):5795-5800.
153. Madore N, Smith KL, Graham CH, Jen A, Brady K, Hall S, Morris R: **Functionally different GPI proteins are organized in different domains on the neuronal surface**. *The EMBO journal* 1999, **18**(24):6917-6926.
154. Shogomori H, Brown DA: **Use of detergents to study membrane rafts: the good, the bad, and the ugly**. *Biological chemistry* 2003, **384**(9):1259-1263.
155. Abi-Rizk G, Besson F: **Interactions of Triton X-100 with sphingomyelin and phosphatidylcholine monolayers: influence of the cholesterol content**. *Colloids and surfaces* 2008, **66**(2):163-167.
156. Ingelmo-Torres M, Gaus K, Herms A, Gonzalez-Moreno E, Kassan A, Bosch M, Grewal T, Tebar F, Enrich C, Pol A: **Triton X-100 promotes a cholesterol-dependent condensation of the plasma membrane**. *The Biochemical journal* 2009, **420**(3):373-381.
157. Heerklotz H: **Triton promotes domain formation in lipid raft mixtures**. *Biophysical journal* 2002, **83**(5):2693-2701.
158. Pathak P, London E: **Measurement of lipid nanodomain (raft) formation and size in sphingomyelin/POPC/cholesterol vesicles shows TX-100 and transmembrane helices increase domain size by coalescing**

preexisting nanodomains but do not induce domain formation. *Biophysical journal* 2011, **101**(10):2417-2425.

159. Foster LJ, De Hoog CL, Mann M: **Unbiased quantitative proteomics of lipid rafts reveals high specificity for signaling factors**. *Proceedings of the National Academy of Sciences of the United States of America* 2003, **100**(10):5813-5818.
160. Friedrichson T, Kurzchalia TV: **Microdomains of GPI-anchored proteins in living cells revealed by crosslinking**. *Nature* 1998, **394**(6695):802-805.
161. Macdonald JL, Pike LJ: **A simplified method for the preparation of detergent-free lipid rafts**. *Journal of lipid research* 2005, **46**(5):1061-1067.
162. Song KS, Li S, Okamoto T, Quilliam LA, Sargiacomo M, Lisanti MP: **Co-purification and direct interaction of Ras with caveolin, an integral membrane protein of caveolae microdomains. Detergent-free purification of caveolae microdomains**. *The Journal of biological chemistry* 1996, **271**(16):9690-9697.
163. Smart EJ, Ying YS, Mineo C, Anderson RG: **A detergent-free method for purifying caveolae membrane from tissue culture cells**. *Proceedings of the National Academy of Sciences of the United States of America* 1995, **92**(22):10104-10108.
164. Persaud-Sawin DA, Lightcap S, Harry GJ: **Isolation of rafts from mouse brain tissue by a detergent-free method**. *Journal of lipid research* 2009, **50**(4):759-767.

165. Liu J, Oh P, Horner T, Rogers RA, Schnitzer JE: **Organized endothelial cell surface signal transduction in caveolae distinct from glycosylphosphatidylinositol-anchored protein microdomains**. *The Journal of biological chemistry* 1997, **272**(11):7211-7222.

166. Harder T, Scheiffele P, Verkade P, Simons K: **Lipid domain structure of the plasma membrane revealed by patching of membrane components**. *The Journal of cell biology* 1998, **141**(4):929-942.

167. Janes PW, Ley SC, Magee AI: **Aggregation of lipid rafts accompanies signaling via the T cell antigen receptor**. *The Journal of cell biology* 1999, **147**(2):447-461.

168. Prior IA, Muncke C, Parton RG, Hancock JF: **Direct visualization of Ras proteins in spatially distinct cell surface microdomains**. *The Journal of cell biology* 2003, **160**(2):165-170.

169. Munro S: **Lipid rafts: elusive or illusive?** *Cell* 2003, **115**(4):377-388.

170. Ostrom RS, Liu X: **Detergent and detergent-free methods to define lipid rafts and caveolae**. *Methods in molecular biology* 2007, **400**:459-468.

171. Schneider A, Rajendran L, Honsho M, Gralle M, Donnert G, Wouters F, Hell SW, Simons M: **Flotillin-dependent clustering of the amyloid precursor protein regulates its endocytosis and amyloidogenic processing in neurons**. *J Neurosci* 2008, **28**(11):2874-2882.

172. Levental I, Lingwood D, Grzybek M, Coskun U, Simons K: **Palmitoylation regulates raft affinity for the majority of integral raft proteins**. *Proceedings of the National Academy of Sciences of the United States of America* 2010, **107**(51):22050-22054.
173. Varma R, Mayor S: **GPI-anchored proteins are organized in submicron domains at the cell surface**. *Nature* 1998, **394**(6695):798-801.
174. Dietrich C, Bagatolli LA, Volovyk ZN, Thompson NL, Levi M, Jacobson K, Gratton E: **Lipid rafts reconstituted in model membranes**. *Biophysical journal* 2001, **80**(3):1417-1428.
175. Kahya N, Brown DA, Schwille P: **Raft partitioning and dynamic behavior of human placental alkaline phosphatase in giant unilamellar vesicles**. *Biochemistry* 2005, **44**(20):7479-7489.
176. Resh MD: **Palmitoylation of ligands, receptors, and intracellular signaling molecules**. *Sci STKE* 2006, **2006**(359):re14.
177. Liang X, Nazarian A, Erdjument-Bromage H, Bornmann W, Tempst P, Resh MD: **Heterogeneous fatty acylation of Src family kinases with polyunsaturated fatty acids regulates raft localization and signal transduction**. *The Journal of biological chemistry* 2001, **276**(33):30987-30994.
178. Balamuth F, Brogdon JL, Bottomly K: **CD4 raft association and signaling regulate molecular clustering at the immunological synapse site**. *J Immunol* 2004, **172**(10):5887-5892.

179. Arcaro A, Gregoire C, Boucheron N, Stotz S, Palmer E, Malissen B, Luescher IF: **Essential role of CD8 palmitoylation in CD8 coreceptor function**. *J Immunol* 2000, **165**(4):2068-2076.

180. Prior IA, Harding A, Yan J, Sluimer J, Parton RG, Hancock JF: **GTP-dependent segregation of H-ras from lipid rafts is required for biological activity**. *Nature cell biology* 2001, **3**(4):368-375.

181. Guirland C, Zheng JQ: **Membrane lipid rafts and their role in axon guidance**. *Advances in experimental medicine and biology* 2007, **621**:144-155.

182. Benarroch EE: **Lipid rafts, protein scaffolds, and neurologic disease**. *Neurology* 2007, **69**(16):1635-1639.

183. Mayor S, Rao M: **Rafts: scale-dependent, active lipid organization at the cell surface**. *Traffic* 2004, **5**(4):231-240.

184. Normanno N, De Luca A, Bianco C, Strizzi L, Mancino M, Maiello MR, Carotenuto A, De Feo G, Caponigro F, Salomon DS: **Epidermal growth factor receptor (EGFR) signaling in cancer**. *Gene* 2006, **366**(1):2-16.

185. Lopez-Torrejon I, Querol E, Aviles FX, Seno M, de Llorens R, Oliva B: **Human betacellulin structure modeled from other members of EGF family**. *Journal of molecular modeling* 2002, **8**(4):131-144.

186. Ben-Levy R, Paterson HF, Marshall CJ, Yarden Y: **A single autophosphorylation site confers oncogenicity to the Neu/ErbB-2 receptor and enables coupling to the MAP kinase pathway**. *The EMBO journal* 1994, **13**(14):3302-3311.

187. Prigent SA, Gullick WJ: **Identification of c-erbB-3 binding sites for phosphatidylinositol 3'-kinase and SHC using an EGF receptor/c-erbB-3 chimera**. *The EMBO journal* 1994, **13**(12):2831-2841.

188. Citri A, Skaria KB, Yarden Y: **The deaf and the dumb: the biology of ErbB-2 and ErbB-3**. *Experimental cell research* 2003, **284**(1):54-65.

189. Ayyappan S, Prabhakar D, Sharma N: **Epidermal growth factor receptor (EGFR)-targeted therapies in esophagogastric cancer**. *Anticancer research* 2013, **33**(10):4139-4155.

190. Roskoski R, Jr.: **ERK1/2 MAP kinases: structure, function, and regulation**. *Pharmacol* Res 2012, **66**(2):105-143.

191. de Laurentiis A, Donovan L, Arcaro A: **Lipid rafts and caveolae in signaling by growth factor receptors**. *The open biochemistry journal* 2007, **1**:12-32.

192. Mlcochova J, Faltejskova P, Nemecek R, Svoboda M, Slaby O: **MicroRNAs targeting EGFR signalling pathway in colorectal cancer**. *Journal of cancer research and clinical oncology* 2013, **139**(10):1615-1624.

193. Roepstorff K, Thomsen P, Sandvig K, van Deurs B: **Sequestration of epidermal growth factor receptors in non-caveolar lipid rafts inhibits ligand binding**. *The Journal of biological chemistry* 2002, **277**(21):18954-18960.

194. Pike LJ, Han X, Gross RW: **Epidermal growth factor receptors are localized to lipid rafts that contain a balance of inner and outer leaflet lipids: a shotgun lipidomics study**.

The Journal of biological chemistry 2005, **280**(29):26796-26804.

195. Patra SK, Rizzi F, Silva A, Rugina DO, Bettuzzi S: **Molecular targets of (-)-epigallocatechin-3-gallate (EGCG): specificity and interaction with membrane lipid rafts**. *J Physiol Pharmacol* 2008, **59**:217-235.
196. Kumler I, Tuxen MK, Nielsen DL: **A systematic review of dual targeting in HER2-positive breast cancer**. *Cancer treatment reviews* 2013, **40**(2):259-270.
197. Calladine, CR, Drew, HR: **Understanding DNA, the molecule and how it works**. *Academic Press Limited* 1997.
198. Binnig G, Rohrer H, Gerber C, Weibel, E: **Surface studies by scanning tunneling microscopy**. *Phys. Rev. Lett.* 1982, **49**:57-61.
199. Binnig G, Quate CF, Gerber C: **Atomic force microscope**. *Physical review letters* 1986, **56**(9):930-933.
200. Siegel J, Polivkova M, Kasalkova NS, Kolska Z, Svorcik V: **Properties of silver nanostructure-coated PTFE and its biocompatibility**. *Nanoscale research letters* 2013, **8**(1):388.
201. Marshall BT, Sarangapani KK, Wu J, Lawrence MB, McEver RP, Zhu C: **Measuring molecular elasticity by atomic force microscope cantilever fluctuations**. *Biophysical journal* 2006, **90**(2):681-692.
202. Wagner KC, Wang Y, Regen SL, Vezenov DV: **Yield strength of glued Langmuir-Blodgett films determined by friction force microscopy**. *Phys Chem Chem Phys* 2013, **15**(33):14037-14046.

203. Liu LN, Scheuring S: **Investigation of photosynthetic membrane structure using atomic force microscopy**. *Trends in plant science* 2013, **18**(5):277-286.

204. Fotiadis D: **Atomic force microscopy for the study of membrane proteins**. *Current opinion in biotechnology* 2012, **23**(4):510-515.

205. Ido S, Kimura K, Oyabu N, Kobayashi K, Tsukada M, Matsushige K, Yamada H: **Beyond the helix pitch: direct visualization of native DNA in aqueous solution**. *ACS nano* 2013, **7**(2):1817-1822.

206. Santacroce M, Daniele F, Cremona A, Scaccabarozzi D, Castagna M, Orsini F: **Imaging of Xenopus laevis oocyte plasma membrane in physiological-like conditions by atomic force microscopy**. *Microsc Microanal* 2013, **19**(5):1358-1363.

207. Allen S, Rigby-Singleton SM, Harris H, Davies MC, O'Shea P: **Measuring and visualizing single molecular interactions in biology**. *Biochemical Society transactions* 2003, **31**(5):1052-1057.

208. Santos NC, Castanho MA: **An overview of the biophysical applications of atomic force microscopy**. *Biophysical chemistry* 2004, **107**(2):133-149.

209. Kienberger F, Ebner A, Gruber HJ, Hinterdorfer P: **Molecular recognition imaging and force spectroscopy of single biomolecules**. *Accounts of chemical research* 2006, **39**(1):29-36.

210. Picas L, Milhiet PE, Hernandez-Borrell J: **Atomic force microscopy: a versatile tool to probe the physical and chemical properties of supported membranes at the nanoscale**. *Chemistry and physics of lipids* 2012, **165**(8):845-860.
211. Czajkowsky DM, Shao Z: **Submolecular resolution of single macromolecules with atomic force microscopy**. *FEBS letters* 1998, **430**(1-2):51-54.
212. Albrecht TR, Akamine S, Carver TE, Quate CF: **Microfabrication of cantilever styli for the atomic force microscope**. *J. Vac. Sci. Technol. A* 1990, **8**:3386-3396.
213. Meyer G, Amer NM: **Novel optical approach to atomic force microscopy**. *Appl. Phys. Lett.* 1988, **53**:1045-1047.
214. Alexander S, Hellemans L, Marti O, Schneir J, Elings V, Hansma PK, Longmire M, Gurley J: **An atomic-resolution atomic-force microscope implemented using an optical lever**. *J. Appl. Phys.* 1989, **65**:164-167.
215. Putman CA, van der Werf KO, de Grooth BG, van Hulst NF, Greve J: **Viscoelasticity of living cells allows high resolution imaging by tapping mode atomic force microscopy**. *Biophysical journal* 1994, **67**(4):1749-1753.
216. Ogletree DF, Carpick RW, Salmeron M: **Calibration of frictional forces in atomic force microscopy**. *Rev. Sci. Instrum.* 1996, **67**:3298-3306.
217. Wiesendanger R: **Scanning Probe Microscopy and Spectroscopy**. *Cambridge University Press*, 1994.

218. Weisenhorn AL, Hansma PK, Albrecht TR, Quate CF: **Forces in atomic force microscopy in air and water**. *Appl. Phys. Lett.* 1989, **54**:2651-2653.

219. Martin Y, Williams CC, Wickramasinghe J: **Atomic force microscope force mapping and profiling on a sub 100-A scale**. *J. Appl. Phys.* 1987 **61**:4723-4729.

220. Luthi R, Meyer E, Howald I, Haefke H, Anselmetti D, Dreier M, Ruetsche M, Bonner T, Overney RM, Fromer J, Guntherodt HJ: **Progress in noncontact dynamic force microscopy**. *J. Vac. Sci. Tech. B* 1994, **12**:1673-1676.

221. Zhong Q, Innis D, Kjoller K, Ellings V: **Fractured polymer/silica fiber structure studied by tapping mode atomic force microscopy**. *Surf. Sci. Lett.* 1993, **290**:L688-L692.

222. McPherson A, Kuznetsov YG, Malkin A, Plomp M: **Macromolecular crystal growth as revealed by atomic force microscopy**. *Journal of structural biology* 2003, **142**(1):32-46.

223. Hansma HG: **Surface biology of DNA by atomic force microscopy**. *Annual review of physical chemistry* 2001, **52**:71-92.

224. Tamayo J, Humphris AD, Owen RJ, Miles MJ: **High-Q dynamic force microscopy in liquid and its application to living cells**. *Biophysical journal* 2001, **81**(1):526-537.

225. Hansma HG, Kasuya K, Oroudjev E: **Atomic force microscopy imaging and pulling of nucleic acids**. *Current opinion in structural biology* 2004, **14**(3):380-385.

226. Orsini F, Cremona A, Arosio P, Corsetto PA, Montorfano G, Lascialfari A, Rizzo AM: **Atomic force microscopy imaging of lipid rafts of human breast cancer cells**. *Biochimica et biophysica acta* 2012, **1818**(12):2943-2949.
227. Jacobson K, Mouritsen OG, Anderson RG: **Lipid rafts: at a crossroad between cell biology and physics**. *Nature cell biology* 2007, **9**(1):7-14.
228. Sorice M, Parolini I, Sansolini T, Garofalo T, Dolo V, Sargiacomo M, Tai T, Peschle C, Torrisi MR, Pavan A: **Evidence for the existence of ganglioside-enriched plasma membrane domains in human peripheral lymphocytes**. *Journal of lipid research* 1997, **38**(5):969-980.
229. Hakomori S, Yamamura S, Handa AK: **Signal transduction through glyco(sphingo)lipids. Introduction and recent studies on glyco(sphingo)lipid-enriched microdomains**. *Annals of the New York Academy of Sciences* 1998, **845**:1-10.
230. Jost P, Brooks UJ, Griffith OH: **Fluidity of phospholipid bilayers and membranes after exposure to osmium tetroxide and gluteraldehyde**. *Journal of molecular biology* 1973, **76**(2):313-318.
231. Fujita A, Cheng J, Fujimoto T: **Quantitative electron microscopy for the nanoscale analysis of membrane lipid distribution**. *Nature protocols* 2010, **5**(4):661-669.
232. Fujita A, Cheng J, Fujimoto T: **Segregation of GM1 and GM3 clusters in the cell membrane depends on the intact actin cytoskeleton**. *Biochimica et biophysica acta* 2009, **1791**(5):388-396.

233. Lagerholm BC, Weinreb GE, Jacobson K, Thompson NL: **Detecting microdomains in intact cell membranes**. *Annual review of physical chemistry* 2005, **56**:309-336.
234. Leung BO, Chou KC: **Review of super-resolution fluorescence microscopy for biology**. *Applied spectroscopy*, **65**(9):967-980.
235. Muller T, Schumann C, Kraegeloh A: **STED microscopy and its applications: new insights into cellular processes on the nanoscale**. *Chemphyschem* 2012, **13**(8):1986-2000.
236. Eggeling C, Willig KI, Barrantes FJ: **STED microscopy of living cells--new frontiers in membrane and neurobiology**. *Journal of neurochemistry* 2013, **126**(2):203-212.
237. Sahl SJ, Leutenegger M, Hilbert M, Hell SW, Eggeling C: **Fast molecular tracking maps nanoscale dynamics of plasma membrane lipids**. *Proceedings of the National Academy of Sciences of the United States of America* 2010, **107**(15):6829-6834.
238. Sengupta P, Jovanovic-Talisman T, Skoko D, Renz M, Veatch SL, Lippincott-Schwartz J: **Probing protein heterogeneity in the plasma membrane using PALM and pair correlation analysis**. *Nature methods* 2011, **8**(11):969-975.
239. Sengupta P, Lippincott-Schwartz J: **Quantitative analysis of photoactivated localization microscopy (PALM) datasets using pair-correlation analysis**. *Bioessays* 2012, **34**(5):396-405.
240. Mizuno H, Dedecker P, Ando R, Fukano T, Hofkens J, Miyawaki A: **Higher resolution in localization microscopy**

by slower switching of a photochromic protein. *Photochem Photobiol Sci* 2010, **9**(2):239-248.

241. Anderton CR, Lou K, Weber PK, Hutcheon ID, Kraft ML: **Correlated AFM and NanoSIMS imaging to probe cholesterol-induced changes in phase behavior and non-ideal mixing in ternary lipid membranes**. *Biochimica et biophysica acta* 2011, **1808**(1):307-315.
242. Giocondi MC, Boichot S, Plenat T, Le Grimellec CC: **Structural diversity of sphingomyelin microdomains**. *Ultramicroscopy* 2004, **100**(3-4):135-143.
243. Connell SD, Smith DA: **The atomic force microscope as a tool for studying phase separation in lipid membranes**. *Molecular membrane biology* 2006, **23**(1):17-28.
244. Rinia HA, Snel MM, van der Eerden JP, de Kruijff B: **Visualizing detergent resistant domains in model membranes with atomic force microscopy**. *FEBS letters* 2001, **501**(1):92-96.
245. El Kirat K, Morandat S: **Cholesterol modulation of membrane resistance to Triton X-100 explored by atomic force microscopy**. *Biochimica et biophysica acta* 2007, **1768**(9):2300-2309.
246. Giocondi MC, Seantier B, Dosset P, Milhiet PE, Le Grimellec C: **Characterizing the interactions between GPI-anchored alkaline phosphatases and membrane domains by AFM**. *Pflugers Arch* 2008, **456**(1):179-188.
247. Giocondi MC, Yamamoto D, Lesniewska E, Milhiet PE, Ando T, Le Grimellec C: **Surface topography of membrane**

domains. *Biochimica et biophysica acta* 2010, **1798**(4):703-718.

248. Cai M, Zhao W, Shang X, Jiang J, Ji H, Tang Z, Wang H: **Direct evidence of lipid rafts by in situ atomic force microscopy**. *Small* 2012, **8**(8):1243-1250.

Chapter 4

Chemical-physical changes in cell membrane microdomains of breast cancer cells after DHA incorporation

This chapter is based on: Corsetto PA, Cremona A, Montorfano G, Jovenitti IE, Orsini F, Arosio P, Rizzo AM. (2012) Chemical-physical changes in cell membrane microdomains of breast cancer cells after omega-3 PUFA incorporation. Cell Biochem Biophys. 64(1):45-59.

4.1 Introduction

Breast cancer is one of the most common cancers and the leading cause of death from cancer among women worldwide. The dietary habit plays an important role in the etiology of breast cancer. Indeed, for the past few decades, epidemiologic studies have suggested a relationship between dietary lipids and development/progression of cancer **[1]**. PUFAs are grouped into two main families, n-6 and n-3, distinguished on the position of the first double bond closest to the methyl end. The main dietary sources of Eicosapentaenoic (EPA, 20:5n-3) and Docosahexaenoic acid (DHA, 22:6n-3) are cold-water fish oils. There are *in vitro* and *in vivo* evidences that the administration DHA and EPA is able to reduce cancer proliferation and to increase apoptosis **[2,3]** as well as inhibit angiogenesis and metastasis, and to influence cancer differentiation **[4,5]**. A number of mechanisms have been proposed for the anticancer actions of n-3 PUFAs, including suppression of neoplastic transformation, inhibition of cell proliferation, enhancement of apoptosis, and antiangiogenic action. Numerous experimental data indicate that the presence of PUFAs in the membrane bilayer seem to involve changes in cell membrane fatty acid composition.

n-3 PUFAs incorporated into membrane PLs can potentially affect a variety of plasma membrane physical properties including membrane thickness, fluidity, elasticity, permeability, the structure and function of membrane microdomains (lipid rafts) and alterations of cell signaling pathways that lead to altered transcription factor activity and changes in gene expression **[6]**. In fact the structure and dynamics of these polyunsaturated chains at the molecular level are profoundly different from their saturated counterpart, with very short reorientational correlation times and extremely low chain order. Moreover, much attention has been given to how DHA can alter membrane properties **[7,8]** and the organization and composition of membrane microdomains **[6,9-11]**.

Lipid rafts are heterogeneous microdomains enriched in Chol, SM, saturated PLs. These microdomains are characterized physicochemically by a relative rigidity and reduced fluidity compared with the surrounding plasma membrane, which is in part caused by their Chol content **[12,13]**. Lipid rafts are highly dynamic and may rapidly assemble and disassemble, leading to a dynamic segregation of proteins **[12-14]**. In fact raft localization is shown to modulate a variety of proteins, such as receptor activities and therefore signal transduction **[15,16]**. Chol alterations, which affect on raft structure, also might alter the receptor function **[15]**.

In the present work, we treated breast cancer cells with DHA to assess if they are incorporated in membrane microdomain PLs and are able to change chemical and physical properties of these structures.

We analyzed the incorporation of PUFAs in cancer cell DRMs by High Performance Liquid Chromatography/Evaporative Light Scattering Detector (HPLC/ELSD) and Gas Chromatography (GC) analyses of raft phospholipid fatty acid composition. In addition, morpho-dimensional changes in DRMs have been visualized and evaluated by AFM studying purified membrane samples both before and after the n-3 PUFA treatment.

Here I will concentrate on the effect of DHA incorporation in MDA-MB-231 breast cancer cell DRM microdomains.

4.2 Material and methods

Materials

DHA (cis-4,7,10,13,16,19-docosahexaenoic acid sodium salt) was purchased from Sigma-Aldrich (St Louis, MO, USA). In order to prevent oxidation, DHA was dissolved in absolute ethanol, stocked under nitrogen, and stored at −80°C. The rabbit polyclonal anti-flotillin-1, the mouse monoclonal anti-clathrin heavy chain (HC) were purchased from Santa Cruz Biotechnology Inc. (CA, USA). Bound primary antibodies were visualized by the proper secondary horseradish peroxidase (HRP)-linked antibodies (Santa Cruz Biotechnology Inc., Santa Cruz, CA, USA) and immunoreactivity was assessed by chemiluminescence (ECL, PerkinElmer,USA).

Cell Lines and Culture Conditions

Human breast cancer cells MDA-MB-231 (ER-negative and over-expressing EGFR), derived from human mammary adenocarcinoma, were obtained from the IST (Italian National Cancer Research Institute, Genoa Italy, laboratory of Molecular Mutagenesis and DNA repair). The MDA-MB-231 cell line is routinely maintained in DMEM medium (Gibco-BRL, Life Technologies Italia srl, Italy) supplemented with 10% fetal bovine serum (FBS), 100U/ml penicillin, 100mg/ml streptomycin and 2mM glutamine. Cells were grown at 37°C in a 5% CO_2 atmosphere with 98% relative humidity.

Cell Viability Assay

The DHA exposure effects on the cell viability were determined by a colorimetric 3-(4,5-dimethylthiazol-2-yl)-2,5-diphenyltetrazolium bromide (MTT) assay **[17]**. A tetrazolium salt has been used to develop a quantitative colorimetric assay for mammalian cell survival and proliferation. Yellow MTT is reduced to purple formazan in the mitochondria only when mitochondrial reductase enzymes are active, and therefore conversion can be directly related to the number of living cells. When the amount of purple formazan produced by cells treated with an agent is compared with the amount of formazan produced by untreated cells, the effectiveness of the agent in causing death of cells can be deduced, through the production of a dose-response curve. The absorbance of this colored solution can be quantified by measuring at a certain wavelength (usually between 500 and 600nm) by a spectrophotometer.

The main advantages of the colorimetric assay are its rapidly and precision, and the lack of any radioisotope. In details, cells were seeded and cultured in 96-well plates at 37°C to allow adhesion to the plate and to reach 50-60% confluence. After 48h, the medium was replaced with the experimental medium supplemented with DHA and incubated for further 72h. We have studied the effects of different DHA increasing concentrations dissolved in ethanol (50-300μM). The final concentration of ethanol was less than 1% in the culture medium, and it had no anti-proliferative effect on MDA-MB-231 breast cancer cell line. After incubation, cells were incubated with 10μl of MTT stock solution (5mg/ml in PBS, pH 7.5) for 4 h at 37°C. For solubilization of the resultant formazan product, 100μl of solubilizing solution (10% v/v sodium dodecyl sulphate and 0.01M HCl) were added to each well and incubated overnight in a humidified incubator at 37°C. The absorbance of the color product was measured using a microplate reader at 540nm. Data represent the mean of eight values and results are expressed as Relative Growth Rate (RGR) in comparison with controls that were exposed to a concentration of ethanol equal to that in the samples exposed to fatty acids. All the reagents are purchased from Sigma-Aldrich, USA.

Detergent-Resistant Membranes (DRMs) isolation

Data obtained from MTT assay on MDA-MB-231 cells have allowed to determine the concentration of DHA (200μM) required to inhibit cell growth by 20–30%. During treatments the MDA-MB-231 cell line was seeded $1.5x10^4$ cells/cm^2 for 48h.

After this period, fresh medium for treatments (DMEM + 10% FBS) containing DHA (200µM) was added, and the cells were further incubated for 72h without medium replacement. Experiments include control cells, which were not exposed to any exogenous fatty acids but incubated in the same conditions with the same ethanol concentration of treated cells. After treatment cells were washed two times with ice-cold phosphate-buffered saline (PBS), and then harvested by scrapering in PBS containing 0.4mM Na_3VO_4. Cells were centrifuged and lysed in 1.4ml ice-cold lysis buffer (10mM Tris buffer, pH 7.5, 150mM NaCl, 5mM EDTA, 1mM Na_3VO_4, 1mM phenylmethylsulfonyl fluoride, 75milliunits/ml aprotinin) containing 1% Triton X-100 for 20min on ice. Lysates were thoroughly homogenized by a tight-fitting dounce homogenizer (10 strokes tight). The cell lysate was centrifuged at 1300g for 5min at 4°C, and the postnuclear supernatant (PNS) was transferred to an Eppendorf tube. 1ml of PNS was mixed in ultracentrifuge tubes (Beckman Coulter) with 1ml of ice-cold 85% (w/v) sucrose in TNEV (10mM Tris buffer, pH 7.5, 150mM NaCl, 5mM EDTA, and 1mM Na_3VO_4) and then overlaid with 5.5ml of 30% and 4ml 5% (w/v) sucrose in TNEV. The gradient was centrifuged with a TST-41.14 rotor at 4°C for 17h at 200,000g (Beckman Coulter Optima LE-80K Ultracentrifuge, Palo Alto, CA). Different fractions (1ml/fraction) were collected sequentially from the top of the gradient (fraction 1) to the bottom (fraction 11). DRMs were collected in low-density fractions (fractions 5 and 6) corresponding to the 5% and 30% sucrose interface.

Lipid Extraction

Fractionated cell membranes were extracted with three different chloroform/methanol mixtures (1:1, 1:2 and 2:1, v/v) and partitioned with the theoretical upper phase (TUP, chloroform/methanol/water, 47:48:1, by volume) and then with water. The organic phase, after partitioning, was dried and then suspended in chloroform/methanol (2:1, v/v) for the analysis of PLs, Chol and gangliosides content.

Characterization of DRMs

Free Chol and SM were separated by HP-TLC using silice gel HP-TLC plates (Merck, Darmstadt, Germany). Chromatography was performed in hexane/ether/glacial acetic acid (90:10:1 by volume) and with chloroform/methanol/glacial acetic acid/water (60:45:4:2 by volume), respectively. Chol was visualized with a solution of copper sulfate in phosphoric acid at 180°C, while SM with anisaldehyde in acetic acid and sulfuric acid at 120°C. Chol and SM standards were spotted on the same plate to built a calibration curve. Quantitative analysis was performed by scanning densitometry. Known amounts of cholesterol standard, in four different increasing concentrations, were co-chromatographed to obtain a calibration curve. While polar glycosphingolipids, contained in the upper phase, were always separated by HP-TLC using silice gel plates. Chromatography was performed in chloroform/methanol/0.25% aqueous $CaCl_2$ (5:4:1 v/v/v). Plates were air dried and gangliosides visualized with resorcinol at 120°C. Ganglioside standards were spotted on the same plate.

For protein characterization of DRMs, all fractions were separated on SDS-PAGE (10% polyacrylamide gel) and incubated with different antibodies to raft (flotillin-1) and non-raft (clathrin HC) markers **[18]**. In particular, equal volumes of all fractions were re-suspended in SDS loading buffer and boiled at 100°C for 5min to avoid to protein aggregates. Protein contents were quantified by Lowry assay **[19]**. Samples were separated by SDS-PAGE and transferred onto a PVDF membrane with Bio-rad Transfer Blot Apparatus at 150mA overnight at 4°C in a transfer buffer (25mM TrisHCl, 190mM glicine, 20% methanol and 0.05% SDS) and analyzed by WB with anti-flotillin-1 and anti-clathrin HC antibodies. Following transfer, the membrane were first blocked in blocking buffer consisting of 5% (w/v) dried non-fat milk in Tris-buffered saline (T-TBS: 10mM Tris/HCl, pH 7.5, 150mM NaCl, 0.1% (v/v) Tween®20) at room temperature for 1h. The blots were treated with anti-flotillin-1 primary antibody diluted 1:200 in blocking buffer at room temperature for 2h, washed 6 times (5 minutes each) with T-TBS and incubated with the proper horseradish peroxidase (HRP)-linked secondary antibody in blocking buffer at room temperature for 1h. After 6 washes (5 minutes each) with T-TBS, the protein bands were visualized using enhanced chemiluminescence (ECL) reagents (PerkinElmer, USA). Afterward, the same membranes was successively reblotted with the antibody specifically directed to clathrin HC. Briefly, the membranes were blocked in blocking buffer containing 5% dried non-fat milk in T-TBS at room temperature for 1h.

The blots were treated with anti-clathrin HC primary antibody diluted 1:1800 in blocking buffer at room temperature for 2h, washed with T-TBS and, then, incubated with the proper horseradish peroxidase (HRP)-linked secondary antibody in blocking buffer at room temperature for 1h. The protein bands were visualized using ECL reagents (PerkinElmer, USA).

Analysis of Different Classes of DRM PLs and Chol

Purification and quantitative analysis of membrane phospholipids and cholesterol was obtained using a HPLC-ELSD system (Jasco, Japan; Sedex SEDERE, FR) equipped with one pump, a SCL-10 Advp, a degasser module and a Rheodyne manual injector with 20µl sample loop and a column (length 250mm, I.D 4.6mm and film thickness 5µm) packed with silica normal-phase LiChrospher Si 60 (LiChroCART 250-4, Merck, Darmstadt, Germany). The chromatographic separation is carried out as reported in literature **[2]**. In particular, the separation was achieved with a linear binary gradient of 0:100% to 100:0% (eluent B:A) in 14 min and then 100% B for 9min. Eluent A and B consists of chloroform/methanol/water 80:19.5:0.5 and 60:34:6 (v/v/v) respectively. The flow rate of the eluent was 1.0 ml/min. Total chromatographic run time was 40min per sample: 23min analysis, 12min to restore initial conditions and 5min to re-equilibration. Evaporative Light Scattering Detector Sedex (ELSD model 75, S.E.D.E.R.E., Alfortville, France) was used to detect and quantify separated PL species, in comparison with calibration standard curves.

The pressure of nebulizer gas (air) was maintained at 2.2 bar and the drift tube temperature was set at 50°C. After elution, samples are splitted in two aliquots. The ratio is 1:9, i.e., one part to the detector and nine parts were collected by Gilson Fraction Collector Model 201, in order to separate the different PL classes for further GC analysis. After separation, each PL class was analysed for fatty acid composition by GC in following conditions. Fatty acid methyl esters were obtained by transesterification with sodium methoxide in methanol 3.33 % w/v and injected into Agilent (Agilent Technologies 6850 Series II) gas chromatograph, equipped with a flame ionization detector (FID) and a capillary column (AT Silar; length 30m, film thickness 0.25μm). Helium was used as carrier gas with flow rate of 5.0ml/min, the injector temperature was 250°C, the detector temperature was 275°C, the oven temperature was set at 50°C for 20 min and then increased to 200°C at 10°C min^{-1} for 20 min. Eptadecanoic acid methylester (Sigma-Aldrich, St. Louis, MO, USA) was utilized as internal standard.

AFM imaging

AFM is able to collect 3D topography images with high lateral and vertical resolutions, in the order of nanometre, without any sample preparation such as fixation or staining. In addition, AFM can work under near-physiological conditions, the only requirement being that the sample is well-flattened and adhered to a flat support. In fact, samples that have been flattened and tightly fixed to a substrate are required to obtain the highest possible resolution in AFM images.

For these reasons a freshly cleaved mica leaf was chosen as sample support because of its ultra-flat surface and simple preparation that did not require any chemical treatment to improve the sample adhesion.

AFM imaging has been performed in collaboration with the laboratory of Prof. A. Lascialfari Department of Physics, Università degli Studi di Milano (Italy). Purified membrane samples obtained by the ultracentrifugation process, described above, were diluted 1:30 in a adsorption buffer (150mM KCl, 25mM MgC_{l2}, 10mM Tris/HCl pH 7.5). 50µl of the suspension is floated on a freshly cleaved mica leaf and let adhered for 10 min. Then, sample is gently rinsed 3 times with a recording buffer (150mM KCl, 10mM Tris/HCl pH 7.5) to remove membranes that have not been strongly adsorbed to the mica support. AFM imaging is performed in liquid buffer using a Multimode Nanoscope IIId (Veeco, Santa Barbara, CA, USA) equipped with a 12 µm scanner and sharpened Si_3N_4 cantilevers with a constant spring of 0.06N/m and a 10nm curvature radius (Veeco, Santa Barbara, CA, USA). The AFM is operated in *Contact mode* in constant force conditions. The set point is manually adjusted and kept as low as possible to obtain the best resolution while the total force applied on the sample during the imaging is approximately 300pN as measured by force–distance curve. The 512x512 pixel images are recorded at typical scan frequencies of 4–6Hz. AFM images are flattened using the SPMLab NT Ver. 6.0. software (Veeco, Santa Barbara, CA, USA).

Statistical analysis

The data are presented as mean ± SD. Student's t-test was used for comparisons between treated and control cells and the level of statistical significance was set at *$p<0.05$ and **$p<0.01$.

4.3 Results

Numerous studies have demonstrated that DHA is capable of inhibiting proliferation through various mechanisms in vitro cultures of cancer cells **[20]**. To evaluate the effects of DHA on cell growth, MDA-MB-231 breast cancer cells, were incubated for 72h in medium supplemented with various concentrations of DHA in the range 50-300μM. The effects on cell viability were assessed and quantified by the MTT assay.

As illustrated in **Figure 1**, DHA induces a dose-dependent reduction of cell viability at concentrations >200μM. In particular, at 200μM of DHA we can observe a statistically significant decrease (**$p<0.01$) versus control groups of about 30% in cell growth with DHA supplementation. From these experiments, we extrapolated the dose to be used in the experiments to assess DHA incorporation into cell membrane PLs: 200μM which correspond to ~70% of viability of MDA-MB-231 cell line.

We first tested the purity of DRMs isolated from MDA-MB-231 human breast cancer cells using lipid and protein raft and non-raft markers. In particular, biochemical analysis of the distribution of some lipids highly present in lipid rafts, namely Chol, Sm and ganglioside (GM1), carried out by HP-TLC confirmed the presence of the DRMs in the 5 and 6 fractions (**Figure 2**).

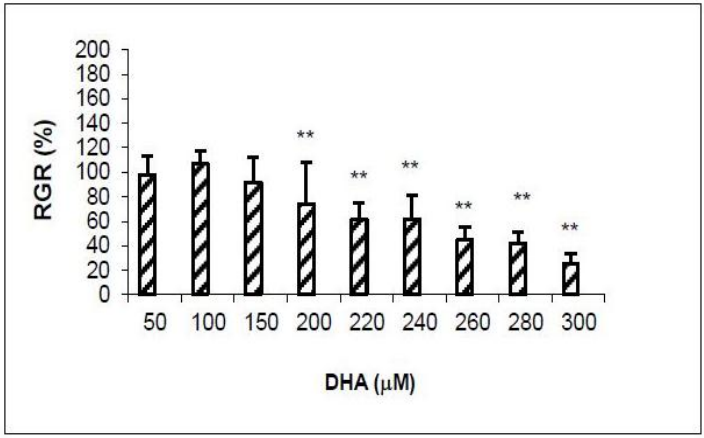

Figure 1. Effect of DHA treatment on cell viability of MDA-MB-231 cells.

The effects of DHA on cell growth inhibition were assessed and quantified by MTT assay. Cells were treated with various concentrations of DHA. Cells were seeded and cultured in a 96-well plate, after 48h, the medium was replaced with fresh medium supplemented with various concentrations of DHA (50-300μM) for further 72h. Data (mean ± DS; n = 8) are expressed as Relative Growth Rate (RGR) compared to the controls (100%), (**$p<0.01$).

Moreover, specific antibody directed to raft marker, flotillin-1, was used to identified raft-enriched fractions, observing that this marker was mostly present in fraction 5 (**Figure 2**). The same membranes were then used to reblot with antibody directed to clathrin HC, a protein highly represented in non-raft fractions of plasma membrane **[18]**, observing that this antibody recognized some bands especially in fraction 11 (**Figure 2**).

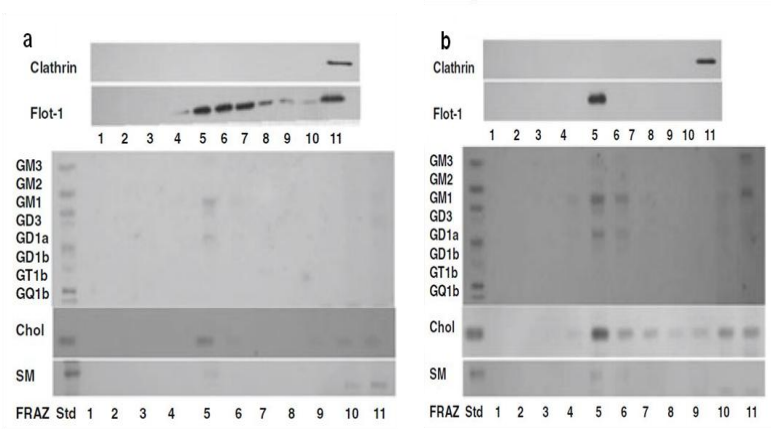

Figure 2. Lipid and protein characterization of DRMs.

Each fraction were analyzed by western blot (**top**) of a raft protein (flotillin-1) and non raft protein (clathrin) markers, and by HP-TLC (**bottom**) of SM, Chol and ganglioside GM1. (**a**) control cells and (**b**) treated with DHA.

Subsequently, we have evaluated the effects of DHA treatment on DRM structure and function. To determine the effects of exogenously added DHA on DRMs composition, the fractions were isolated from untreated and treated cells with DHA. After DRMs isolation we analyzed by GC PL fatty acid of DRMs fraction obtained from both treated and untreated cells. Even if no radiolabel compounds were used, we calculated the percentage of DHA incorporated into cell lipids.

Total fatty acid composition of DRM microdomains changes in DHA-treated cells compared to the untreated cells, as shown in **Table 1**. In particular, the treatment with DHA causes a significant increase of C22:6 n-3 (DHA) from 0.54 ± 0.29% to 6.66 ± 0.69% (mean ± SD; n = 10), and of C20:5 n-3 (EPA) from 0.74 ± 0.35% to 1.49 ± 0.18% (mean ± SD; n = 10). At the same time, the results show a reduction of C20:4 n-6 (AA) from 4.29 ± 1.23% to 2.47 ± 0.38% (mean ± SD; n = 10). The observed differences between the DHA-treated and untreated DRM microdomains was statistically significant (**$p<0.01$). It is worth noting that the percentage of Saturated Fatty Acids (SFA) about 70% was not changed by DHA treatment. These data demonstrated that DHA is incorporated in cell membrane microdomains and is able to alter fatty acid composition without decreasing the total percentage of SFA that characterize these structures. In particular, DHA determines an increase of n-3 PUFA and a decrease of n-6 PUFA.

To detect if DHA treatment induces specific changes in fatty acid composition of DRM microdomain phospholipids, we have carried out a study using a HPLC-ELSD system. In particular, membrane PLs and Chol have been purified and analyzed by HPLC-ELSD system.

	CTR	DHA
C16:0	42.63 ± 3.04	44.88 ± 0.12
C16:1	3.07 ± 1.45	5.00 ± 1.09*
C18:0	33.85 ± 3.96	26.70 ± 6.61
C18:1	10.75 ± 3.55	7.56 ± 2.01
C18:2 (LA)	2.24 ± 0.89	2.49 ± 1.98
C18:3 (ALA)	0.72 ± 0.29	**1.93 ± 0.35****
C20:3	0.61 ± 0.18	**0.25 ± 0.04****
C20:4 (AA)	4.29 ± 1.23	**2.47 ± 0.38****
C20:5 (EPA)	0.74 ± 0.35	**1.49 ± 0.18****
C22:5 (DPA)	0.33 ± 0.15	0.56 ± 0.06*
C22:6 (DHA)	0.54 ± 0.29	**6.66 ± 0.69****
SFA	76.48 ± 6.95	71.58 ± 6.69
MUFA	13.82 ± 4.77	12.56 ± 3.06
n-3 PUFA	2.34 ± 0.94	**10.64 ± 1.27****
n-6 PUFA	7.15 ± 1.91	5.22 ± 2.39

Table 2. FA composition of DRMs purified from DHA-treated and untreated cells. Data (mean ± SD; n = 10) are expressed as % of FAs, *p<0.05; **p<0.01. MUFA: Monounsaturated Fatty Acids; SFA: Saturated Fatty Acids.

The DHA incubation determines its incorporation in all PLs, except in PS, in MDA-MB-231 microdomains, as shown in **Figure 3**. In particular, DHA improves in PE from 1.99 ± 0.64% to 8.61 ± 1.34% (mean ± SD), in PI from 0.88 ± 0.05% to 9.94 ± 2.08% (mean ± SD), in PC from 0.6 ± 0.15% to 10.41 ± 1.99% (mean ± SD), and in SM from 0.3 ± 0.12% to 2.47 ± 0.14% (mean ± SD). At the same time, the results show a reduction of AA from 15.28 ± 3.46% to 5.38 ± 1.54% (mean ± SD) in PE and from 6.27 ± 0.82% to 2.17 ± 0.29% (mean ± SD) in PI. Moreover, DHA causes a significant increase of EPA from 0.46 ± 0.19% to 0.79 ± 0.13% (mean ± SD) in PE, from 0.8 ± 0.51% to 13.16 ± 3.48% (mean ± SD) in PI, from 0.35 ± 0.34% to 1.8 ± 0.21% (mean ± SD) in PC, and from 0.89 ± 0.35% to 3.78 ± 0.26% (mean ± SD) in SM. The observed differences between the DHA-treated and untreated DRM microdomains were statistically significant (*$p<0.05$; **$p<0.01$).

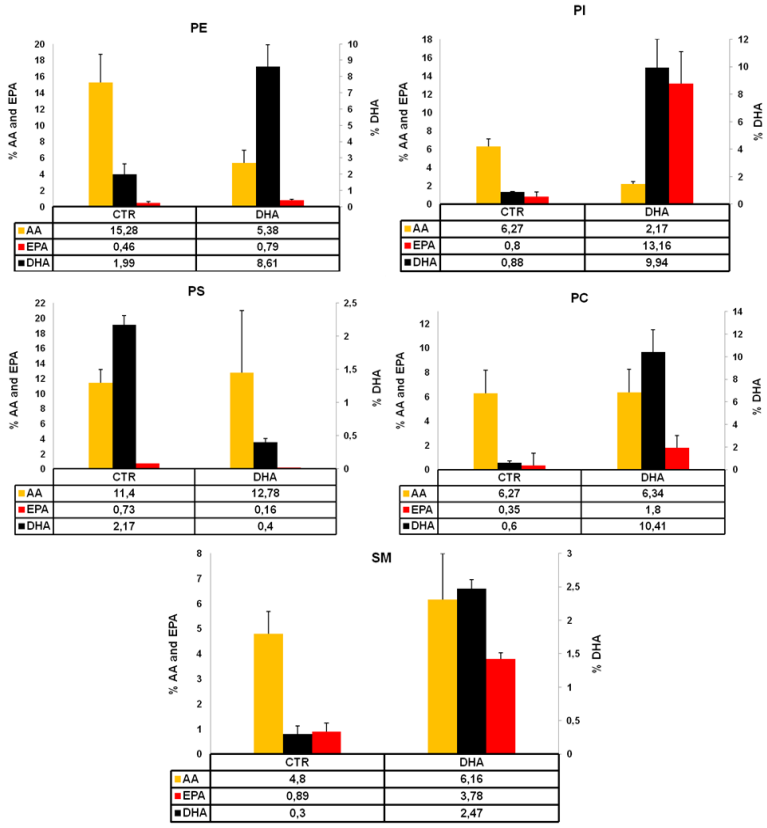

Figure 3. Histogram of DRM phospholipid polyunsaturated fatty acid composition of DHA-treated and untreated cells.

Values (mean ± SD; n = 15 and 6 untreated and DHA-treated cells respectively) are expressed as percentage of total fatty acids. Asterisks indicate significant differences between treated and control cells, *p<0.05; **p<0.01.

We can conclude that our data demonstrated that DHA is incorporated in breast cancer membrane microdomains with different specificity for the PLs moiety. Moreover, we have evaluated the effects of these incorporations on Chol and SM relative content in DRM microdomains. Collected data indicate that n-3 PUFA treatment modifies the content of SM. As show histogram reported in **Figure 4**, the DHA treatment shows a significant reduction (**p<0.01) of SM content about 40% (from 244.22 to 162.35 nmol/mg proteins) in DRMs compared to the control.

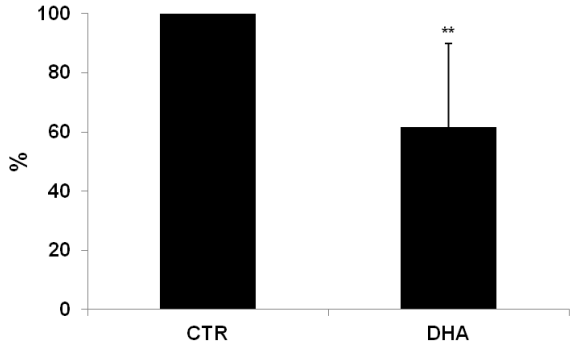

Figure 4 Effects of n-3 PUFAs on SM relative content in DRM.
MDA-MB-231 cells fractionated on sucrose gradient has been analysed by HPLC-ELSD. Cells were treated with DHA for 72h. Measurements were performed in triplicate and data are presented as percentage of control ± SD (n = 3), **p<0.01.

Cholesterol is known to play a key role in maintaining membrane integrity, signal transduction and fluidity. Moreover, cholesterol is a important component of lipid rafts **[21]**. For these reasons, we have also carried out a study to evaluate the effects of n-3 PUFA treatment on Chol content in microdomains. The data indicate that DHA determines a remarkable and significant reduction (*$p<0.05$) of this sterol. As shown in the histogram reported in **Figure 5**, DHA determines a reduction of Chol content about 70% content in DRMs (from 829.39 to 585.62 nmol/mg proteins) compared to the control.

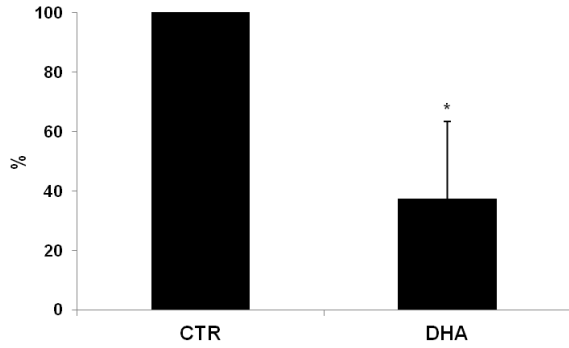

Figure 5. Effects of n-3 PUFAs on Chol relative content in DRM microdomains.
MDA-MB-231 cells fractionated on sucrose gradient has been analysed by HPLC-ELSD. Cells were treated with DHA for 72h. Measurements were performed in triplicate and data are presented as percentage of control ± SD (n = 3), *$p<0.05$.

Previously results obtained by AFM analysis were relative to DRMs isolated from estrogen-sensible human cancer cell, MCF-7. In particular, AFM investigation allowed to relate chemical–physical modifications, induced in breast cancer membrane microdomains by the DHA incubation, to their morpho-dimensional changes. AFM images were collected in a saline liquid buffer operating in Contact mode and in constant force conditions. **Figure 6**, as an example, shows two AFM topography images of MCF-7 DRMs before (**a)** and after (**b**) DHA incorporation. In particular, AFM imaging shows membrane patches with lateral size in the order, on average, of a few microns. After DHA incubation, AFM images clearly show a reduction of the number of membrane patches (in the order of about 20–30%). Moreover, DHA treated DRMs show, on average, a lateral size larger than the control ones. In addition, interestingly the profile lines (see **Figure 6**) show the presence, in the DHA incorporated rafts, of two different height ranges, 4–4.5nm and 6–6.5nm. In particular, the 6 nm thickness of membrane patches could be produced by DHA incorporation effects. On the contrary, untreated samples show a constant height of about 4nm as awaited for a membrane lipid bilayer.

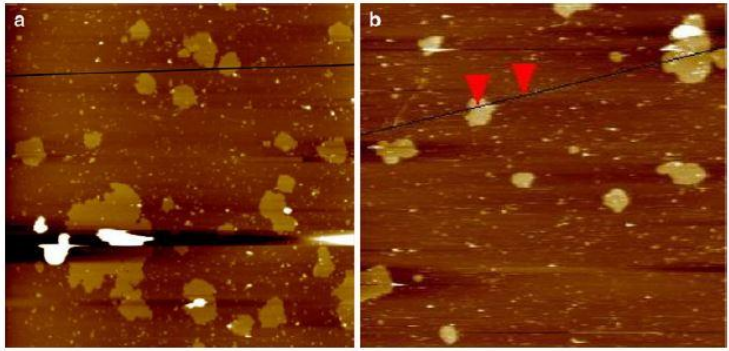

Figure 5. AFM topography images collected in contact mode in buffer solution of MCF-7 DRMs before (a) and after (b) treatment with DHA. For all the images: Vertical scale (from darkest to lightest): 50nm; scan area: 10x10 µm.

Figure 6. Height profiles corresponding to the two black lines drawn in the AFM topography images reported in Figure 5. (a) control sample, (b) DHA-treated sample.

4.4 Discussion

Our study was aimed to understand if the n-3 PUFA effects on cancer cells may be related to alteration of biochemical and biophysical characteristics of DRMs.

There are in vitro and in vivo evidences that the administration of EPA and DHA is able to reduce cancer proliferation and to increase apoptosis **[2,3]** as well as inhibit angiogenesis and metastasis, and to influence cancer differentiation **[4,5]**. The plasma membrane is involved in many aspects of cell biology, including proliferation, differentiation and apoptosis. Fatty acids in the PLs of cell membranes play a key role in maintaining the fluidity, structure and function of the cell membrane. Thus, changes in membrane PL fatty acid composition can influence the function of cells. In particular, n-3 PUFAs incorporated into membrane PLs can potentially affect a variety of plasma membrane physical properties including membrane thickness, fluidity, elasticity, permeability, cell signaling pathways, and the structure and function of membrane microdomains, known as lipid rafts **[6,22,23]**.

Lipid rafts are known to be rich in signalling proteins, such as Src, and tyrosin kinases receptors as EGFR, and to regulate signal transduction in normal and cancer cells **[24,25]**. The key difference between the lipid rafts and the surrounding membrane bilayers is their lipid composition. Rafts contain Chol and SLs at concentrations up to 50% higher than rest of the membrane. Moreover, the hydrophobic alkyl chains of lipids within the rafts are more saturated compared to the surrounding bilayer and hence tightly packed **[26-28]**.

In the present paper, we treated MDA-MB-231 cells with DHA in relative high concentration to assess if they were incorporated in membrane microdomain PLs and were able to change chemical and physical properties of these structures. We chosen relative high concentration of PUFA because in our condition the cells were relatively resistant to FA treatment. Moreover, the EPIC-Norfolk cohort study showed that the average concentration of DHA in plasma is 236.2μmol/l, with a high individual variability **[29]**. These data demonstrate that in vivo the doses used in our study can be reached and in some case are relative normal.

Focusing on MDA-MB-231 breast cancer cells treated with DHA, our data demonstrate that DHA and its metabolites are inserted with different yield in cell membrane microdomains and are able to alter fatty acid composition without decreasing the total percentage of SFA that characterize these structures. We have also analyzed the changes in content of SM in DRMs. In particular, DHA treatment determines a reduction of SM content of about 40%. These reductions might be due to an activation of Sphingomyelinase (SMase). SMase is an enzyme that catalyzes the hydrolysis of SM to ceramide. A variety of studies has shown that the ceramide is ubiquitously produced during cellular stress and is associated with apoptosis **[31,31]**. The neutral SMase (N-SMase) is a plasma membrane-bound enzyme that is implicated in mediating apoptosis and it resides in lipid rafts **[30]**. Therefore, factors influencing the lipid composition of membranes can influence the activity and distribution of N-SMase in microdomains.

Wu *et al.*, already demonstrated that in Jurkat leukemic cells, EPA and DHA increase the N-SMase activity inducing SM hydrolysis **[32]**, our data are in agreement with these observations. Moreover, we also analyzed the changes in content of Chol of DRMs. Our results showed that DHA determines a reduction of Chol content of about 70%. Sterols are the major non-polar lipids of cell membranes, and Chol predominates in mammalian cell. The unique puckered four-ring structure of Chol confers special biophysical properties that increase the ordering (cohesion and packing) of neighbouring lipids. Because of the rigid sterol backbone, Chol is preferentially positioned in close proximity to saturated hydrocarbon chains of neighbouring lipids, as these are more inflexible and elongated compared with those of unsaturated lipids. It therefore plays a very important and dominant role in raft formation and stabilization **[28,33,34]**.

Cholesterol accumulation is known to be associated in many tumors, including prostate cancer and oral cancer **[35,36]**, and dysregulated in lung and breast cancers **[37,38]**. Moreover, depletion of Chol results in the disorganization of DRMs microdomains and dissociation of proteins bound to the lipid rafts **[9]**. Grimm *et al.*, recently demonstrated that treatment of SH-SY5Y cells with DHA displaces Chol from DRMs to "non-raft" detergent soluble membranes (DSMs) **[39]**. The laboratory of Chapkin, have evaluated the effects of n-3 PUFA administration on Chol and SM content in lipid rafts in multiple cell types, such as immortalized young adult mouse colonocytes (YAMC) and mouse splenic T-cells.

Their results have showed a reduction of Chol (46%) and SM (30%) in YAMC and mouse splenic T-cells fed n-3 PUFAs, respectively **[40]**. Thus, our data are in agreement with these observations. Unfavorable interaction between Chol and PUFA chains has been clearly demonstrated by the exclusion of Chol from dipolyunsaturated PC liposomes where it is forced to directly contact polyunsaturated chains. Studies using a variety of techniques including Differential Scanning Calorimetry (DSC), ^{2}H NMR spectroscopy, indicate of that the poor affinity of DHA for Chol provides a lipid-driven mechanism for lateral phase separation of cholesterol-rich lipid microdomains from the surrounding bulk membrane. This could in principle alter the size, stability and distribution of cell surface lipid microdomains such as rafts **[22]**. Since lipid rafts are predominantly enriched in saturated fatty acids-containing SLs and Chol, the incorporation of PUFA, especially DHA, determines a reorganization of membrane microdomains. In particular, different models have been proposed: Wassall and Stillwell hypothesized that the energetically less favorable interaction between Chol and DHA promotes lateral phase segregation into sterol-poor/PUFA-rich and sterol-rich/saturated fatty acid-rich microdomains **[41]**. Moreover, Shaikh proposed the formation of ‘‘declustered rafts’’. His model shows that n-3 PUFAs disrupt the molecular organization of membrane microdomains by directly incorporating into the raft, shifting out the Chol into non-rafts domains with reorganization of lipids and proteins **[42]**. Finally, Chapkin and his lab have demonstrated that n-3 PUFAs modify lipid raft organization, leading to altered cell signaling and function.

They have proposed a putative model for the effect of n-3 PUFAs on lipid rafts where n-3 PUFAs are incorporated into PLs which are inserted into both raft and non-raft regions of the plasma membrane. This results in a deplete of Chol and SM and a clustering of lipid raft regions. Moreover, many lipid raft associated proteins are relocated to the bulk membrane. This results in a suppression of lipid raft mediated processes, including the activation and downstream signal transduction **[40]**.

AFM imaging was useful to characterize morpho-dimensionally changes in DRMs studying purified membrane samples both before and after the DHA incorporation. In particular, preliminary data showed that, in breast cancer cells after DHA incorporated, membrane patches had two different height ranges, 4-4.5nm and 6-6.5nm (in the order of about 20%). On the contrary, untreated samples showed a constant height of about 4 nm as awaited for a membrane lipid bilayer. Moreover, DHA-treated samples show, a decrease the number of membrane patches in the order of about 20-30%, and, in on average, a lateral size larger than the control ones. These changes might influence resident protein conformation turning on and/or off signaling proteins, and modulate cellular events. In fact acyl moieties of proteins partition in the cytoplasmic leaflet of the membrane lipid bilayer. Lipid alterations in the cytoplasmic lipid leaflet of membrane rafts would hence be particularly effective in displacing palmitoylated proteins.

4.5 Conclusions

Complex SLs and Chol are required to facilitate raft formation. Because of its polyunsaturation, DHA is sterically incompatible with SLs and Chol and, therefore, is believed to alter lipid raft behavior and protein function. Our results showed that n-3 PUFAs are able to modify membrane microdomain biochemical and biophysical features leading to decrease of breast cancer cell proliferation probably through different mechanisms related to acyl chain length and unsaturation. In particular, DHA may change the biophysical properties of lipid rafts decreasing the content of Chol and SM. We suggest that the alteration of microdomains lipid composition might determine the displacement of proteins, such as EGFR and Ras, from rafts in n-3 PUFA treated cells with alteration of signal transduction. Although caution is needed when drawing conclusions based solely on the capacity of detergent to solubilize lipids, collectively, these data support our hypothesis that n-3 PUFAs can alter specific lipid microdomains.

References

1. Hardman WE: **Omega-3 fatty acids to augment cancer therapy**. *The Journal of nutrition* 2002, **132**:3508S-3512S.
2. Corsetto PA, Montorfano G, Zava S, Jovenitti IE, Cremona A, Berra B, Rizzo AM: **Effects of n-3 PUFAs on breast cancer cells through their incorporation in plasma membrane**. *Lipids in health and disease* 2011, **10**:73.
3. Serini S, Piccioni E, Merendino N, Calviello G: **Dietary polyunsaturated fatty acids as inducers of apoptosis: implications for cancer**. *Apoptosis* 2009, **14**(2):135-152.
4. Merendino N, Costantini L, Manzi L, Molinari R, D'Eliseo D, Velotti F: **Dietary omega -3 polyunsaturated fatty acid DHA: a potential adjuvant in the treatment of cancer**. *BioMed research international* 2013, **2013**:310186.
5. Vaughan VC, Hassing MR, Lewandowski PA: **Marine polyunsaturated fatty acids and cancer therapy**. *British journal of cancer* 2013, **108**(3):486-492.
6. Wassall SR, Brzustowicz MR, Shaikh SR, Cherezov V, Caffrey M, Stillwell W: **Order from disorder, corralling cholesterol with chaotic lipids. The role of polyunsaturated lipids in membrane raft formation**. *Chemistry and physics of lipids* 2004, **132**(1):79-88.
7. Williams EE, Jenski LJ, Stillwell W: **Docosahexaenoic acid (DHA) alters the structure and composition of membranous vesicles exfoliated from the surface of a murine leukemia cell line**. *Biochimica et biophysica acta* 1998, **1371**(2):351-362.

8. Shaikh SR, Brzustowicz MR, Stillwell W, Wassall SR: **Formation of inverted hexagonal phase in SDPE as observed by solid-state (31)P NMR**. *Biochemical and biophysical research communications* 2001, **286**(4):758-763.
9. Schley PD, Brindley DN, Field CJ: **(n-3) PUFA alter raft lipid composition and decrease epidermal growth factor receptor levels in lipid rafts of human breast cancer cells**. *The Journal of nutrition* 2007, **137**(3):548-553.
10. Chapkin RS, Wang N, Fan YY, Lupton JR, Prior IA: **Docosahexaenoic acid alters the size and distribution of cell surface microdomains**. *Biochimica et biophysica acta* 2008, **1778**(2):466-471.
11. Shaikh SR, Teague H: **N-3 fatty acids and membrane microdomains: from model membranes to lymphocyte function**. *Prostaglandins, leukotrienes, and essential fatty acids* 2012, **87**(6):205-208.
12. Simons K, Toomre D: **Lipid rafts and signal transduction**. *Nature reviews* 2000, **1**(1):31-39.
13. Razani B, Woodman SE, Lisanti MP: **Caveolae: from cell biology to animal physiology**. *Pharmacological reviews* 2002, **54**(3):431-467.
14. Fastenberg ME, Shogomori H, Xu X, Brown DA, London E: **Exclusion of a transmembrane-type peptide from ordered-lipid domains (rafts) detected by fluorescence quenching: extension of quenching analysis to account for the effects of**

domain size and domain boundaries. *Biochemistry* 2003, **42**(42):12376-12390.

15. Gimpl G, Burger K, Fahrenholz F: **Cholesterol as modulator of receptor function**. *Biochemistry* 1997, **36**(36):10959-10974.
16. Pike LJ, Casey L: **Cholesterol levels modulate EGF receptor-mediated signaling by altering receptor function and trafficking**. *Biochemistry* 2002, **41**(32):10315-10322.
17. Mosmann T: **Rapid colorimetric assay for cellular growth and survival: application to proliferation and cytotoxicity assays**. *Journal of immunological methods* 1983, 65(1-2):55-63.
18. Fabelo N, Martin V, Santpere G, Marin R, Torrent L, Ferrer I, Diaz M: **Severe alterations in lipid composition of frontal cortex lipid rafts from Parkinson's disease and incidental Parkinson's disease**. *Molecular* medicine 2011, **17**(9-10):1107-1118.
19. Lowry OH, Rosebrough NJ, Farr AL, Randall RJ: **Protein measurement with the Folin phenol reagent**. *The Journal of biological chemistry* 1951, **193**(1):265-275.
20. Biondo PD, Brindley DN, Sawyer MB, Field CJ: **The potential for treatment with dietary long-chain polyunsaturated n-3 fatty acids during chemotherapy**. *The Journal of nutritional biochemistry* 2008, **19**(12):787-796.
21. Patra SK: **Dissecting lipid raft facilitated cell signaling pathways in cancer**. *Biochimica et biophysica acta* 2008, **1785**(2):182-206.

22. Stillwell W, Wassall SR: **Docosahexaenoic acid: membrane properties of a unique fatty acid**. *Chemistry and physics of lipids* 2003, **126**(1):1-27.
23. Roynette CE, Calder PC, Dupertuis YM, Pichard C: **n-3 polyunsaturated fatty acids and colon cancer prevention**. *Clinical nutrition (Edinburgh, Scotland)* 2004, **23**(2):139-151.
24. Edidin M: **Membrane cholesterol, protein phosphorylation, and lipid rafts**. *Sci STKE* 2001, **2001**(67):pe1.
25. Zajchowski LD, Robbins SM: **Lipid rafts and little caves. Compartmentalized signalling in membrane microdomains**. *European journal of biochemistry / FEBS* 2002, **269**(3):737-752.
26. Silvius JR: **Role of cholesterol in lipid raft formation: lessons from lipid model systems**. *Biochimica et biophysica acta* 2003, **1610**(2):174-183.
27. Maxfield FR, Tabas I: **Role of cholesterol and lipid organization in disease**. *Nature* 2005, **438**(7068):612-621.
28. Epand RM: **Proteins and cholesterol-rich domains**. *Biochimica et biophysica acta* 2008, **1778**(7-8):1576-1582.
29. Welch AA, Shakya-Shrestha S, Lentjes MA, Wareham NJ, Khaw KT: **Dietary intake and status of n-3 polyunsaturated fatty acids in a population of fish-eating and non-fish-eating meat-eaters, vegetarians, and vegans and the product-precursor ratio [corrected] of alpha-linolenic acid to long-chain n-3 polyunsaturated fatty acids: results from the EPIC-Norfolk cohort**. *The American journal of clinical nutrition* 2010, **92**(5):1040-1051.

30. Jayadev S, Liu B, Bielawska AE, Lee JY, Nazaire F, Pushkareva M, Obeid LM, Hannun YA: **Role for ceramide in cell cycle arrest**. *The Journal of biological chemistry* 1995, **270**(5):2047-2052.
31. Veldman RJ, Maestre N, Aduib OM, Medin JA, Salvayre R, Levade T: **A neutral sphingomyelinase resides in sphingolipid-enriched microdomains and is inhibited by the caveolin-scaffolding domain: potential implications in tumour necrosis factor signalling**. *The Biochemical journal* 2001, **355**(Pt 3):859-868.
32. Wu M, Harvey KA, Ruzmetov N, Welch ZR, Sech L, Jackson K, Stillwell W, Zaloga GP, Siddiqui RA: **Omega-3 polyunsaturated fatty acids attenuate breast cancer growth through activation of a neutral sphingomyelinase-mediated pathway**. *International journal of cancer* 2005, **117**(3):340-348.
33. London E, Brown DA: **Insolubility of lipids in triton X-100: physical origin and relationship to sphingolipid/cholesterol membrane domains (rafts)**. *Biochimica et biophysica acta* 2000, **1508**(1-2):182-195.
34. Wang TY, Silvius JR: **Cholesterol does not induce segregation of liquid-ordered domains in bilayers modeling the inner leaflet of the plasma membrane**. *Biophysical journal* 2001, **81**(5):2762-2773.
35. Kolanjiappan K, Ramachandran CR, Manoharan S: **Biochemical changes in tumor tissues of oral cancer patients**. *Clinical biochemistry* 2003, **36**(1):61-65.

36. Freeman MR, Solomon KR: **Cholesterol and prostate cancer**. *Journal of cellular biochemistry* 2004, **91**(1):54-69.
37. Bennis F, Favre G, Le Gaillard F, Soula G: **Importance of mevalonate-derived products in the control of HMG-CoA reductase activity and growth of human lung adenocarcinoma cell line A549**. *International journal of cancer* 1993, **55**(4):640-645.
38. El-Sohemy A, Archer MC: **Inhibition of N-methyl-N-nitrosourea- and 7,12-dimethylbenz[a] anthracene-induced rat mammary tumorigenesis by dietary cholesterol is independent of Ha-Ras mutations**. *Carcinogenesis* 2000, **21**(4):827-831.
39. Grimm MO, Kuchenbecker J, Grosgen S, Burg VK, Hundsdorfer B, Rothhaar TL, Friess P, de Wilde MC, Broersen LM, Penke B *et al*: **Docosahexaenoic acid reduces amyloid beta production via multiple pleiotropic mechanisms**. *The Journal of biological chemistry* 2011, **286**(16):14028-14039.
40. Turk HF, Chapkin RS: **Membrane lipid raft organization is uniquely modified by n-3 polyunsaturated fatty acids**. *Prostaglandins, leukotrienes, and essential fatty acids* 2013, **88**(1):43-47.
41. Wassall SR, Stillwell W: **Polyunsaturated fatty acid-cholesterol interactions: domain formation in membranes**. *Biochimica et biophysica acta* 2009, **1788**(1):24-32.
42. Shaikh SR: **Biophysical and biochemical mechanisms by which dietary N-3 polyunsaturated fatty acids from fish oil**

disrupt membrane lipid rafts. *The Journal of nutritional biochemistry* 2012, **23**(2):101-105.

Chapter 5

Atomic Force Microscopy imaging of lipid rafts of human breast cancer cells

This chapter is based on: Cremona A, Orsini F, Arosio P, Corsetto PA, Montorfano G, Lascialfari A, Rizzo AM. (2012). Atomic force microscopy imaging of lipid rafts of human breast cancer cells. Biochim Biophys Acta. 1818(12):2943-9

5.1 Introduction

Accumulating evidence indicates that cell membrane constituents might be not randomly distributed but rather organized in small lipid/protein domains enriched in sphingomyelin (SM) and cholesterol (Chol), known as lipid rafts **[1,2]**. Lipid rafts are tiny, dynamic, and ordered microdomains, enriched in cholesterol and sphingolipids **[3]**. These domains are characterized physic-chemically by a relative rigidity and reduced fluidity compared with the surrounding plasma membrane, which is in part caused by their cholesterol content **[4,5]**. Moreover, they are highly dynamic and may rapidly assemble and disassemble, leading to a dynamic segregation of proteins **[6]**. Proof of the existence of lipid rafts is based largely on biochemical evidence even if the lipid raft hypothesis is still a contentious topic, with much of the scientific community divided. In particular, the inability to visualize lipid rafts directly in cell membranes, as well as a lack of understanding of some basic properties (e.g. size and lifetime), has led to controversy over their definition and existence.

The coexistence of domains in liquid-ordered (Lo) and liquid-disordered (Ld) phases has been extensively characterized **[7,8]**. Studies of membrane model systems strongly suggest that lipids could laterally segregate in membranes under certain conditions, and could form distinct lipid domains with particular structural characteristics (i.e. a particular lipid phase). Self-associative properties unique to sphingolipids and Chol *in vitro* could facilitate selective lateral segregation in the membrane plane and serve as a basis for lipid sorting *in vivo* **[1]**. Studying lipid rafts is challenging since they are probably too small to be resolved by techniques such as optical and fluorescence microscopy. Today, high-resolution techniques that utilize fluorescent probes are available for studies of membrane heterogeneity in intact cells, allowing the study of small and elusive microdomains *in vivo* **[9,10,11]**. Some of these techniques are particularly appealing because of their capability to reveal the dynamics of membrane domains. For example, Stimulated-Emission-Depletion (STED) nanoscopy **[12]** provided direct evidence in live cells that certain lipids are transiently trapped in Chol-assisted molecular complexes. In particular, these studies have demonstrated that lipid raft markers, such as GPI-anchored proteins, SM, and GM1, were confined into membrane areas with diameters about 20nm. These complexes were transient and had an average lifespan about 10^{-2} sec. The complexes appeared to be cholesterol-dependent, as the trapping was reduced upon cholesterol depletion **[9,13,14]**. Photoactivated Localization Microscopy (PALM) is another powerful approach for investigating protein/lipid organization.

PALM imaging proved that Chol- and sphingolipid-enriched microdomains occupy different regions on the plasma membrane with lateral dimensions in the order of a hundred of nanometers **[15]**. In the past decade, Atomic force microscopy (AFM) has emerged as a powerful tool to obtain nano-structural details of soft and fragile materials such as proteins and lipids.

AFM operating in physiological-like conditions and providing nanometer spatial resolution without fixation, staining, or labeling, appears to be a powerful tool to quantitatively perform a morpho-dimensional characterization of lipid rafts **[16]**. Moreover, thanks to its high signal-to-noise ratio, AFM allows to monitor function related structural conformational changes and to observe structural details of membrane proteins under physiological conditions, revealing information on the protein oligomeric state and on the supramolecular architecture of membrane protein complexes **[17,18]**.

In this work we applied AFM, together with biochemical assays, Western Blotting (WB) and High Performance Thin Layer Chromatography (HP-TLC), to the study of Detergent-Resistant Membranes (DRMs) of MDA-MB-231 human breast cancer cells. In particular, the different fractions, isolated in the purification process by ultracentrifugation on sucrose gradient, have been analyzed with respect to their protein content and morpho-dimensionally characterized.

5.2 Materials and methods

Cell Lines and Culture Conditions

See **Chapter 4**, section Materials and methods, for a detailed description of human breast cancer cells MDA-MB-231 and culture conditions

DRMs Isolation

See **Chapter 4**, section Materials and methods, for a detailed description of DRM isolation from MDA-MB-231 cells.

Western blot analysis for flotillin-1

All fractions were separated by SDS-PAGE (10% polyacrylamide gel) and transferred onto a polyvinylidene difluoride (PVDF) membrane overnight then blocked in blocking buffer consisting of 5% (w/v) dried non-fat milk in Tris-buffered saline (T-TBS: 10mM Tris/HCl, pH 7.5, 150mM NaCl, 0.1% (v/v) Tween®20) at room temperature for 1h. The blots were treated with anti-flotillin-1 primary antibodies diluted 1:200 in blocking buffer at room temperature for 2h, washed with T-TBS and incubated with the proper secondary antibody in blocking buffer at room temperature for 1h. The protein bands were visualized using ECL reagents (PerkinElmer, USA).

Lipid composition analysis

See **Chapter 4**, section Materials and methods, for a detailed description of DRM lipid composition analyses.

AFM imaging

See **Chapter 4**, section Materials and methods, for a detailed description of AFM imaging conditions. AFM imaging has been performed in collaboration with the laboratory of Prof. A. Lascialfari Department of Physics, Università degli Studi di Milano (Italy).

Sample preparation protocol for AFM imaging

See **Chapter 4**, section Materials and methods, for a detailed description of the purified membrane sample preparation protocol for AFM imaging.

AFM-immunolabeling and analysis procedures

Membrane samples, adsorbed onto mica surface and prepared as above described, were incubated with different antibodies such as to raft marker as rabbit polyclonal anti flotillin-1 antibodies raised against amino acids 324–427 of flotillin-1, a protein segment near the C-terminus and fully exposed in the cytoplasmic side of the plasma membrane, and non-raft marker such as anti-clathrin hc mouse monoclonal antibody raised against the N-terminus of clathrin heavy chain of human origin (Santa Cruz Biotechnology, USA).

The antibodies were diluted 1:4 in recording buffer as reported in literature **[19]** and the sample was imaged prior and after 60min to assess the antibody binding, allowing the direct comparison of the same membrane patches before and after antibody binding. We have evaluated the difference of the surface area both, before and after the antibodies incubation, as follows.

The contour line of a number of membrane patches as well as of microdomains protruding from the patch surface were marked before and after 60min treatment with anti flotillin-1 and anti-clathrin hc antibodies directly from several AFM images using the ImageJ 1.45 software (NIH, USA).

Statistical analysis

The data are presented as mean ± SD (or SE). Student's t-test was used for comparisons between treated and control cells and the level of statistical significance was set at $*p<0.01$.

5.3 Results

In the present work, lipid rafts were isolated from MDA-MB-231 human breast cancer cells as DRMs by ultracentrifugation on a discontinuous sucrose gradient as described in details in Materials and Methods. We have applied biochemical assays WB and HP-TLC, together with AFM, to characterize the DRMs of MDA-MB-231 cells.

As reported in **Chapter 4** "*Chemical-physical changes in cell membrane microdomains of breast cancer cells after omega-3 PUFA incorporation",* the purity of isolated DRMs was demonstrated using lipid and protein raft and non-raft markers. In particular, biochemical analysis of the distribution of some lipids highly present in lipid rafts, namely Chol, Sm and ganglioside (GM1), carried out by HP-TLC confirmed the presence of the DRMs in the 5 and 6 fractions.

The presence of DRMs was verified detecting in all the 11 collected fractions the raft and non-raft protein marker, flotillin-1 and clathrin HC, respectively **[20]** by SDS-PAGE assay and WB analysis.

In particular, as shown in **Figure 1**, WB analysis showed that in the low-density fractions (fractions 5 and 6), corresponding to the 5% and 30% sucrose interface, are enriched of flotillin-1 and depleted of clathrin HC indicating that these fractions are enriched with DRMs

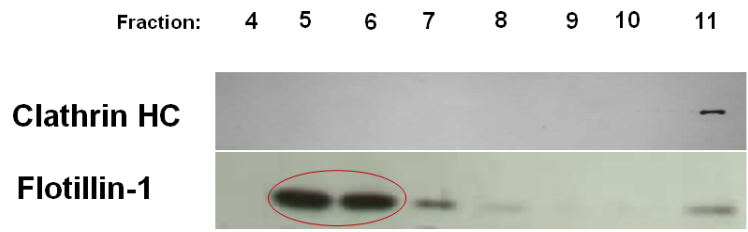

Figure 1. Distribution of flotillin-1 and clathrin HC in DRMs.
Triton X-100 lysates of cell cultures were purified and fractionated by sucrose gradient ultracentrifugation. Equal volumes of each fraction were analyzed by WB using anti-flotillin-1 and anti-clathrin HC antibodies.

In order to perform a morpho-dimensional characterization of DRMs, all the 11 fractions purified in the ultracentrifugation process were visualized by AFM. AFM images were collected in a saline liquid buffer operating in tapping mode. Tapping mode can reduce significantly the lateral forces, allowing to study samples too fragile to withstand the lateral forces of Contact mode as biological samples.

It uses an oscillating cantilever at its resonance frequency, placed a few nanometers above the sample surface, and only at the end of each oscillation cycle the tip interacts with the surface. Because the tip is not continuously in contact with the surface, the sample degradations are minimized.

Figure 2 shows AFM topography images of some among the 11 fractions isolated and visualized in a saline buffer. Depending on the fractions visualized, the situation dramatically changes. In particular, AFM imaging of fractions 5 and 6 shows the higher number of membrane patches, which decreases moving from fractions 5 to 7.

Moreover, only small membrane fragments with lateral dimensions of a few dozen of nanometers are visualized on the mica support in fractions from 1 to 4, 8 and 9. Fractions 10 and 11 show a continuous and homogeneous distribution of membrane fragments on the whole mica surface. It is worth noting that these fractions are recovered at the bottom of the tube exactly where the post-nuclear supernatant (PNS) is placed before the ultracentrifugation process.

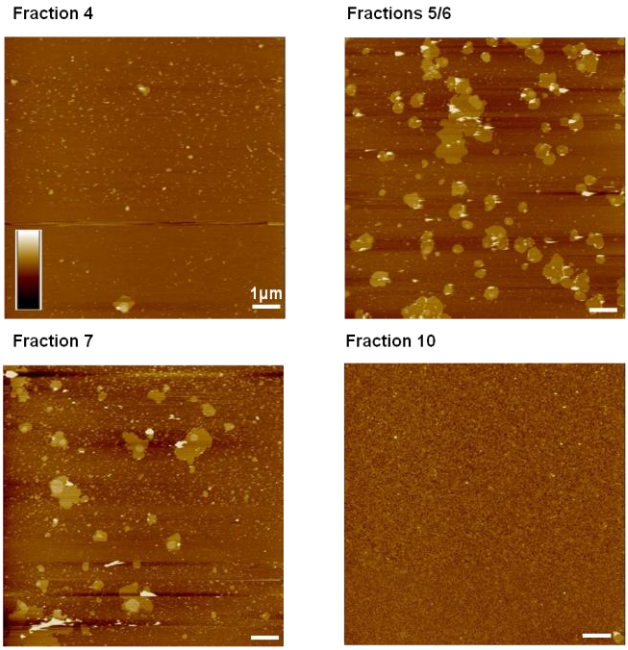

Figure 2. AFM topography images of some isolated fractions.

Purified membranes were diluted 1:30 in adsorbtion buffer and placed on a mica support. For all the images: scan area: 10×10µm; vertical scale: 20nm (see insert in **Fig.)**.

Taken together, the biochemical analyses and AFM imaging indicate that DRMs are mainly present in the low-density fractions (fractions 5 and 6). For these reasons a detail AFM study of these fractions have been performed. As an example, an AFM topography image of membrane samples prepared from fraction 5 is reported in **Figure 3**.

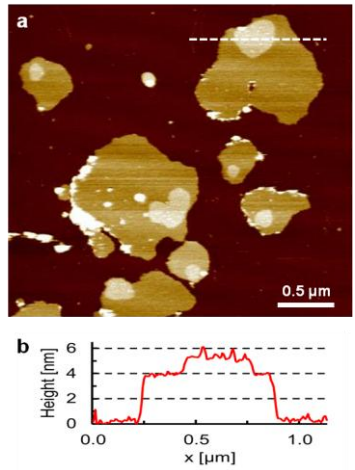

Figure 3. AFM topography image of membrane samples collected in liquid buffer in tapping mode (a). (b) Height profile corresponding to the white line drawn in **(a).** Scan area: 2.5×2.5µm; vertical scale: 9nm (see insert in **Fig. 2)**.

Different regions can be easily identified in **Figure 3**: the mica support, membrane patches and microdomains protruding from the membrane surface. Analyzing several AFM topography images collected in tapping mode in buffer solution we have morpho-dimensionally characterized the structures visualized in **Figure 3a**.

In particular, the membrane patches showed lateral size in the order, on average, of a few microns and height of about 4 nm, as awaited for lipid bilayers. Moreover, the microdomains, protruding by 1-2nm from the surrounding membrane as shown in the height profile reported in **Figure 3b**, exhibited lateral dimensions in the range of 100–500nm, in agreement with the data obtained using artificial membranes **[21]**.

The brighter areas visible on membrane patches could be identified as protein aggregates probably produced during the sample deposition process and induced by the interactions with the mica support.

Microdomains have a highest surface roughness compared to the surrounding membrane that appears very smooth. Surface roughness of membrane patches as well as of the membrane microdomains, expressed as differences in the root-mean-square of the vertical Z dimension values within the examined areas, was calculated according to the following equation:

$$rms_{xy} = \sqrt{\sum_{x,y=1}^{N} \frac{\left(Z_{x,y} - Z_{average}\right)^2}{N^2}}$$

where $Z_{average}$ is the average Z value within the examined area, $Z_{x,y}$ is the local Z value and N indicates the number of points within the area.

Rms surface roughness values were calculated as the mean of at least 15 measurements on 50 × 50nm square areas collected on the surface of membrane patches and membrane microdomains observed in several AFM topography images.

In particular, the microdomain has a mean rms surface roughness of 0.26 ± 0.03nm (mean ± SD; n = 18), while the surrounding membrane is very smooth with a mean rms surface roughness of only 0.11 ± 0.01nm (mean ± SD; n = 15).

The microdomains visualized on the membrane patch surface appear to be very interesting since their dimensions are in line with the range expected for lipid rafts as reported extensively in literature **[22,23]**.

For this reason we also performed a high resolution AFM imaging of these areas aiming at obtaining more detailed insights.

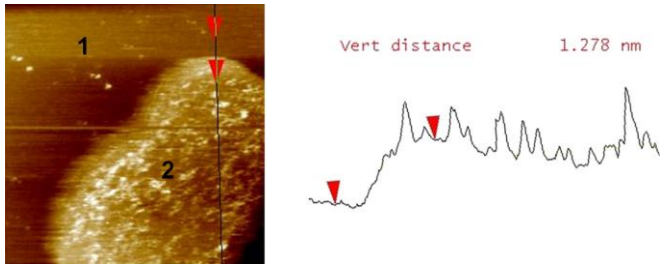

Figure 4. High resolution AFM topography image.
AFM image of a membrane sample prepared from fraction 5 collected in liquid buffer in tapping mode **(left).** Height profile corresponding to the black line drawn in AFM image **(right).** Scan area=200×200nm; vertical scale: 9nm (see insert in **Fig. 2)**.

In particular, the AFM image obtained by scanning an area of a few hundred square nanometers and reported in **Figure 4**, shows a microdomain protruding by about 1nm from the membrane surface (red arrows). Moreover, the height profile (see **Figure 4 right**) shows some structural features on the microdomain surface with heights of about

1nm and lateral sizes of a few nanometers, thus suggesting the presence of proteins embedded in the microdomain.

Unfortunately these nanometer structures cannot be identified, but their structural features appear to be in good agreement with the dimensions of proteins observed by AFM on biological membranes **[24]**.

In order to obtain more information regarding the nature of the microdomains we incubated at room temperature the purified membrane samples adsorbed onto mica with specific antibody against a lipid raft protein marker, flotillin-1. In particular, rabbit polyclonal antibodies raised against amino acids 324–427 of flotillin-1, a protein segment near the C-terminus and fully exposed in the cytoplasmic side of the plasma membrane were injected into the AFM liquid cell. The sample was visualized before and after 60min to assess the antibody binding, allowing the direct comparison of the same membrane patches before and after antibody binding. As shown in **Figure 5**, the microdomains visualized after the antibody incubation changed in their dimensions and shape (see circled areas in **Figure 5a** and **b**). In particular, microdomains protruding from the smooth lipid membrane increased their surface area by about 20% upon antibody binding. We found a surface area increase of 22.3 ± 4.9% (mean ± SD; n = 25) and 9.3 ± 2.3% (mean ± SD; n = 25) for microdomains and membrane patches respectively as indicated in the histogram in **Figure 5c**.

The observed difference among the surface area increase of the microdomains, induced by the anti-flotillin-1 treatment, and of membrane patches both in the anti-flotillin-1 treated and control

experiment as well as of the microdomains in the control experiment is statistically significant (*p<0.01).

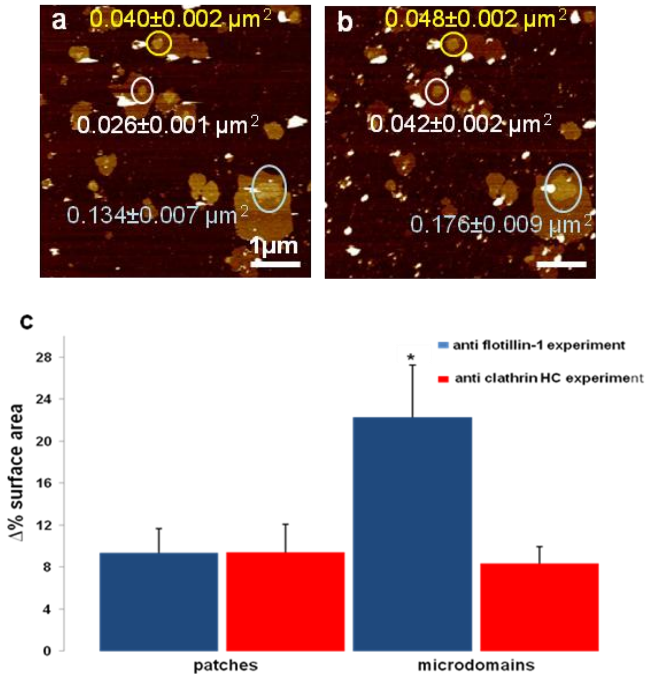

Figure 5. AFM-immunolabeling.

AFM topography images of membrane samples prepared from fraction 5 and collected in liquid buffer in tapping mode at room temperature. Membrane patches **(a)** were incubated with anti-flotillin-1 antibody for different times. Just after 60min of treatment **(b)** the surface area of microdomains clearly increases (see circled areas). Scan area: 5×5µm; vertical scale: 9nm (see insert in **Fig. 2)**. **(c)** Histogram of the surface area increase for membrane patches and microdomains, after 60min anti-flotillin-1 antibody incubation (blue bars) and of the surface area increase for membrane patches, and microdomains in the control experiment after 60min anti-clathrin hc antibody incubation (red bars). Asterisk indicates significant differences between room and physiological temperature (*p<0.01).

To demonstrate specificity and get rid of possible physisorption phenomena, we carried out experiments using non-rafts marker antibody. In particular, membrane samples were incubated with antibodies raised against a non raft protein marker, clathrin hc, **[25]** as described in Material and methods. After 60min incubation with anti-clathrin hc antibody, microdomains did not show significant variation in shape and lateral dimensions. In particular, after anti-clathrin hc incubation, surface area increases of 8.1 ± 1.6% (mean ± SD; n = 10) and 9.4 ± 2.5% (mean ± SD; n = 10) for microdomains and membrane patches, respectively (see histogram reported in **Figure 5c**). However, the difference between the surface area increase of microdomains and membrane patches in these experiments was not statistically significant. The experimental data suggest that the protein nature of the visualized nanometer structures and confirm the presence of flotillin-1, a protein marker of lipid rafts, in the membrane microdomains.

Moreover, although the enlargement of the microdomain surface area is the more evident effect visible in AFM images (see **Figure 5**), it is expected that antibody binding should also result in an increase of height and surface corrugation of the microdomains **[26]**. The analysis of the height profiles derived from cross-sections perpendicular to the microdomain long axis and obtained by AFM topography images collected before and after the anti flotillin-1 treatment made difficult to quantify a reliable difference even if the experimental data showed a slight increase of the microdomain height and the height profiles exhibited a higher corrugation after the antibody binding.

Quantitative information was obtained by the analysis of the rms surface roughness. In particular, the rms surface roughness of the membrane microdomains, measured on 50×50nm square areas, increased from 0.25 ± 0.03nm (mean ± SD; n = 11) to 0.34 ± 0.03nm (mean ± SD; n = 11) after the antibody binding.

5.4 Discussion

AFM has been shown to be a very useful technique to visualize and quantitatively characterize the topology of biological membranes also in physiological-like conditions **[24,27]**. Moreover, AFM has been employed to study structure and dynamics of lipid rafts based on ternary lipid mixtures commonly used to mimic membrane rafts **[28]** and, more recently, also in native membranes **[29]**.

In the present study we applied Tapping mode AFM imaging, coupled with WB and HP-TLC to obtain a biochemical characterization of the structures visualized in AFM images, to characterize lipid rafts extract as Detergent-Resistant Membranes (DRMs) of MDA-MB-231 human breast cancer cells.

Membrane patches of MDA-MB-231 cell resistant to Triton X-100 extraction were purified by ultracentrifugation on a discontinuous sucrose gradient. All the 11 isolated fractions were analyzed with respect to raft lipid (Chol and SM) and protein (flotillin-1) marker. The biochemical data therefore confirm a larger presence of lipid rafts marker in the low-density fractions 5 and 6 corresponding to the 5% and 30% sucrose interface.

In agreement with biochemical analyses, AFM imaging visualized large and planar membrane patches with lateral sizes of a few microns and a height of about 4–5nm, as awaited for single lipid bilayers, only in the fractions with the richest content of flotillin-1, Chol and SM (**Fig. 2**). Moreover, the number of the membrane patches decreases from fractions 5 to 7 as well as the flotillin-1, Chol and SM content.

The standard method of isolation of membrane rafts involves solubilization of the membrane at 4°C using the non-ionic detergent, typically Triton X-100. Thank to their low relative density, due to of their high lipid-to-protein ratio, membrane rafts are separated by centrifugation on discontinuous or continuous sucrose gradients. Usually DRMs are isolated in the low-density fractions corresponding to the 5% and 30% sucrose interface **[30]**. Although Triton X-100 is the best characterized and most widely used detergent for DRMs purification, some observations raised the hypothesis that treatment of cells with detergents may generate clusters of raft lipids and proteins that did not exist in the intact cells **[31]**.

AFM imaging of samples prepared from fractions 5 and 6 showed many membrane patches with lateral dimension in the order of 1–3μm that may be formed through a mechanism of coalescence as a result of detergent treatment. However, a recent study demonstrated that Triton X-100 does not induce domain formation or increase the fraction of the bilayer in the ordered state,although it does increase domain size by coalescing pre-existing domains **[32]**. Thus our observations are in agreement with this theory.

It is worth noting that, high resolution AFM imaging of samples prepared from fraction 5 showed microdomains that protruding by 1–2nm from the membrane patches, with lateral dimensions in the range of 100–500nm in line with the data obtained using model membranes to study lipid rafts **[21]**. Moreover, the microdomains exhibit a surface corrugation (surface roughness = 0.26 ± 0.03nm; mean ± SD, n = 18) with nanometer features on its surface which resemble proteins in both size and shape. The AFM-immunolabeling with anti flotillin-1 antibody showed that the microdomains changed their size and appearance showing an evident enlargement of the surface area (about 20%), and a higher surface corrugation after the antibody binding. On the contrary, control experiments carried out using anti clathrin hc, a non specific antibody raised against a non raft protein marker **[25]**, did not show a statistically significant variation of surface area of microdomains (**Fig. 5**). It is worth noting that the increase of the surface area of the membrane microdomains induced by the anti flotillin-1 treatment showed values distributed in two different ranges, 8–10% and 24–27%. These differences can be justified taken in account that the sample preparation protocol for AFM imaging does not allow to select the orientation of the membrane patches on the mica support. Since anti flotillin-1 binds to the cytoplasmic side of the plasma membrane, the 8–10% surface area increase could be induced by non specific physisorption phenomena on microdomains exposing the external face of the membrane. As a result the increase of the micro-domain surface area of about 20% induced by the anti flotillin-1 antibody binding could be an underestimation of the real value.

5.5 Conclusions

Taken together the biochemical data as well as the flotillin-1 recognition and its high content in the membrane microdomains, strongly indicate that the nanometer areas protruding from the membrane patch surface and visualized in AFM images could be identified as lipid rafts. As a final comment, it is worth speculating on the utility of nanoscale methods, such as AFM, for probing raft domains in cells. In this context, our results on the presence of flotillin-1 and their co-localization with membrane microdomains is an important step toward the direct visualization of lipid and protein components of rafts in native membranes.

References

1. Simons K, Ikonen E: **Functional rafts in cell membranes**. *Nature* 1997, **387**(6633):569-572.
2. Simons K, Vaz WL: **Model systems, lipid rafts, and cell membranes**. *Annual review of biophysics and biomolecular structure* 2004, **33**:269-295.
3. Kraft ML: **Plasma membrane organization and function: moving past lipid rafts**. *Molecular biology of the cell* 2013, **24**(18):2765-2768.
4. Simons K, Toomre D: **Lipid rafts and signal transduction**. *Nature reviews* 2000, **1**(1):31-39.
5. van Meer G, Lisman Q: **Sphingolipid transport: rafts and translocators**. *The Journal of biological chemistry* 2002, **277**(29):25855-25858.
6. Fastenberg ME, Shogomori H, Xu X, Brown DA, London E: **Exclusion of a transmembrane-type peptide from ordered-lipid domains (rafts) detected by fluorescence quenching: extension of quenching analysis to account for the effects of domain size and domain boundaries**. *Biochemistry* 2003, **42**(42):12376-12390.
7. London E: **How principles of domain formation in model membranes may explain ambiguities concerning lipid raft formation in cells**. *Biochimica et biophysica acta* 2005, **1746**(3):203-220.

8. Almeida PF, Pokorny A, Hinderliter A: **Thermodynamics of membrane domains**. *Biochimica et biophysica acta* 2005, **1720**(1-2):1-13.
9. Eggeling C, Ringemann C, Medda R, Schwarzmann G, Sandhoff K, Polyakova S, Belov VN, Hein B, von Middendorff C, Schonle A *et al*: **Direct observation of the nanoscale dynamics of membrane lipids in a living cell**. *Nature* 2009, **457**(7233):1159-1162.
10. Owen DM, Magenau A, Williamson D, Gaus K: **The lipid raft hypothesis revisited--new insights on raft composition and function from super-resolution fluorescence microscopy**. *Bioessays* 2012, **34**(9):739-747.
11. Owen DM, Williamson D, Magenau A, Gaus K: **Optical techniques for imaging membrane domains in live cells (live-cell palm of protein clustering)**. *Methods in enzymology* 2012, **504**:221-235.
12. Hell SW, Wichmann J: **Breaking the diffraction resolution limit by stimulated emission: stimulated-emission-depletion fluorescence microscopy**. *Optics letters* 1994, **19**(11):780-782.
13. Eggeling C, Ringemann C, Medda R, Schwarzmann G, Sandhoff K, Polyakova S, Belov VN, Hein B, von Middendorff C, Schonle A *et al*: **Direct observation of the nanoscale dynamics of membrane lipids in a living cell**. *Nature* 2009, **457**(7233):1159-1162.
14. Sahl SJ, Leutenegger M, Hilbert M, Hell SW, Eggeling C: **Fast molecular tracking maps nanoscale dynamics of plasma**

membrane lipids. *Proceedings of the National Academy of Sciences of the United States of America* 2010, **107**(15):6829-6834.

15. Mizuno H, Abe M, Dedecker P, Makino A, Rocha S, Ohno-Iwashita Y, Hofkens J, Kobayashi T, Miyawaki A: **Fluorescent probes for superresolution imaging of lipid domains on the plasma membrane**. *Chem. Sci.* 2011, **2**:1548–1553
16. Anderton CR, Lou K, Weber PK, Hutcheon ID, Kraft ML: **Correlated AFM and NanoSIMS imaging to probe cholesterol-induced changes in phase behavior and non-ideal mixing in ternary lipid membranes**. *Biochimica et biophysica acta* 2011, **1808**(1):307-315.
17. Scheuring S: **AFM studies of the supramolecular assembly of bacterial photosynthetic core-complexes**. *Current opinion in chemical biology* 2006, **10**(5):387-393.
18. Goncalves RP, Buzhynskyy N, Prima V, Sturgis JN, Scheuring S: **Supramolecular assembly of VDAC in native mitochondrial outer membranes**. *Journal of molecular biology* 2007, **369**(2):413-418.
19. Buzhynskyy N, Salesse C, Scheuring S: **Rhodopsin is spatially heterogeneously distributed in rod outer segment disk membranes**. *J Mol Recognit* 2011, **24**(3):483-489.
20. Pike LJ: **Lipid rafts: bringing order to chaos**. *Journal of lipid research* 2003, **44**(4):655-667.
21. Rinia HA, Snel MM, van der Eerden JP, de Kruijff B: **Visualizing detergent resistant domains in model**

membranes with atomic force microscopy. *FEBS letters* 2001, **501**(1):92-96.

22. Schutz GJ, Kada G, Pastushenko VP, Schindler H: **Properties of lipid microdomains in a muscle cell membrane visualized by single molecule microscopy**. *The EMBO journal* 2000, **19**(5):892-901.
23. Lingwood D, Simons K: **Lipid rafts as a membrane-organizing principle**. *Science* 2010, **327**(5961):46-50.
24. Santacroce M, Daniele F, Cremona A, Scaccabarozzi D, Castagna M, Orsini F: **Imaging of Xenopus laevis oocyte plasma membrane in physiological-like conditions by atomic force microscopy**. *Microsc Microanal* 2013, **19**(5):1358-1363.
25. Fabelo N, Martin V, Santpere G, Marin R, Torrent L, Diaz M: **Severe alterations in lipid composition of frontal cortex lipid rafts from Parkinson's disease and incidental Parkinson's disease**. *Mol. Med*. 2011, **17**:1107–1118.
26. Muller DJ, Schoenenberger CA, Buldt G, Engel A: **Immuno-atomic force microscopy of purple membrane**. *Biophysical journal* 1996, **70**(4):1796-1802.
27. Hoogenboom BW, Suda K, Engel A, Fotiadis D: **Supramolecular assemblies of the voltage-dependent anion channel in the native membrane**. *J. Mol. Biol.* 2007, **370**:246–255
28. El Kirat K, Morandat S: **Cholesterol modulation of membrane resistance to Triton X-100 explored by atomic**

force microscopy. *Biochimica et biophysica acta* 2007, **1768**(9):2300-2309.

29. Cai M, Zhao W, Shang X, Jiang J, Ji H, Tang Z, Wang H: **Direct evidence of lipid rafts by in situ atomic force microscopy**. *Small* 2012, **8**(8):1243-1250.
30. London E, Brown DA: **Insolubility of lipids in triton X-100: physical origin and relationship to sphingolipid/cholesterol membrane domains (rafts)**. *Biochimica et biophysica acta* 2000, **1508**(1-2):182-195.
31. Ingelmo-Torres M, Gaus K, Herms A, Gonzalez-Moreno E, Kassan A, Bosch M, Grewal T, Tebar F, Enrich C, Pol A: **Triton X-100 promotes a cholesterol-dependent condensation of the plasma membrane**. *The Biochemical journal* 2009, **420**(3):373-381.
32. Pathak P, London E: **Measurement of lipid nanodomain (raft) formation and size in sphingomyelin/POPC/cholesterol vesicles shows TX-100 and transmembrane helices increase domain size by coalescing preexisting nanodomains but do not induce domain formation**. *Biophysical journal* 2011, **101**(10):2417-2425.

Chapter 6

Reversible dissolution of microdomains in native plasma membranes at physiological temperature

This chapter is based on: Reversible dissolution of microdomains in native plasma membranes at physiological temperature (article in preparation). Data have been obtained during my Erasmus placement in the laboratory of Dr. B.W. Hoogenboom London Centre for Nanotechnology, University College London (UK).

6.1 Introduction

A typical membrane is overwhelmingly complex, contains hundreds of lipid species, such as glycerophospholipids (GPLs), sphingolipids (SLs) and cholesterol (Chol), that differ in their physico-chemical properties, lipophilic molecules and membrane proteins in two asymmetric leaflets **[1]**. It is becoming increasingly apparent that such a complex assortment of lipids is necessary to accomplish the manifold functions that lipids perform. Thanks to electron microscopy (EM) images, S.J. Singer and G.L. Nicolson proposed the model to "fluid mosaic" of biological membranes **[2]**. This model assigned to the lipid bilayer a certain degree of fluidity. In fact, at physiological temperature, the fatty acyl chains of the phospholipids (PLs) of the lipid bilayer are in a fluid phase. Thus, the cellular membrane appear to be a two-dimensional solutions of integral membrane proteins in a lipid bilayer solvent **[3]**, allowing the lateral movement of membrane components. As a consequence of the lipid bilayer fluidity, the membrane components can create “membrane domains” that differ in lipid and/or protein composition from that of the surrounding lipid matrix **[4]**.

Such bilayer domains, also called "lipid rafts", are known to be dynamic, small and ordered domains enriched in Chol, SM and specific proteins that may formed into larger structures due to lipid–lipid, lipid–protein, and protein–protein interactions **[5]**. The organization of membranes into dynamic platforms serves to bring about a functional compartmentalization so that multimolecular interactions, such as membrane trafficking, signal transduction, and regulation of the activity of membrane proteins, can be executed and regulated in space and time **[6]**. Under physiological conditions, lipid bilayers exist in a liquid disordered (Ld) phase, upon cooling below the melting point, the lipid acyl chains are frozen in an solid-ordered phase (So) where their mobility is restricted. However, because of the high concentration of Chol in the plasma membrane, a third physical phase, the liquid ordered (Lo) phase, can be observed. In the Lo state, acyl chains of lipids are extended and tightly packed. In this sense, the Lo state is similar to the gel state, and lipids that favor gel state formation, and thus have a high melting temperature (Tm) in the absence of Chol, tend to form the Lo state in the presence of Chol. On the other hand, lateral diffusion in the Lo state appears to be almost as rapid as in the fluid Ld state **[7]**.

The "lipid rafts" structure appears to arise from the phase separation of a Ld/Lo phase. The coexistence of domains in Lo and Ld phases has been extensively characterized. Studies of membrane model systems using a variety of techniques, such as Fluorescence Resonance Energy Transfer (FRET), Deuterium-based Nuclear Magnetic Resonance (^{2}H-NMR) and Atomic Force Microcopy (AFM) strongly suggest that lipids could laterally segregate into macroscopic (>200nm) or

microscopic (<100nm) membrane domains under certain conditions **[8]**. Model systems have greatly improved our understanding of the structure and function of cell membranes, but the model membranes don't reflect the complexity of the lipid environment or the interactions between lipids and proteins in a cell membrane.

Giant plasma membrane vesicles (GPMVs), microscopic spheres of plasma membranes harvested from live cells following chemical treatment **[9]** are probably the closest models of cell plasma membranes in terms of chemical composition, as in addition to lipids they contain also membrane proteins. Fluid phase separation has been reported in giant GPMVs obtained from mast cells and fibroblasts **[10,11]**, from A431 **[12]** and RBL-2H3 **[13]** cells. Bernardino de la Serna *et al.*, **[14]** using Fluorescence Microscopy (FM) and AFM under physiological conditions, observed the coexistence of two distinct micrometer sized fluid phases (ordered and disordered-like phases) in GPMVs obtained from native pulmonary surfactant membranes. Moreover, their results showed that the phase separation was dramatically affected by the extraction of Chol. Model membranes and GMPVs show clearly separated microscopic domains of Lo/Ld phases, while in cell plasma membranes these domains have not been really observed except in some rare exceptions **[15,16]**, due to the complexity of cell membrane organization.

In the past decade, AFM has emerged as a powerful tool to obtain nano-structural details of soft and fragile materials such as proteins and lipids. AFM operating in physiological-like conditions and providing nanometer spatial resolution without fixation, staining, or labeling, appears to be a powerful tool to quantitatively perform a morpho-dimensional characterization of membrane microdomains, such as Detergent-Resistant Membrane (DRM) microdomains **[17-18]**.

In this work we applied AFM to the study DRM microdomains of MDA-MB-231 human breast cancer cells. In particular, we carried out a study using a heating control system to obtain more information regarding the temperature-induced phase behavior on membrane microdomains resistant to non-ionic detergent (Triton X-100) extraction.

6.2 Materials and methods

Cell Lines and Culture Conditions

See **Chapter 4**, section Materials and methods, for a detailed description of human breast cancer cells MDA-MB-231 and culture conditions

DRMs Isolation

See **Chapter 4**, section Materials and methods, for a detailed description of DRM isolation from MDA-MB-231 cells.

AFM imaging

See **Chapter 5**, section Materials and methods, for a detailed description of AFM imaging conditions.

AFM imaging has been performed in collaboration with the laboratory of Dr. B.W. Hoogenboom London Centre for Nanotechnology, University College London (UK).

Sample preparation protocol for AFM imaging

See **Chapter 4**, section Materials and methods, for a detailed description of the purified membrane sample preparation protocol for AFM imaging.

Temperature-controlled AFM imaging

AFM imaging was performed at different temperatures in liquid buffer using a Multimode Nanoscope IIIa (Bruker, Santa Barbara, CA, USA) equipped with a J piezo scanner (125x125μm) AS 130V and with a heating control system (Multimode AFM high temperature heater, Bruker, Santa Barbara, CA, USA) which allows to control the temperature in the range 25-250°C. Mica support was glued to a Teflon layer which in turn was glued to a metal disk that was magnetically fixed to the AFM sample holder. Basically, the temperature setup consists of a sample heater and a electronic heater controller that allows for setting a desired sample temperature.

The sample heater is a ceramic block that carries an embedded micro-heater placed between the scanner and the sample that transmits the heat to the sample from underneath.

Although the distance between the heating element and the sample inside the buffer droplet is typically in the range of a few mm, there can be the problem of thermal gradients from the heater element to the mica support. To reduce this problem, before to observe the sample, we have evaluated the real temperature inside the AFM fluid cell. Briefly, using a control system we have measured the temperature inside the buffer droplet just in contact with the sample surface.

Temperature-controlled experiments were performed with a temperature controller stage (Multimode AFM temperature heater controller with a range of 25-250°C, Bruker, Santa Barbara, CA, USA). In particular, membrane samples adsorbed onto the mica surface, as described above, were visualized changing the temperature over a large range (25-45°C). Moreover, once the desired temperature was reached, the system was allowed to thermally equilibrate for approximately 30sec before the tip approaching the sample surface. Starting from room temperature (~25°C), the temperature was incremented in 2°C steps till to ~40°C. Then, the sample was cooled back to room temperature to return to the initial conditions. AFM images were collected at different steps of temperature, for example, 25°C, 30°C, 37°C and 25°C ("thermal cycle"). AFM images were collected approximately every 10min allowing the direct comparison of the same membrane patches before and after the temperature increase.

AFM-imunolabeling and analysis procedures

See **Chapter 5**, section Materials and methods, for a detailed description of the purified membrane sample labeling and AFM imaging.

Statistical analysis

The data are presented as mean ± SD (or SE). Student's t-test was used for comparisons between treated and control cells and the level of statistical significance was set at *p< 0.01.

6.3 Results

As reported in **Chapter 4** "*Chemical-physical changes in cell membrane microdomains of breast cancer cells after omega-3 PUFA incorporation",* the purity of isolated DRMs was demonstrated using lipid and protein raft and non-raft markers. In particular, biochemical analysis of the distribution of some lipids highly present in lipid rafts, namely Chol, Sm and ganglioside (GM1), carried out by HP-TLC confirmed the presence of the DRMs in the 5 and 6 fractions. Moreover, the same fractions, showed higher content of flotillin-1, a protein marker of lipid rafts, indicating that these fractions are enriched with DRMs. Moreover, as reported in **Chapter 5** "*Characterization of DRMs Microdomains from Human Breast Cancer Cells",* AFM imaging of the purified fractions enriched in DRMs, showed membrane microdomains with lateral dimensions of a few hundreds of nanometers. Moreover, treating the samples with a specific antibody against the protein flotillin-1, an increase of the microdomain surface area occurs thus suggesting the presence of flotillin-1, a lipid raft-associated protein **[19]**, in the visualized membrane microdomains.

Starting from these results, we have decided to apply AFM to characterize the phase behavior of DRM microdomains. In particular, we carried out a study using a heating control system to elucidate the kinetics on the phase transition process. Briefly, AFM images were collected at different steps of temperature, for example, 25°C, 30°C, 37°C and 25°C ("thermal cycle").

This experiment allowed the direct comparison of the same membrane patches during the thermal cycle. As an example, an AFM topography image of thermal cycle collected in Tapping mode in buffer solution is reported in **Figure 1**. In particular membrane patches and microdomains protruding from their surface are clearly identified at 25°C. As described in **Chapter 5**, the membrane patches showed lateral size in the order, on average, of a few microns and height of about 4nm, as awaited for lipid bilayers. While the microdomains, protruding by 1-2nm from the surrounding membrane exhibited lateral dimensions in the range of 100–500nm, in agreement with the data obtained using artificial membranes **[20]**. Interestingly, when the temperature is increased (till 37°C), the membrane patches are even visible on mica support, while, as clearly visible in **Figure 1**, the size and shape of the microdomains depend strongly on the temperature. In particular, when the temperature is increased (above 30°C) the smaller microdomains (less than 100nm in diameter) disappear while the larger microdomains are reduced in size. It is worth of notice that at physiological temperature (around 37°C), it is possible to see only a few and smaller microdomains which lateral dimensions, of the order of an tens of nanometers.

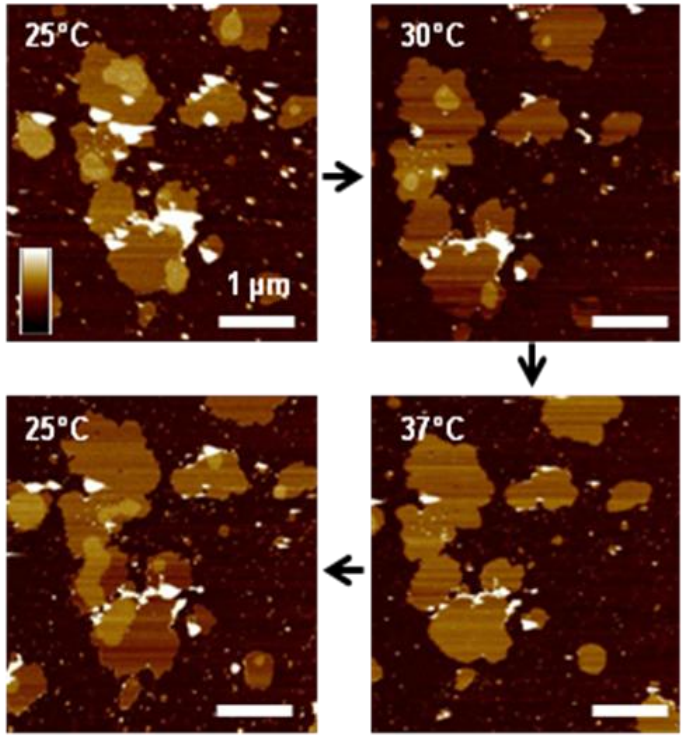

Figure 1. Reversible dissolution of microdomains at physiological temperature.
AFM topography images of DRMs collected at different temperatures. For all AFM images Scan area: 3 × 3 µm; vertical scale: 9 nm (see insert in **Fig**.).

In addition, when the sample was cooled back to room temperature, the microdomains become again visible on membrane patch surface even if they change in shape and size and/or position, thus suggesting a dynamic nature of these structure (**Figure 1**).

The quantitative analysis of AFM images corresponding at many thermal cycles allowed to calculate the total surface area of the microdomains at different temperature. In particular, **Figure 2** shows the plot of microdomains surface area collected at different temperatures, obtained analyzing 8 thermal cycles, and normalized to the mean total area of microdomains collected at room temperature (25°C). In particular we found a decrease of the microdomains total surface area of 77.2 ± 1.9% and 96.7 ± 0.9% (mean ± SEM) at 30°C and 36°C respectively. The observed difference between the total surface area decrease of microdomains at 25°C and 36°C is statistically significant (*p<0.01).

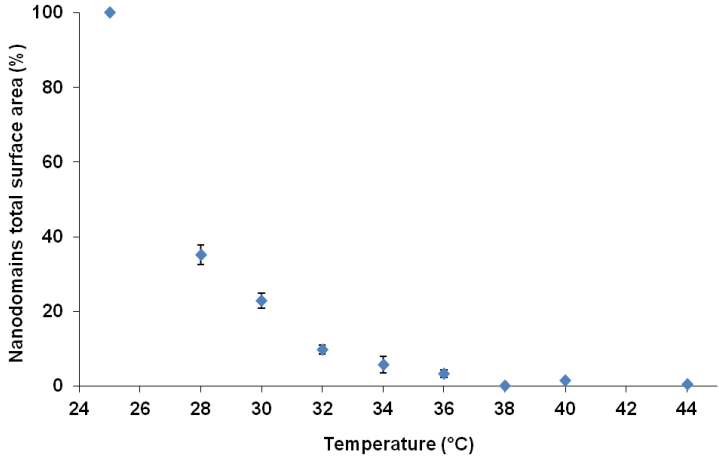

Figure 2. Microdomain area as a function of temperature.

Scattering of the mean total surface area of microdomains at different temperatures. Data (mean ± SEM) have been obtained analyzing different thermal cycles (n= 8). Total surface area at 25°C was used to normalized results.

Figure 3 shows the plot of microdomains height (measured with respect to the membrane patches surface) observed at different temperatures, obtained analyzing 8 thermal cycles. In particular, the microdomains protrude by about 1.5nm from the surrounding membrane at room temperature, while they show an height about 1nm in the range of physiological temperature.

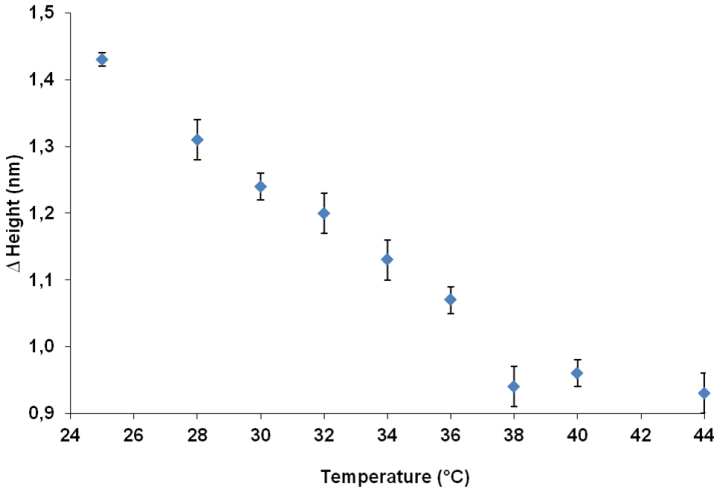

Figure 3. Microdomain height above the membrane as a function of temperature. Scattering of the mean height for microdomains at different temperatures. Data (mean ± ES) have been obtained analyzing different AFM images collected at different temperatures.

To verify that the microdomain size modifications were not induced by the mechanic effect produced by the AFM tip during the sample scanning, we have carried out a study at physiological temperature scanning the membrane patches after a long period of temperature stabilization. As shown in **Figure 4**, scanning the sample till to 180min changes in the microdomain dimensions do not occur. These results strongly indicate that the microdomain size is totally temperature dependent.

Finally, in order to verify the presence, at room temperature, of proteins in reshaped DRMs after the thermal cycles treatment, we carried out a new study using anti-flotillin-1 antibody. The purified DRMs adsorbed onto mica were heated till to 40°C and then cooled back to the room temperature. Subsequently, the samples were incubated with anti-flotillin-1 antibody (diluition 1:4) and imaged at room temperature after 60min of treatment.

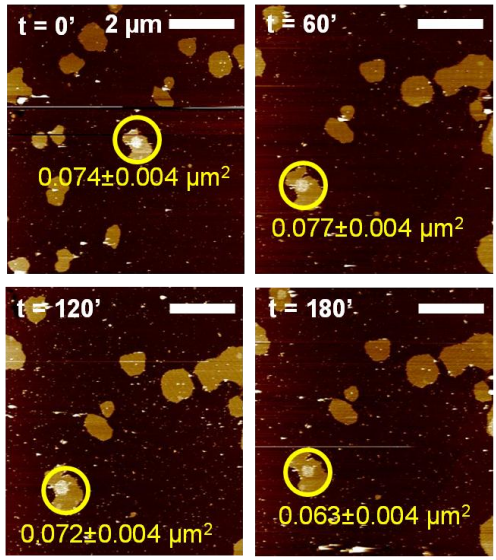

Figure 4. Membrane and microdomain stability at 37°C.
AFM topography images of membrane samples prepared from fraction 5 and collected in liquid buffer in Tapping mode at same temperature (37°C) for long times. For all images scan area: 5 x 5µm; vertical scale: 9nm (see insert in **Fig. 1**).

The reshaped microdomains after thermal cycle showed an enlargement of their surface area (about 25%). In particular, we found a surface area increase of 25.3 ± 6.3% (mean ± SD; n = 17) and 9.2 ± 2.5% (mean ± SD; n = 15) for microdomains and membrane patches respectively as shown in the histogram in **Figure 5**. The observed difference between the surface area increase of membrane patches and microdomains after antibody incubation was statistically significant (*$p<0.01$). These data suggest the presence of flotillin-1 in the membrane microdomains after the thermal treatment.

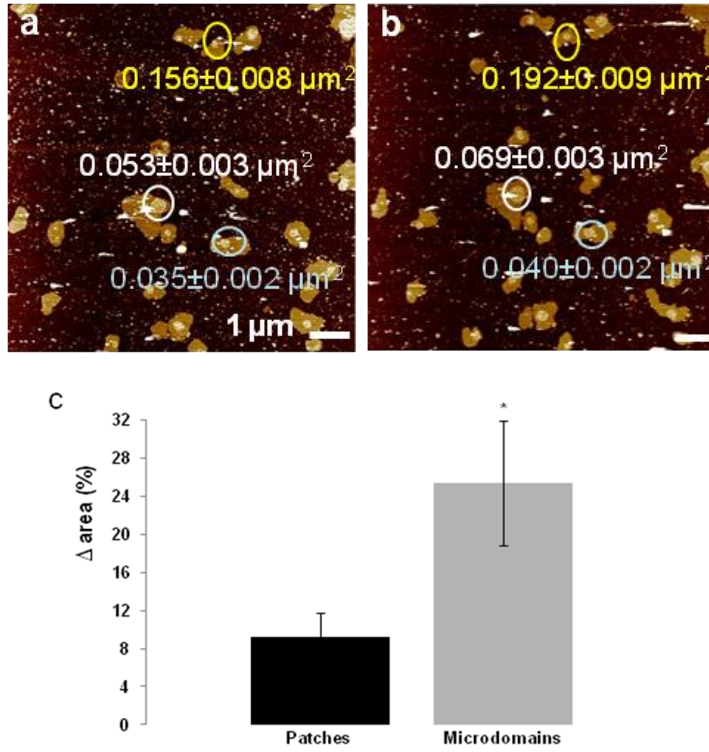

Figure 5. AFM-imunolabeling.

AFM topography images of membrane samples prepared from fraction 5 and collected in liquid buffer in tapping mode after the thermal cycle. For all images scan area: 8 x 8µm; vertical scale: 9nm (see insert in **Fig. 1**). Membrane patches **(a)** were incubated with anti Flot-1 antibodies. After 60 min of treatment **(b)** the surface area of microdomains clearly increases. For all images scan area: 8 x 8 µm; vertical scale: 9nm (see insert in **Fig. 1**). **(c)** Histogram of the surface area increase after anti-flotillin-1 antibody incubation (*$p<0.01$).

6.4 Discussion

A typical membrane is overwhelmingly complex, contains hundreds of lipids species that differ in their physico-chemical properties, lipophilic molecules and membrane proteins in two asymmetric leaflets **[1]**. Such a multicomponent mixture exhibits a complex phase behavior. This phase behavior can modify the orientation and mobility of membrane lipids and proteins, and will therefore affect membrane functionality. At physiological temperatures, membranes are fluid, thus both, lipids and proteins can diffuse laterally within the membrane lipid bilayer plane, creating membrane domains with lipid and/or protein composition different from that of the surrounding lipid matrix **[4]**.

The domain structure appears to arise from the phase separation of a Ld phase enriched in low melting temperature lipids, characterized by high fluidity in which the lipid acyl chains are disordered and highly mobile, and a Lo phase enriched in Chol and high melting temperature lipids such as SM **[7]**.

The forces that control the formation and dynamics of this membrane microdomains are not yet fully understood. Thus, the observation and the characterization of phase separation in purified plasma membranes becames important for better understand the lateral organization of microdomains within the plasma membrane.

In the past decade, AFM has emerged as a powerful tool to obtain nano-structural details of soft and fragile materials such as proteins and lipids. In particular, operating in physiological-like conditions and providing nanometer spatial resolution without fixation, staining, or labeling, AFM appears to be a powerful tool to quantitatively perform a morpho-dimensional characterization of membrane microdomains **[18,21-23]**.

Taken together, the biochemical analyses and AFM imaging reported above (see **Chapter 4** and **5**) indicate that the DRMs (fractions 5 and 6) were enriched with lipid and protein raft marker, such as Chol, SM and flotillin-1. Moreover, AFM imaging of these fractions, showed membrane lipid bilayers and microdomains with lateral dimensions in the range of 100–500nm that protrude of about 1-2nm from the membrane surface. For these reasons, the phase behavior, of the purified DRM microdomain, has been studied as a function of the temperature using an AFM equipped with a heating control system. Moreover, the use of isolated and purified membranes, in our case DRM purified by ultracentrifugation process, offers the possibility to observe nano-scale domains and small height differences by AFM, in order to study temperature effects without deregulating the whole cell.

Our results show that, when the temperature is increased (till 37°C), the membrane patches are even visible on mica support while, the surface area of the microdomains depend strongly on the temperature and were not induced by the mechanic effect produced by the AFM tip during the sample scanning.

In particular, when the temperature is increased the smaller microdomains (less than 100nm in diameter) disappear while the larger microdomains are reduced in size. Moreover, the height of microdomains is temperature dependent (**Fig. 3**). In addition, when the sample was cooled back to room temperature, the microdomains become again visible on membrane patch surface even if they change in shape and size and/or position, thus suggesting a dynamic nature of these structure. Take together these data suggest that the microdomains and their behavior as function of the temperature, appear to be in agreement with the phase separation of a Ld and Lo phase observed both, in model membrane and GPMVs **[24]**.

It is worth of notice that at physiological temperature, it is possible to see only a few and smaller microdomains which lateral dimensions, of the order of a tens of nanometers. These data suggest that these microdomains might exist in living cells, indeed their lateral dimension are in agreement with the range expected for membrane microdomains observed in living cell using a Stimulated Emission Depletion (STED) far-field fluorescence microscopy **[25]**.

Finally, we observed an enlargement of reshaped microdomains surface area after anti-flotillin-1 antibody incubation (**Fig. 5**). These data suggest the presence of flotillin-1 in the membrane microdomains after the thermal treatment, sustaining the dynamics of these structures and their ability to carry around proteins. Moreover, our findings demonstrate the high affinity of flotillin-1 proteins to the visualized microdomains.

6.5 Conclusions

These preliminary results suggest that AFM could be an useful tool to study the phase coexistence of a Ld and Lo domain in purified plasma membrane.

References

1. van Meer G, Voelker DR, Feigenson GW: **Membrane lipids: where they are and how they behave**. *Nature reviews* 2008, **9**(2):112-124.
2. Singer SJ, Nicolson GL: **The fluid mosaic model of the structure of cell membranes**. *Science (New York, NY* 1972, **175**(4023):720-731.
3. Coskun U, Simons K: **Membrane rafting: from apical sorting to phase segregation**. *FEBS letters* 2010, **584**(9):1685-1693.
4. Sonnino S, Prinetti A: **Membrane domains and the "lipid raft" concept**. *Current medicinal chemistry*, **20**(1):4-21.
5. Kraft ML: **Plasma membrane organization and function: moving past lipid rafts**. *Molecular biology of the cell* 2013, **24**(18):2765-2768.
6. Simons K, Gerl MJ: **Revitalizing membrane rafts: new tools and insights**. *Nature reviews* 2010, **11**(10):688-699.
7. Heberle FA, Feigenson GW: **Phase separation in lipid membranes**. *Cold Spring Harbor perspectives in biology* 2011, **3**(4): a004630.
8. Hancock JF: **Lipid rafts: contentious only from simplistic standpoints**. *Nature reviews* 2006, **7**(6):456-462.
9. Scott RE: **Plasma membrane vesiculation: a new technique for isolation of plasma membranes**. *Science* 1976 ,**194**:743–745.
10. Baumgart T, Hammond AT, Sengupta P, Hess ST, Holowka DA, Baird BA, Webb WW: **Large-scale fluid/fluid phase**

separation of proteins and lipids in giant plasma membrane vesicles. *Proceedings of the National Academy of Sciences of the United States of America* 2007, **104**(9):3165-3170.

11. Veatch SL, Cicuta P, Sengupta P, Honerkamp-Smith A, Holowka D, Baird B: **Critical fluctuations in plasma membrane vesicles**. *ACS chemical biology* 2008, **3**(5):287-293.
12. Lingwood D, Ries J, Schwille P, Simons K: **Plasma membranes are poised for activation of raft phase coalescence at physiological temperature**. *Proceedings of the National Academy of Sciences of the United States of America* 2008, **105**(29):10005-10010.
13. Sezgin E, Levental I, Grzybek M, Schwarzmann G, Mueller V, Honigmann A, Belov VN, Eggeling C, Coskun U, Simons K *et al*: **Partitioning, diffusion, and ligand binding of raft lipid analogs in model and cellular plasma membranes**. *Biochimica et biophysica acta* 2012, **1818**(7):1777-1784.
14. Bernardino de la Serna J, Perez-Gil J, Simonsen AC, Bagatolli LA: **Cholesterol rules: direct observation of the coexistence of two fluid phases in native pulmonary surfactant membranes at physiological temperatures**. *The Journal of biological chemistry* 2004, **279**(39):40715-40722.
15. Gaus K, Gratton E, Kable EP, Jones AS, Gelissen I, Kritharides L, Jessup W: **Visualizing lipid structure and raft domains in living cells with two-photon microscopy**. *Proceedings of the National Academy of Sciences of the United States of America* 2003, **100**(26):15554-15559.

16. Gousset K, Wolkers WF, Tsvetkova NM, Oliver AE, Field CL, Walker NJ, Crowe JH, Tablin F: **Evidence for a physiological role for membrane rafts in human platelets**. *Journal of cellular physiology* 2002, **190**(1):117-128.
17. Anderton CR, Lou K, Weber PK, Hutcheon ID, Kraft ML: **Correlated AFM and NanoSIMS imaging to probe cholesterol-induced changes in phase behavior and non-ideal mixing in ternary lipid membranes**. *Biochimica et biophysica acta* 2011, **808**(1):307-315.
18. Orsini F, Cremona A, Arosio P, Corsetto PA, Montorfano G, Lascialfari A, Rizzo AM: **Atomic force microscopy imaging of lipid rafts of human breast cancer cells**. *Biochimica et biophysica acta* 2012, **1818**(12):2943-2949.
19. Pike LJ: **Lipid rafts: bringing order to chaos**. *Journal of lipid research* 2003, **44**(4):655-667.
20. Rinia HA, Snel MM, van der Eerden JP, de Kruijff B: **Visualizing detergent resistant domains in model membranes with atomic force microscopy**. *FEBS letters* 2001, **501**(1):92-96.
21. Connell SD, Smith DA: **The atomic force microscope as a tool for studying phase separation in lipid membranes**. *Molecular membrane biology* 2006, **23**(1):17-28.
22. El Kirat K, Morandat S: **Cholesterol modulation of membrane resistance to Triton X-100 explored by atomic force microscopy**. *Biochimica et biophysica acta* 2007, **1768**(9):2300-2309.

23. Cai M, Zhao W, Shang X, Jiang J, Ji H, Tang Z, Wang H: **Direct evidence of lipid rafts by in situ atomic force microscopy**. *Small* 2012, **8**(8):1243-1250.
24. Risselada HJ, Marrink SJ: **The molecular face of lipid rafts in model membranes**. *Proceedings of the National Academy of Sciences of the United States of America* 2008, **105**(45):17367-17372.
25. Eggeling C, Ringemann C, Medda R, Schwarzmann G, Sandhoff K, Polyakova S, Belov VN, Hein B, von Middendorff C, Schonle A *et al*: **Direct observation of the nanoscale dynamics of membrane lipids in a living cell**. *Nature* 2009, **457**(7233):1159-1162.

Chapter 7

DHA alters membrane microdomain organization and EGFR-related signaling in MDA-MB-231 breast cancer cells

This chapter is based on: DHA alters membrane microdomain organization and EGFR-related signaling in MDA-MB-231 breast cancer cells (article in preparation).

7.1 Introduction

Lipid rafts are defined as small, dynamic, ordered domains of Chol, SLs, and specific proteins that may combine into larger structures due to lipid–lipid, lipid–protein, and protein–protein interactions **[1]**. Moreover, they can include or exclude proteins, for this reason, they may be involved in a wide variety of cellular functions and biological events **[2,3]** such as signal transduction and regulation of the activity of membrane proteins **[4,5]**. Several classes of proteins involved in signal transduction mechanisms, have been reported to be associated with lipid rafts in cancer cells. Among the proteins known to be localized in lipid rafts there is the EGFR **[6]**. EGFR is a tyrosine kinase mitogenic receptor whose function has been implicated in many biological processes. Several ligands, including EGF bind and activate the EGF receptors **[7]**. Upon ligand binding, EGFR stimulates signaling pathways involved in cell growth, survival, and migration. The EGFR signaling has multiple pathways, including the Ras/Raf/MAP-kinase and the PI3K/Akt **[8,9]**. These intracellular signaling cascades result in alterations of gene expression, which determines the biological response to receptor activation.

Specific dietary fatty acids, such as n-3 PUFAs, have been suggested to play a key role in the normal development and function of the organism.

Epidemiological studies have suggested that an increased n-3 PUFA intake might be associated with a reduced breast cancer incidence in humans **[10,11]**.

A number of mechanisms have been proposed for the anticancer actions of n-3 PUFAs, DHA and EPA in particular, including inhibition of cell proliferation, enhancement of apoptosis, as well as inhibition of angiogenesis and metastasis, and cancer differentiation **[12-15]**. In addition, it has also been suggested that these FAs might change the localization and function of raft-associated signaling proteins by inducing changes in physical properties **[16]**. DHA, a 22 carbon n-3 FA with six cis double bonds, is the longest and most highly unsaturated FA founds in most membranes. DHA, due to its high degree of unsaturation, has poor affinity and it is sterically incompatible with Chol. Studies conducted in various cell types have shown that treatment with DHA can alter the structure of lipid rafts as well as the signaling pathways that is known to occur within rafts **[17-19]**. Wong *et al.,* have demonstrated that Toll-like receptors, TLR2 and TLR4, signaling pathways and target gene expression are modulated by PUFAs. In particular, their results demonstrate that DHA inhibits saturated fatty acid-induced dimerization and recruitment of TLR4 to lipid rafts, which is the initial step of TLR4 signaling pathways, suggesting a possibility that n-3 PUFAs inhibit the formation of lipid rafts by altering the fatty acid composition of polar

lipids that are required to be acylated with saturated fatty acid for the formation of liquid-ordered lipid rafts **[17]**.

The EGFR localization in lipid rafts **[20,21]** is believed to be crucial for downstream receptor signaling controlling proliferation and apoptosis, which in turn could be altered by n-3 PUFA incorporation. Many experimental data have showed in several cell types that administration of n-3 PUFAs, in particular DHA, can exclude EGFR proteins from lipid raft, suppressing the activation of several downstream pathways, including Erk1/2 and Fatty Acid Synthase (FASN) protein **[22-26]**.

Based on these studies, it has been proposed that lipid raft modification can change the localization of raft-associated proteins, which could lead to cell death. Therefore, we hypothesized that DHA can inhibit breast cancer cell proliferation by altering the localization and the signaling pathways of EGFR. In the present work, we have examined the effect of DHA administration on DRM microdomains, isolated from MDA-MB-231 breast cancer cells by ultracentrifugation, with particular interest on EGFR protein localization and its downstream signaling.

7.2 Material and methods

Materials

DHA (cis-4,7,10,13,16,19-docosahexaenoic acid sodium salt) was purchased from Sigma-Aldrich (St Louis, MO, USA). In order to prevent oxidation, DHA was dissolved in absolute ethanol, stocked under

nitrogen, and stored at −80°C. Epidermal Growth Factor (EGF) was purchased from Sigma-Aldrich (St Louis, MO, USA).

The rabbit polyclonal anti-flotillin-1, the mouse monoclonal anti-clathrin heavy chain (HC), the rabbit polyclonal anti-EGFR (1005), the mouse monoclonal anti-pan Ras (F132), the rabbit polyclonal anti-p-Erk1/2 (Thr 202/Tyr 204) and the rabbit polyclonal anti-Erk1/2 antibodies were purchased from Santa Cruz Biotechnology Inc. (CA, USA). The sheep anti-Akt and the mouse monoclonal anti-Akt pS473 were purchased from Rockland Immunochemicals Inc. (Gilbertsville, PA, USA). The monoclonal anti-β-actin (AC-40) antibody was purchased from Sigma-Aldrich (St Louis, MO, USA). Bound primary antibodies were visualized by the proper secondary horseradish peroxidase (HRP)-linked antibodies (Santa Cruz Biotechnology Inc., Santa Cruz, CA, USA) and immunoreactivity was assessed by chemiluminescence (ECL, PerkinElmer,USA).

Cell Lines and Culture Conditions

See **Chapter 4**, section Materials and methods, for a detailed description of human breast cancer cells MDA-MB-231.

During treatments the MDA-MB-231 cell line was seeded $1.5x10^4$ cells/cm^2 for 48h. After this period, fresh medium for treatments (DMEM + 10% FBS) containing DHA (200μM) was added, and the cells were further incubated for 72h without medium replacement. Experiments include control cells, which were not exposed to any exogenous fatty acids but incubated in the same conditions with the same ethanol concentration of treated cells.

Cells were then stimulated with EGF. In particular, cells treated or not with DHA were cultured in medium for treatments supplemented with 10nM EGF and incubated at 37°C for 10min of stimulation. Experiments include not stimulated cells, which were not exposed to EGF but incubated in the same conditions with fresh medium for treatments.

DRMs Isolation

See **Chapter 4**, section Materials and methods, for a detailed description of DRM isolation from MDA-MB-231 cells.

WB analysis for EGFR, pan-Ras, Erk1/2, p-Erk1/2, Akt, p-Akt

Control and DHA-treated cell lysates (PNS) were analyzed by WB with anti-Erk1/2, anti-p-Erk1/2, anti-Akt and p-Akt antibodies. While control and DHA-treated DRMs (fraction 5) were analyzed by WB with anti-EGFR and anti-pan-Ras. All samples, 100μg protein/lane of total cellular protein, were separated by 10% SDS-PAGE. The proteins were then transferred onto a PVDF membrane with Bio-rad Transfer Blot Apparatus at 150mA overnight at 4°C in a transfer buffer (25mM TrisHCl, 190mM glicine, 20% methanol and 0.05% SDS). Following transfer, the samples were analyzed by WB with anti-EGFR (1:200), anti-pan-Ras (1:200), anti-Erk1/2 (1:200), anti-p-Erk1/2 (1:200), anti-Akt and p-Akt (1:1000) antibodies. The PVDF membranes were blocked in blocking buffer to prevent non-specific binding to the antibodies. In particular, the membranes were blocked in blocking buffer 3% dried non-fat milk in Tris-buffered saline (T-TBS: 10mM Tris/HCl,

pH 7.5, 150mM NaCl, 0.1% (v/v) Tween®20), for detection EGFR, and 5% dried non-fat milk in T-TBS, for detection Erk1/2 and p-Erk1/2, Akt, p-Akt and pan-Ras at room temperature for 1h. Subsequently, the membranes were incubated with an appropriate primary antibody in blocking buffer overnight at 4°C.

The blots were washed 6 times (5 minutes each) with T-TBS at room temperature, and then incubated with the proper secondary antibody in blocking buffer at room temperature for 1 h. Finally, after 6 washes with T-TBS, the specific antibody signals were visualized by using the ECL-PLUS (Perkin Elmer, USA), followed by autoradiography. The relative intensities of band signals were determined by digital scanning densitometry and β-actin, or flotillin-1, were used to normalize the results to protein content.

Statistical analysis

The data are presented as mean ± SD (or SE). Student's t-test was used for comparisons between treated and control cells and the level of statistical significance was set at */§$p < 0.05$ and **$p < 0.01$.

7.3 Results

Previously we observed that n-3 PUFAs are inserted with different yield in cell membrane microdomains and are able to alter FA composition without decreasing the total percentage of SFA that characterize these structures. Moreover, DHA decreased the content of Chol and SM in DRM microdomains. Thus, we have hypothesized that the alteration of microdomains lipid composition might determine the displacement of protein, such as EGFR, from DRMs in n-3 PUFA-treated cells, with alteration of signal transduction. For these reasons, we examined whether DHA redistributes DRM-associated proteins, including Ras and EGFR.

As shows WB in **Figure 1A**, when DRM preparations from cell cultures supplemented with DHA were assessed, the level of EGFR protein in DRM fraction was reduced compared to the same fraction of untreated cells. Moreover, DHA induces a reduction of EGFR content in DRM enriched fraction. A semi-quantitative analysis (**Figure 1B**) showed that the EGFR levels was decreased of 53.65 ± 17.6% in DHA-treated compared to the control cells (mean ± SEM; n = 3; *$p < 0.05$).

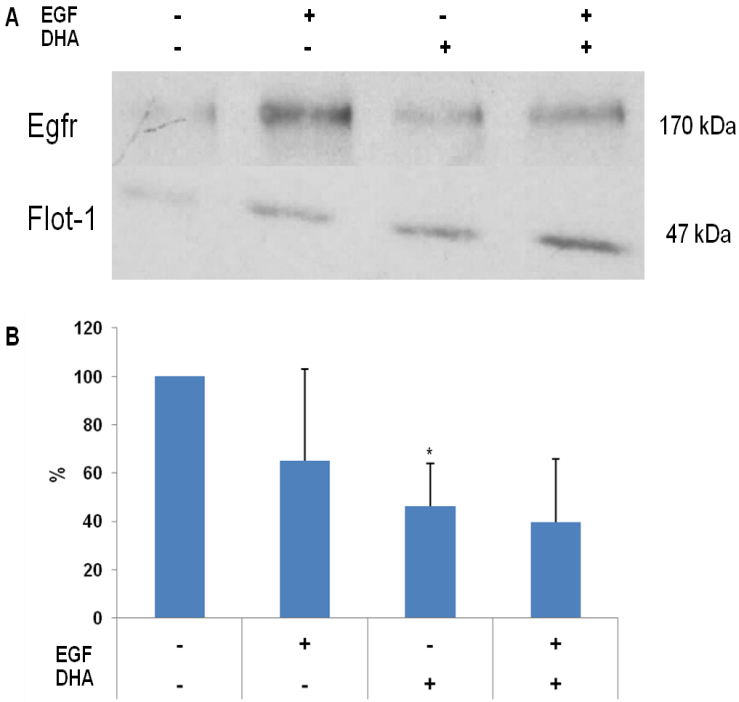

Figure 1. DHA reduces EGFR levels in DRMs.

Cells were treated with or without DHA (200μM). Some DHA-treated cells were incubated with EGF (10nM) before harvest. Following isolation the PNS was fractionated into 11 distinct fractions by ultracentrifugation. Fractions 5 were collected and analyzed by WB using the indicated antibodies **(A).** Each immunoblot is representative of at least 3 independent experiments. Flotilli-1 was used to normalized results. **(B)** Histogram of EGFR content in DRMs. Data (mean ± SEM; n=3) are represented as % of control. Asterisks indicate significant differences between treated and control cells (*$p<0.05$).

Lateral organization of EGFR within the plasma membrane is directly linked to receptor function. In particular, the ability of EGFR to activate downstream pathways is correlated to its localization in lipid raft domains of the plasma membrane **[20,21,27]** probably due to co-localization with downstream mediators within lipid rafts. Previous reports have shown that n-3 PUFAs can alter the localization of EGFR within the plasma membrane of lung and colon cells **[23,24]**.

Therefore, we have examined whether DHA can redistributes DRM-associated EGFR in MDA-MB-231 cells. As shows WB analysis reported in **Figure 2A**, the low-density fractions (fractions 5 and 6) from each treatment were enriched in flotillin-1, which served as lipid raft markers, and depleted of clathrin HC, which is excluded from lipid rafts, indicating that these fractions were enriched in lipid rafts. When we fractionated cells with TX-100 at 4°C, we found that EGFR was present in DRM enriched fractions of untreated cells. However, in DHA-treated cells EGFR protein was not found predominately in the DRM fractions as the lipid raft marker protein flotillin-1 (**Figure 2A**). In particular, as shown in the histogram in **Figure 2B**, we have observed a reduction of EGFR levels in DRM fractions and an increase of EGFR levels in detergent soluble membrane (DSM) fractions, indicating a lateral reorganization of EGFR across the plasma membrane.

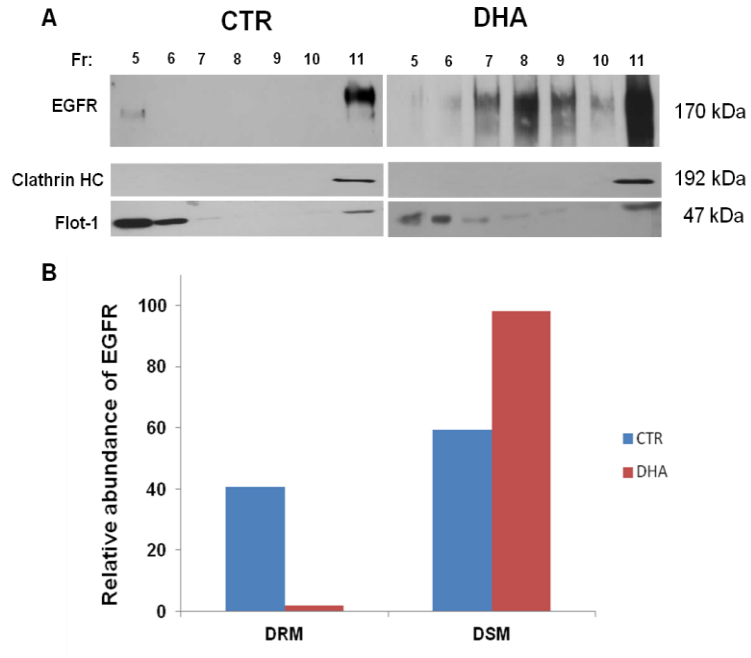

Figure 2. Lateral organization of EGFR.

Cells were treated with or without DHA (200μM). After 72h cells were incubated with or without EGF (10nM). Following isolation the PNS was fractionated into 11 distinct fractions by ultracentrifugation. **(A)** Fractions were collected and an equal amount of proteins from each fraction was analyzed by WB using antibodies against EGFR, flotillin-1, and clathrin HC. **(B)** Quantification of band intensity was performed, and data are presented as the relative amount of EGFR in each fraction, with the sum of each fraction equaling 100. DRM detergent resistant membrane; DSM detergent soluble membrane.

Upon ligand binding, EGFR stimulates signaling pathways involved in cell growth, survival, and migration.

The main signaling pathways activated by EGFR receptors are mediated by PI3K/Akt, MAP-kinase and STAT3 **[28]**. We have decided to study the alteration of EGFR-Ras-MAPK and PI3K/Akt pathways. To understand the mechanism by which DHA suppresses EGFR signal transduction, we assessed the individual components of the EGFR signaling axis. In particular, we first determined the effect of DHA on localization of Ras within the plasma membrane. Ras, a lipidated proto-oncogene product, is expressed in three distinct isoforms, H-Ras, N-Ras and K-Ras. While K-Ras is exclusively located in the bulk membrane, H-Ras is enriched in lipid rafts **[29]**. The localization of Ras within the plasma membrane, the main signaling platform of Ras, and its subsequent binding to GTP are required for activation and downstream signaling.

Previous observations reported that DHA can decrease membrane association of Ras and concomitantly reduce Ras-dependent signaling, cell proliferation, and tumor incidence in transformed mouse colonocytes and colonic epithelium from carcinogen-injected rats **[30,31]**.

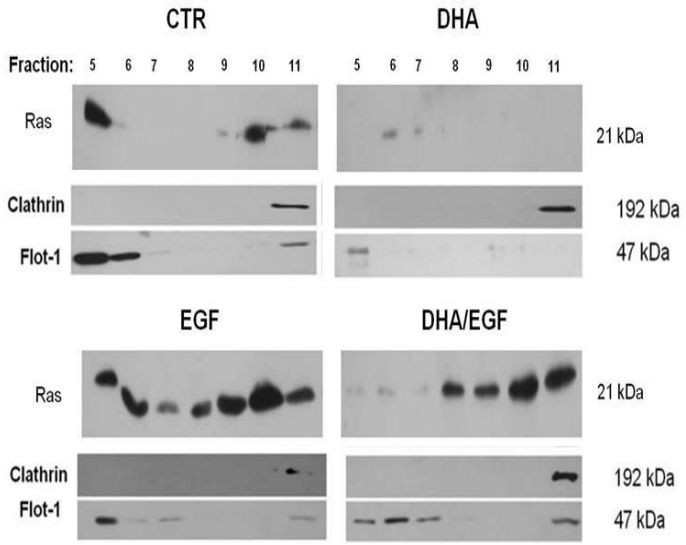

Figure 3. Lateral organization of Ras.

MDA-MB-231 cells were untreated or treated with DHA (200μM). After 72h cells were incubated with or without EGF (10nM), and the PNS was isolated. Following isolation PNS was fractionated into 11 distinct fractions by ultracentrifugation. Fractions were collected and an equal amount of proteins from each fraction was analyzed by WB using antibodies against Ras, flotillin-1, and clathrin HC.

We hypothesized that DHA may influence Ras membrane localization by modifying membrane lipid composition. We evaluated the effect of DHA treatment on Ras protein to evaluate as DHA can inhibit EGF-induced Ras activation. Our data showed that the localization of Ras protein appears to be influenced by DHA treatment (**Figure 3**). In particular, the EGF-stimulation not determine a significant change in Ras content within DRMs.

However, upon ligand binding, EGFR appear to recruit the Ras protein within the plasma membrane. Moreover, after DHA treatment most of the protein does not remain in the DRM enriched fractions. A semi-quantitative analysis allowed to calculate Ras levels in DRMs. In particular, **Figure 4** shows a reduction of Ras content in DRMs of 74.1 ± 7.4% (mean ± SEM; n = 3) after DHA treatment compared to the untreated cells (**p< 0.01).

Also, as reported in **Figure 4B**, our findings showed that a combination of EGF- and DHA treatment determines a reduction of Ras content of 82.0 ± 5.1% (mean ± SEM; n = 3) compared to control (**p< 0.01), and a reduction of 84.4 ± 10.2% (mean ± SEM; n = 3) compared to EGF-treated cells (§p< 0.05). These results indicate that, in addition to the altered localization of EGFR, also Ras protein appears to be affected by DHA treatment.

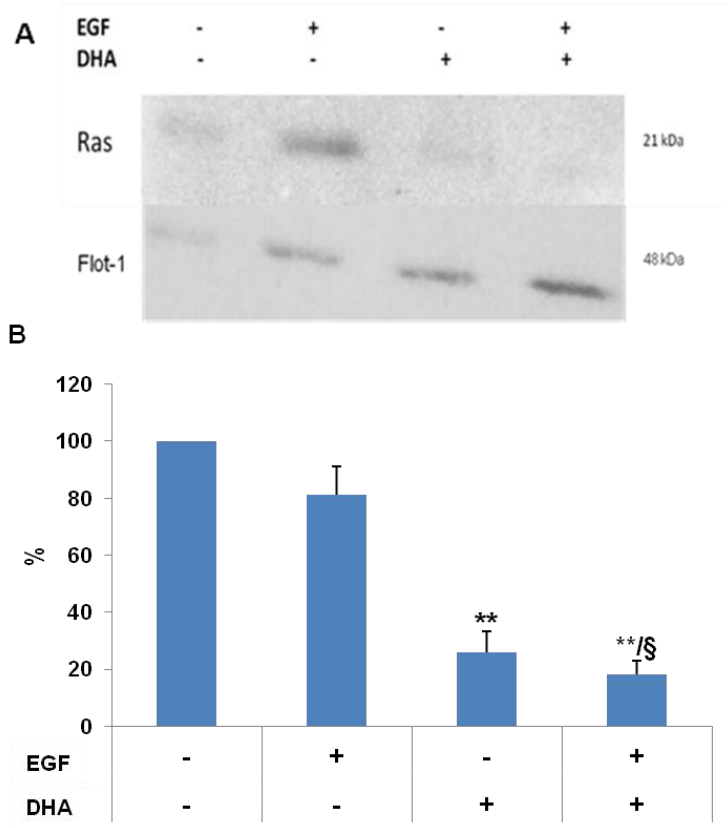

Figure 4. DHA reduces Ras levels in DRMs. Cells were treated with or without DHA (200μM). Some DHA-treated cells were incubated with EGF (10nM) before harvest. PNS were fractionated and fractions 5 were collected and analyzed by WB using antibodies against Ras and flotillin-1 **(A).** Flotillin-1 was used to normalized results. (**B**) Data (mean ± SEM; n=3) are represented as % of control (**p<0.01; §p<0.05). Each immunoblot is representative of at least 3 independent experiments.

Some studies link the tumour-suppressive action of n-3 PUFA with the MAP-kinase pathway and the inactivation of its components with the induction of apoptosis **[32]** suggesting that there may be tissue or cancer specific mechanisms of n-3 PUFA action. In particular, as regards Extracellular signal-regulated Kinase 1/2 (Erk1/2), some studies showed that n-3 PUFAs promote apoptosis in cancer cells by reducing the levels of p-Erk1/2 **[33,34]**. Moreover, in recent years, a second pathway downstream of receptor tyrosine kinases (RTKs), sometimes via Ras, that involves PI3K and AKT has come onto the scene. AKT, also known as protein kinase B, is a serine/threonine kinase and promotes cell survival and growth by potentiating NF-κB activity and the mammalian target of rapamycin (mTOR) **[35]**. Because the PI3K/Akt signalling pathway mediates cell proliferation, survival and motility, Akt is implicated in the oncogenesis of many cancers.

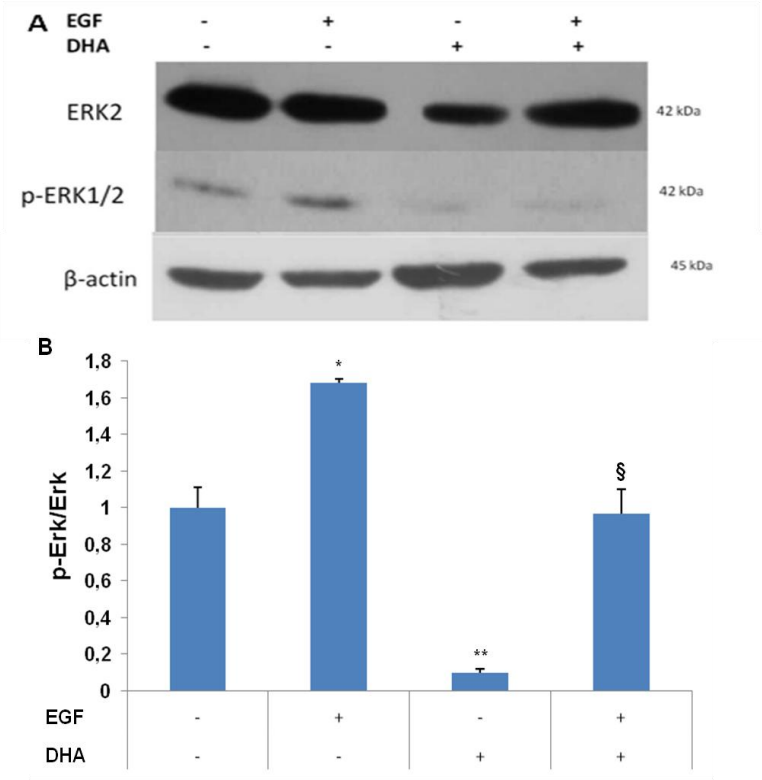

Figure 5. DHA reduces activation of Erk1/2.

Cells were treated with or without DHA (200μM). Some DHA-treated cells were incubated with EGF (10nM) before harvest. PNS were collected and processed by WB using the indicated antibodies **(A).** Each immunoblot is representative of at least 3 independent experiments**. (B)** Quantification of band volume was performed and data are presented as mean ± SEM; n=3. Data are expressed as the ratio of the p-Erk1/2 to total Ekr1/2 protein and normalized to control (mean ± SEM; n=3). Asterisks indicate significant differences between DHA- and EGF-treated compared to CTR cells (**p<0.01; *p<0.05), and between DHA/EGF- and EGF-treated cells (§p<0.05).

Since EGFR phosphorylation is characteristically associated with activation of downstream signaling, we further probed cell lysates (PNS) for phosphorylation of EGFR downstream effector proteins, including Erk1/2 and Akt. As shown in **Figure 5A**, Erk1/2 was phosphorylated after incubation with EGF (10nM) for 10min, while the incubation with DHA decreased the phosphorylation of Erk1/2 both in EGF-treated and untreated cells. A semi-quantitative analysis allowed to calculate the variation of p-Erk1/2, see histogram reported in **Figure 5B**. In particular, the EGF-stimulation increases the phosphorylation of Erk1/2 of 1.5 fold compared to untreated cells (*$p<0.05$). p-Erk1/2 showed to be sensitive to the DHA treatment, its levels markedly decreased. DHA treatment resulted in a ~90% reduction in the activation of Erk1/2 in DHA treated compared to the control cells. Moreover, DHA determines a reduction of p-Erk1/2 about of 60% compared to the EGF-treated cells.

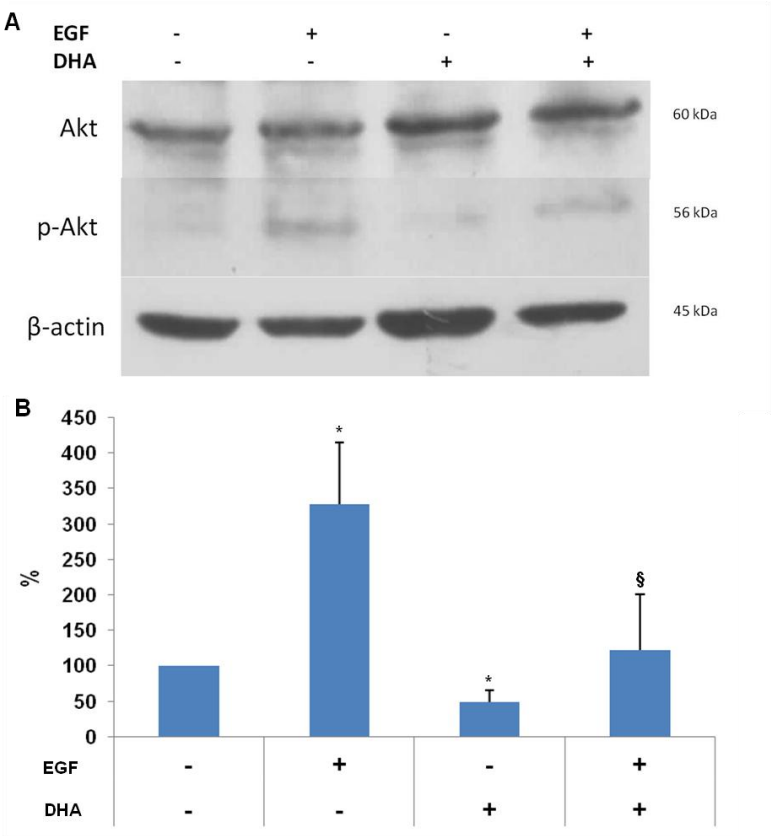

Figure 5. DHA reduces activation of Akt.

Cells were treated with or without DHA (200μM). Some DHA-treated cells were incubated with EGF (10nM) before harvest. PNS were collected and processed by WB **(A)** using the indicated antibodies. Each immunoblot is representative of at least 3 independent experiments. **(B)** Data (mean ± SEM; n=3) are represented as % of control (*/§$p<0.05$) and β-actin was used to normalized results

PI3K is implicated in protecting cells against apoptosis **[36]**, moreover, the Akt signaling pathway plays a crucial role in cancer progression. It has been reported that inactivation of PI3K/Akt signaling by DHA enhances cell death, although the mechanisms involved in DHA-induced Akt inactivation have not been well addressed **[37]**. For this reason, we tested alterations of the levels of phosphorylation of the downstream target of PI3 kinase, Akt. As shown **Figure 5A**, incubation with EGF (10nM) for 10min determines an increased of the phosphorylation of Akt, while DHA-incubation decreases p-Akt levels. In particular, a semi-quantitative analysis **(Figure 5B)** allowed to observe a reduction of p-Akt levels of 52.2 ± 15.5% in DHA-treated cells compared to the untreated cells (mean ± SEM; n = 3; *p< 0.05). Our findings showed that the EGF-stimulation increases the phosphorylation of Akt of 3 fold compared to untreated cells (*p< 0.05), while the combination of DHA/EGF treatment determines a reduction of p-Akt levels of 57.9 ± 18.8% compared to the EGF-treated cells (mean ± SEM; n = 3; §p< 0.05).

Take together these data indicate that the DHA can redistribute lipid raft-associated proteins, such as EGFR, and its downstream signaling, in particular EGFR-Ras-Erk and PI3K/Akt pathways.

7.4 Discussion

Epidemiological studies support the hypothesis that an increased n-3 PUFA intake can inhibit the formation and progression of cancers **[38-39]**. However, although it is acknowledged that n-3 PUFAs may act on the cancer, the specific mechanisms by these FAs may exert their modulatory effects on cancer are not fully understood. n-3 PUFAs appear to be involved in multiple mechanisms that connect the cell membrane, the cytosol, and the nucleus.

This study was prompted by the observation on previously results obtained in our laboratory. We observed that DHA may change the biophysical properties of DRM microdomains by decreasing the content of Chol and SM, due to its incorporation in membrane PLs **[19]**. Thus, we suggest that the alteration of microdomains lipids composition might determine the displacement of proteins, such as EGFR, from rafts in n-3 PUFA treated cells with alteration of signal transduction and induction of apoptosis.

Membrane microdomains, known as lipid rafts, are heterogeneous microdomains enriched in Chol, SM and saturated PLs. They are highly dynamic and may rapidly assemble and disassemble, leading to a dynamic segregation of proteins. They can include or exclude a variety of proteins, such as receptor activities and therefore signal transduction **[4]**. Among the proteins known to be localized in lipid rafts there is the EGFR **[6]**. EGFR is a 170 kDa transmembrane receptor tyrosine kinase, which is frequently over-expressed in many human tumours such as lung and breast cancers **[40].**

We have chosen MDA-MB-231 cells because they express high levels of the EGFR **[39]** and are a good model to study EGFR raft modulation by n-3 PUFAs. Upon ligand binding, EGFR recruits downstream signalling proteins, triggering signal cascades along a number of pathways that eventually lead to cell growth, migration and apoptosis resistance. Key to the ability of EGFR to activate downstream pathways is its localization in lipid raft domains of the plasma membrane **[20,22,24,42]**. Our results shown that DHA is able to reduce EGFR content in DRM enriched fractions compared to the same fractions of untreated cells. We have hypothesized that the reduction of EGFR content in DRM microdomains by DHA might be the consequences of membrane microdomains alterations induced by FA.

Our recent studies **[13,19]** suggest that n-3 PUFA induce modifications of membrane structure and function of breast cancer cells, thereby increasing the degree of unsaturation. In particular, we have observed that EPA and DHA were incorporated in membrane microdomains with different specificity for PLs. Moreover, DHA determines a reduction of SM (about 40%) and Chol (about 70%) content in membrane microdomains.

Since lipid rafts are predominantly enriched in saturated fatty acids and Chol, the incorporation of DHA determines a structural reorganization of microdomains rafts due to steric incompatibility between Chol and DHA **[16,43]**. In fact, the poor affinity of DHA for Chol alter the size, stability and distribution of membrane microdomains.

Thus, the reorganization of membrane microdomains could be the mechanism by which DHA can exclude EGFR proteins from membrane microdomains. Lateral organization of EGFR within the plasma membrane is directly linked to receptor function. Coskun *et al.*, have recently showed that the membrane lipid environment can modulate the localization and function of EGFR. In particular, they have observed that in a three-component lipid mixture consisting of unsaturated PC, SM an Chol, not occurs the EGFR autophosphorylation in absence of EGF, though allowing the ligand-mediated receptor dimerization and its activation. Moreover, when GM3 was added to the ternary lipid mixture EGFR autophosphorylation was inhibited without affecting ligand binding. Their result shows that lipids can function in the allosteric regulation of EGFR function **[44]**. Analyzing DRM and DSM fractions we observed a lateral reorganization of EGFR within the plasmatic membrane after DHA incubation. In particular, we observed a reduction of EGFR level in DRM fractions, and an increase of EGFR level in DSM fractions (**Fig. 2**) compared to the untreated cells.

Therefore, the DHA-induced shift of EGFR localization within the plasma membrane alters the ability of the receptor to dimerize and transphosphorylate Our finding is in favorable agreement with the model proposed by Turk *et al.*, according to which receptor modulation by FAs is mediated by the membrane **[24]**.

The main signaling pathways activated by EGFR receptors are mediated by PI3K/Akt, MAP-kinase and STAT3 **[28]**. To understand the mechanism by which DHA suppresses EGFR signal transduction, we assessed the individual components of the EGFR signaling axis.

Ras is expressed in three distinct isoforms, H-Ras (enriched in lipid rafts), N-Ras and K-Ras (exclusively located in the bulk membrane) **[29]**. The localization of Ras within the plasma membrane is required for activation and downstream signaling. Previous observations reported that DHA can decrease membrane association of Ras and concomitantly reduce Ras-dependent signalling and cell cell proliferation, and tumor incidence in transformed mouse colonocytes and colonic epithelium from carcinogen-injected rats **[39]**.

Our data showed that the localization of Ras protein appears to be influenced by DHA treatment and EGF stimulation (**Fig. 3**). In particular, after EGF-stimulation we observed an increases of Ras level within plasmatic membrane suggesting the recruitment of this protein for activate the EGFR-Ras-MAPK pathway. Moreover, after DHA treatment most of the protein not appear to be associate within plasmatic membrane, especially within membrane microdomains (**Fig. 4**). Moreover, DHA is able to suppress the EGF-stimulated activation of Ras. Recent findings have demonstrated a partitioning of Ras into lipid rafts and caveolae, and effects of n-3 PUFAs on Ras membrane compartmentalization have been examined *in vivo* and *in vitro* models **[39]**.

The Chapkin laboratory showed that dietary n-3 PUFAs are capable of displacing acylated proteins from lipid raft both *in vivo* and *in vitro* models. Feeding mice a diet enriched in n-3 PUFA and treating immortalized YAMC cells with DHA decreased the localization of H-Ras in lipid raft domains, suggesting that changes in membrane lipid composition directly influence the intracellular trafficking and

subcellular localization of lipidated proteins **[45,46]**. Our results are in agreement with these observation. In particular, our results indicate that, in addition to the altered localization of EGFR, also Ras protein appears to be affected by DHA treatment, due to its incorporation in membrane microdomain PLs, which structural reorganization of microdomains. In addition to Ras down-regulation, we found that in breast cancer cells DHA is able to cause a decrease in the phosphorylation state of Erk1/2. Our results indicate that DHA is probably decreasing cell proliferation in part, by down regulating Ras/Erk signaling. Many cancer cells are associated with aberrant PI3K/Akt signaling that up regulates cell proliferation mechanisms and suppresses apoptosis **[47,48]**. Our results showed that DHA interferes with Akt phosphorylation on S473 in MDA-MB-231 breast cancer cells. In our previously work **[13]** we have observed that n-3 PUFA were incorporated in breast cancer cell membrane with different specificity for the PLs moiety. The enrichment was significant, especially in PE, PI and PC. Moreover, in agreement with the results obtained by Gu *et al.,* **[49]** we supposed that the incorporation of DHA into cell membrane could modify PL content and consequently the membrane protein localization, including Akt.

PI3K phosphorylates PIP2 to PIP3 that stimulates the activity of Akt. PIPs (PIP2 and 3) are PLs composed of a glycerol backbone with FAs at the sn-1 and sn-2 position and inositol at the sn-3 position. When Akt is recruited to the plasma membrane through direct contact with PIP3, it is phosphorylated and activated. Akt can phosphorylate proteins, such as pro-caspase-9 and BAD, and is involved in the regulation of apoptosis, gene expression, cell proliferation migration and angiogenesis

[39]. Gu *et al.*, have showed that DHA can replace the FA at the sn-2 position of the glycerol backbone, thereby changing the species of PLs. In particular, DHA alters PIP3 and, consequently, the activation of Akt (S473) protein, suppressing AKT signaling pathway and prostate tumor growth **[49]**.

7.5 Conclusion

Based on the work presented here, DHA play a key role in regulating signal transduction. In particular, we demonstrated that DHA can exclude key proteins, such as EGFR and Ras, from membrane microdomains, thus modifying their downstream signaling, such as Erk and Akt.

In conclusion, the treatment with DHA determines a reduction of cell proliferation by inhibiting of EGFR activity, thus suggesting that these effects might be the consequences of the alteration in membrane microdomains induced by this FA.

References

1. Kraft ML: **Plasma membrane organization and function: moving past lipid rafts**. *Molecular biology of the cell* 2013, **24**(18):2765-2768.
2. Guirland C, Zheng JQ: **Membrane lipid rafts and their role in axon guidance**. *Advances in experimental medicine and biology* 2007, **621**:144-155.
3. Benarroch EE: **Lipid rafts, protein scaffolds, and neurologic disease**. *Neurology* 2007, **69**(16):1635-1639.
4. Simons K, Toomre D: **Lipid rafts and signal transduction**. *Nature reviews* 2001, **1**(1):31-39.
5. Mayor S, Rao M: **Rafts: scale-dependent, active lipid organization at the cell surface**. *Traffic (Copenhagen, Denmark)* 2004, **5**(4):231-240.
6. Foster LJ, De Hoog CL, Mann M: **Unbiased quantitative proteomics of lipid rafts reveals high specificity for signaling factors**. *Proceedings of the National Academy of Sciences of the United States of America* 2003, **100**(10):5813-5818.
7. Lopez-Torrejon I, Querol E, Aviles FX, Seno M, de Llorens R, Oliva B: **Human betacellulin structure modeled from other members of EGF family**. *Journal of molecular modeling* 2002, **8**(4):131-144.
8. Ben-Levy R, Paterson HF, Marshall CJ, Yarden Y: **A single autophosphorylation site confers oncogenicity to the Neu/ErbB-2 receptor and enables coupling to the MAP kinase pathway**. *The EMBO journal* 1994, **13**(14):3302-3311.

9. Prigent SA, Gullick WJ: **Identification of c-erbB-3 binding sites for phosphatidylinositol 3'-kinase and SHC using an EGF receptor/c-erbB-3 chimera**. *The EMBO journal* 1994, **13**(12):2831-2841.
10. Manni A, Xu H, Washington S, Aliaga C, Cooper T, Richie JP, Jr., Bruggeman R, Prokopczyk B, Calcagnotto A, Trushin N *et al*: **The impact of fish oil on the chemopreventive efficacy of tamoxifen against development of N-methyl-N-nitrosourea-induced rat mammary carcinogenesis**. *Cancer prevention research* 2010, **3**(3):322-330.
11. Gillet L, Roger S, Bougnoux P, Le Guennec JY, Besson P: **Beneficial effects of omega-3 long-chain fatty acids in breast cancer and cardiovascular diseases: voltage-gated sodium channels as a common feature?** *Biochimie* 2011, **93**(1):4-6.
12. Serini S, Piccioni E, Merendino N, Calviello G: **Dietary polyunsaturated fatty acids as inducers of apoptosis: implications for cancer**. *Apoptosis* 2009, **14**(2):135-152.
13. Corsetto PA, Montorfano G, Zava S, Jovenitti IE, Cremona A, Berra B, Rizzo AM: **Effects of n-3 PUFAs on breast cancer cells through their incorporation in plasma membrane**. *Lipids in health and disease* 2011, **10**:73.
14. Merendino N, Costantini L, Manzi L, Molinari R, D'Eliseo D, Velotti F: **Dietary omega -3 polyunsaturated fatty acid DHA: a potential adjuvant in the treatment of cancer**. *BioMed research internationa*, 2013, **2013**:310186.

15. Vaughan VC, Hassing MR, Lewandowski PA: **Marine polyunsaturated fatty acids and cancer therapy**. *British journal of cancer* 2013, **108**(3):486-492.
16. Turk HF, Chapkin RS: **Membrane lipid raft organization is uniquely modified by n-3 polyunsaturated fatty acids**. *Prostaglandins, leukotrienes, and essential fatty acids* 2013,**88**(1):43-47.
17. Wong SW, Kwon MJ, Choi AM, Kim HP, Nakahira K, Hwang DH: **Fatty acids modulate Toll-like receptor 4 activation through regulation of receptor dimerization and recruitment into lipid rafts in a reactive oxygen species-dependent manner**. *The Journal of biological chemistry* 2009, **284**(40):27384-27392.
18. Shaikh SR, Rockett BD, Salameh M, Carraway K: **Docosahexaenoic acid modifies the clustering and size of lipid rafts and the lateral organization and surface expression of MHC class I of EL4 cells**. *The Journal of nutrition* 2009, **139**(9):1632-1639.
19. Corsetto PA, Cremona A, Montorfano G, Jovenitti IE, Orsini F, Arosio P, Rizzo AM: **Chemical-physical changes in cell membrane microdomains of breast cancer cells after omega-3 PUFA incorporation**. *Cell biochemistry and biophysics* 2012, **64**(1):45-59.
20. Pike LJ, Han X, Gross RW: **Epidermal growth factor receptors are localized to lipid rafts that contain a balance of inner and outer leaflet lipids: a shotgun lipidomics study**. *The Journal of biological chemistry* 2005, **280**(29):26796-26804.

21. Patra SK: **Dissecting lipid raft facilitated cell signaling pathways in cancer**. *Biochimica et biophysica acta* 2008, **1785**(2):182-206.
22. Schley PD, Brindley DN, Field CJ: **(n-3) PUFA alter raft lipid composition and decrease epidermal growth factor receptor levels in lipid rafts of human breast cancer cells**. *The Journal of nutrition* 2007, **137**(3):548-553.
23. Rogers KR, Kikawa KD, Mouradian M, Hernandez K, McKinnon KM, Ahwah SM, Pardini RS: **Docosahexaenoic acid alters epidermal growth factor receptor-related signaling by disrupting its lipid raft association**. *Carcinogenesis* 2010, **31**(9):1523-1530.
24. Turk HF, Barhoumi R, Chapkin RS: **Alteration of EGFR spatiotemporal dynamics suppresses signal transduction**. *PloS one* 2012, **7**(6):e39682.
25. Ravacci GR, Brentani MM, Tortelli T, Jr., Torrinhas RS, Saldanha T, Torres EA, Waitzberg DL: **Lipid raft disruption by docosahexaenoic acid induces apoptosis in transformed human mammary luminal epithelial cells harboring HER-2 overexpression**. *The Journal of nutritional biochemistry* 2013, **24**(3):505-515.
26. Lee EJ, Yun UJ, Koo KH, Sung JY, Shim J, Ye SK, Hong KM, Kim YN: **Down-regulation of lipid raft-associated onco-proteins via cholesterol-dependent lipid raft internalization in docosahexaenoic acid-induced apoptosis**. *Biochimica et biophysica acta* 2013, **1841**(1):190-203.

27. Roepstorff K, Thomsen P, Sandvig K, van Deurs B: **Sequestration of epidermal growth factor receptors in non-caveolar lipid rafts inhibits ligand binding**. *The Journal of biological chemistry* 2002, **277**(21):18954-18960.
28. Zandi R, Larsen AB, Andersen P, Stockhausen MT, Poulsen HS: **Mechanisms for oncogenic activation of the epidermal growth factor receptor**. *Cellular signalling* 2007, **19**(10):2013-2023.
29. Roy S, Plowman S, Rotblat B, Prior IA, Muncke C, Grainger S, Parton RG, Henis YI, Kloog Y, Hancock JF: **Individual palmitoyl residues serve distinct roles in H-ras trafficking, microlocalization, and signaling**. *Molecular and cellular biology* 2005, **25**(15):6722-6733.
30. Collett ED, Davidson LA, Fan YY, Lupton JR, Chapkin RS: **n-6 and n-3 polyunsaturated fatty acids differentially modulate oncogenic Ras activation in colonocytes.** *American journal of physiology* 2001, **280**(5):C1066-1075.
31. Davidson LA, Lupton JR, Jiang YH, Chapkin RS: **Carcinogen and dietary lipid regulate ras expression and localization in rat colon without affecting farnesylation kinetics**. *Carcinogenesis* 1999, **20**(5):785-791.
32. Sun H, Hu Y, Gu Z, Owens RT, Chen YQ, Edwards IJ: **Omega-3 fatty acids induce apoptosis in human breast cancer cells and mouse mammary tissue through syndecan-1 inhibition of the MEK-Erk pathway**. *Carcinogenesis* 2011, **32**(10):1518-1524.
33. Calviello G, Di Nicuolo F, Gragnoli S, Piccioni E, Serini S, Maggiano N, Tringali G, Navarra P, Ranelletti FO, Palozza P: **n-3**

PUFAs reduce VEGF expression in human colon cancer cells modulating the COX-2/PGE2 induced ERK-1 and -2 and HIF-1alpha induction pathway. *Carcinogenesis* 2004, **25**(12):2303-2310.

34. Serini S, Trombino S, Oliva F, Piccioni E, Monego G, Resci F, Boninsegna A, Picci N, Ranelletti FO, Calviello G: **Docosahexaenoic acid induces apoptosis in lung cancer cells by increasing MKP-1 and down-regulating p-ERK1/2 and p-p38 expression**. *Apoptosis* 2008, **13**(9):1172-1183.
35. Franke TF: **Intracellular signaling by Akt: bound to be specific**. *Science signaling* 2008, **1**(24):pe29.
36. Gire V, Marshall C, Wynford-Thomas D: **PI-3-kinase is an essential anti-apoptotic effector in the proliferative response of primary human epithelial cells to mutant RAS**. *Oncogene* 2000, **19**(19):2269-2276.
37. Hu Y, Sun H, Owens RT, Gu Z, Wu J, Chen YQ, O'Flaherty JT, Edwards IJ: **Syndecan-1-dependent suppression of PDK1/Akt/bad signaling by docosahexaenoic acid induces apoptosis in prostate cancer**. *Neoplasia* 2010, **12**(10):826-836.
38. Calviello G, Serini S, Piccioni E, Pessina G: **Antineoplastic effects of n-3 polyunsaturated fatty acids in combination with drugs and radiotherapy: preventive and therapeutic strategies**. *Nutrition and cancer* 2009, **61**(3):287-301.
39. Biondo PD, Brindley DN, Sawyer MB, Field CJ: **The potential for treatment with dietary long-chain polyunsaturated n-3 fatty**

acids during chemotherapy. *The Journal of nutritional biochemistry* 2008, **19**(12):787-796.

40. Salomon DS, Brandt R, Ciardiello F, Normanno N: **Epidermal growth factor-related peptides and their receptors in human malignancies**. *Critical reviews in oncology/hematology* 1995, **19**(3):183-232.
41. Biscardi JS, Belsches AP, Parsons SJ: **Characterization of human epidermal growth factor receptor and c-Src interactions in human breast tumor cells**. *Molecular carcinogenesis* 1998, **21**(4):261-272.
42. Irwin ME, Mueller KL, Bohin N, Ge Y, Boerner JL: **Lipid raft localization of EGFR alters the response of cancer cells to the EGFR tyrosine kinase inhibitor gefitinib**. *Journal of cellular physiology* 2011, **226**(9):2316-2328.
43. Chapkin RS, McMurray DN, Davidson LA, Patil BS, Fan YY, Lupton JR: **Bioactive dietary long-chain fatty acids: emerging mechanisms of action**. *The British journal of nutrition* 2008, **100**(6):1152-1157.
44. Coskun U, Grzybek M, Drechsel D, Simons K: **Regulation of human EGF receptor by lipids**. *Proceedings of the National Academy of Sciences of the United States of America* 2011, **108**(22):9044-9048.
45. Ma DW, Seo J, Davidson LA, Callaway ES, Fan YY, Lupton JR, Chapkin RS: **n-3 PUFA alter caveolae lipid composition and resident protein localization in mouse colon**. *Faseb J* 2004, **18**(9):1040-1042.

46. Seo J, Barhoumi R, Johnson AE, Lupton JR, Chapkin RS: **Docosahexaenoic acid selectively inhibits plasma membrane targeting of lipidated proteins**. *Faseb J* 2006, **20**(6):770-772.
47. Manning BD, Cantley LC: **AKT/PKB signaling: navigating downstream**. *Cell* 2007, **129**(7):1261-1274.
48. Liu P, Cheng H, Roberts TM, Zhao JJ: **Targeting the phosphoinositide 3-kinase pathway in cancer**. *Nature reviews* 2009, **8**(8):627-644.
49. Gu Z, Wu J, Wang S, Suburu J, Chen H, Thomas MJ, Shi L, Edwards IJ, Berquin IM, Chen YQ: **Polyunsaturated fatty acids affect the localization and signaling of PIP3/AKT in prostate cancer cells**. *Carcinogenesis*, **34**(9):1968-1975.

Appendix

Pubblications

1. **"Atomic force microscopy imaging of lipid rafts of human breast cancer cells"** Cremona A., Orsini F., Arosio P., Corsetto P.A., Montorfano G., Lascialfari A., Rizzo A.M. *BBA-Biomembranes* (2012) 1818(12):2943-9. **(*)**

2. **"Chemical-Physical changes in cell membrane microdomains of breast cancer cells after omega-3 PUFA incorporation"** Corsetto P.A., Cremona A., Montorfano G., Orsini F., Arosio P., Rizzo A.M. *Cell Biochemistry and Biophysics* (2012) 64:45. **(*)**

3. **"Effects of n-3 PUFAs on breast cancer cells through their incorporation in plasma membrane"** Corsetto P.A., Montorfano G., Zava S., Jovenitti I.E., Cremona A., Berra B., Rizzo A.M. *Lipids in Health and Disease* (2011) 10:73.

(*) *Papers discussed in the thesis.*

Erasmus placement

April – July 2013
Abroad period in the laboratoty of Prof. B.W Hoogenboom.
London Centre for Nanotechnology and Dept. of Physics & Astronomy, University College London, London (UK).

Oral communications

1. **"Atomic Force Microscopy study of lipid rafts in MDA-MB-231 human breast cancer cells after DHA incorporation"** Corsetto P.A., Cremona A., Orsini F., Arosio P., Jovenitti I.E., Zava S., Montorfano G., Rizzo A.M.
   Convegno Annuale della sezione Ligure-Lombardo-Piemontese della Società Italiana di Biochimica e Biologia Molecolare (LLP) Novara 20 May 2011.

Co-author of scientific congress communications

1. **"DHA alters lipid raft organization and function in breast cancer cells".** Corsetto P.A., Cremona A., Montorfano G., Rizzo A.M.
   54st International Conference on the Bioscience of Lipids, 2013, Bari, Italy.
2. **"Omega-3 PUFA modulate P-glicoprotein (Pgp) activity altering lipid raft cholesterol".** Corsetto P.A., Riganti C., Montorfano G., Gelsomino G., Cremona A., Campia I., Ghigo D., Bosia A., Rizzo A.M.
   38th FEBS Congress, July 6-11, 2013, St Petersburg, Russia.
3. **"ω-3 PUFA reduce cholesterol biosynthesis and doxorubicin resistance in colon cancer cells"** Riganti C., Corsetto P.A., Montorfano G., Cremona A., Ghigo D., Bosia A., Rizzo A.M.
   56th National Meeting of the Italian Society of Biochemeistry and Molecular Biology Chieti, Italy 26-29 September 2012.
4. **"DHA modifies lipid raft structure and function in MDA-MB-231 breast cancer cells"** Corsetto P.A., Ami D., Montorfano G., Cremona A., Doglia S.M., Rizzo A.M.
   56th National Meeting of the Italian Society of Biochemeistry and Molecular Biology Chieti, Italy 26-29 September 2012.

5. **"Effects of n-3 PUFAs on structure and function of breast cancer lipid rafts"** Corsetto P.A., Montorfano G., Cremona A., Jovenitti I.E., Orsini F., Arosio P., Rizzo A.M.
   37th FEBS CONGRESS Seville, Spain 4-9 September 2012.
6. **"Atomic Force Microscopy imaging of lipid rafts of human breast cancer cells"** Orsini F., Cremona A., Arosio P., Corsetto P.A., Lascialfari A., Rizzo A.M.
   Seeing at the Nanoscale Bristol, UK 9-11 July 2012.
7. **"Atomic force microscopy imaging of human aquaporin 4 expressed in Xenopus laevis oocytes"** Orsini F., Santacroce M., Cremona A., Arosio P., Hoogenboom B., Lascialfari A.
   Seeing at the Nanoscale Bristol, UK 9-11 July 2012.
8. **"Chemical-Physical changes in cell membrane microdomains of breast cancer cells after omega-3 PUFA incorporation"** Corsetto P.A., Cremona A., Montorfano G., Jovenitti I.E., Orsini F., Arosio P., Rizzo A.M.
   Next-step La Giovane Ricerca Avanzata 3 Milan, Italy 26 June 2012
9. **"Chemical-Physical changes in cell membrane microdomains of breast cancer cells after omega-3 PUFA incorporation"** Cremona A., Corsetto P.A., Rizzo A.M.
   XXIV Convegno "A. Castellani" dei Dottorandi di ricerca in discipline Biochimiche Brallo di Pregola (PV), Italy 11-15 June 2012.
10. **"Effects of DHA incorporation in membrane lipid rafts of MDA-MB-231 human breast cancer cells"** Orsini F., Cremona A., Corsetto P.A., Arosio P., Lascialfari A., Rizzo A.M.
    Fourth International Meeting on AFM in Life Sciences and Medicine Paris, France 23-27 August 2011.

11. **"Imaging of the Xenopus laevis oocyte plasma membrane in physiologicallike conditions by Atomic Force Microscopy"** Orsini F., Santacroce M., Cremona A., Arosio P., Sacchi V., Kramer A., Hoogenboom B.
    Fourth International Meeting on AFM in Life Sciences and Medicine Paris, France 23-27 August 2011.
12. **"Biochemical and biophysical approaches to study the incorporation of omega-3 LCPUFA on breast cancer cells lipid rafts"** Corsetto P.A., Cremona A., Montorfano G., Jovenitti I.E., Orsini F., Arosio P., Rizzo A.M.
    36th FEBS CONGRESS Turin, Italy 25-30 June 2011.

Scientific schools and courses attendante

XXIV Riunione Nazionale dei Dottorandi in discipline Biochimiche "A. Castellani" Brallo di Pregola (PV), Italy 11-15 June 2012.